4. SITE 465: SOUTHERN HESS RISE[1]

Shipboard Scientific Party[2]

HOLE 465

Date occupied: 23 August 1978

Date departed: 24 August 1978

Time on hole: 20.75 hours

Position (latitude; longitude): 33°49.23′N; 178°55.14′E

Water depth (corrected m, echo sounding): 2161

Bottom felt (m, drill pipe): 2165.5

Penetration (m): 96

Number of cores: 11

Total length of cored section (m): 96

Total core recovered (m): 43.89

Core recovery (%): 46.0

Oldest sediment cored:
Depth sub-bottom (m): 96
Nature: Foraminifer nannofossil ooze
Age: Early Maastrichtian

Igneous basement: Not penetrated

HOLE 465A

Date occupied: 24 August 1978

Date departed: 28 August 1978

Time on hole: 83.2 hours

Position (latitude; longitude): 33°49.23′N; 178°55.14′E

Water depth (corrected m, echo sounding): 2161

Bottom felt (m, drill pipe): 2165.5

Penetration (m): 476

Number of cores: 46

Total length of cored section (m): 437

Total core recovered (m): 108.5

Core recovery (%): 24.8

Oldest sediment cored:
Depth sub-bottom (m): 411.7
Nature: Limestone
Age: Late Albian
Measured velocity: 2.89 km/s

Igneous basement:
Depth sub-bottom (m): 411.7
Nature: Altered trachyte
Velocity range (km/s): 3.60 ± 0.12

Principal results: We drilled at Site 465 (Fig. 1) on southern Hess Rise to determine the age of igneous basement, the ages and depositional environments of the sediments, and the paleoenvironmental implications. Southern Hess Rise has been above the local CCD since its formation. This large aseismic structure apparently formed south of the mid-Cretaceous equator and moved northward on the Pacific Plate as it subsided. Two holes (Holes 465 and 465A) were drilled. Hole 465 was cored to a sub-bottom depth of 96 meters. The entire sediment sequence and 64 meters of the volcanic basement (Fig. 2) were continuously cored in Hole 465A to a sub-bottom depth of 476 meters.

In Hole 465, 11 cores of nannofossil ooze and foraminifer nannofossil ooze range in age from early Maastrichtian to early Pleistocene. A hiatus of almost 50 m.y. occurs between upper Paleocene and lower Pliocene sediments, but there appears to be a continuous record across the Cretaceous/Tertiary boundary. Chert is a common constituent, and pyrite is present in trace amounts. Hole 465 was abandoned because the ship drifted off the beacon, making it necessary to pull the drill string above the mud line.

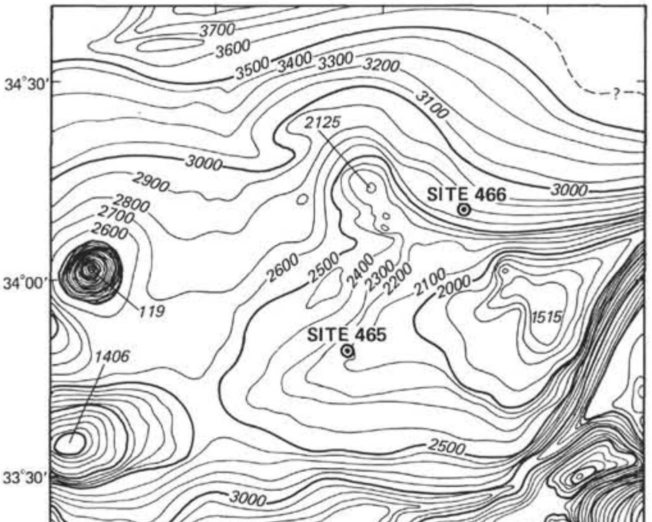

Figure 1. Location of DSDP Sites 465 and 466, southern Hess Rise. Bathymetry from Chase et al. (this volume).

---

[1] *Initial Reports of the Deep Sea Drilling Project*, Volume 62.

[2] Tracy L. Vallier (Co-Chief Scientist), U.S. Geological Survey, Menlo Park, California; Jörn Thiede (Co-Chief scientist), Department of Geology, University of Oslo, Blindern, Oslo 3, Norway; Charles Adelseck, Jr., Deep Sea Drilling Project, Scripps Institution of Oceanography, La Jolla, California; Anne Boersma, Lamont-Doherty Geological Observatory, Palisades, New York; Pavel Čepek, Bundesanstalt für Geowissenschaften und Rohstoffe, Hannover, Federal Republic of Germany; Walter E. Dean, U.S. Geological Survey, Denver, Colorado; Naoyuki Fujii, Department of Earth Sciences, Kobe University, Nada, Kobe, Japan; Vladimir I. Koporulin, Geological Institute, U.S.S.R. Academy of Sciences, Moscow, U.S.S.R.; David K. Rea, Department of Atmospheric and Oceanic Science, University of Michigan, Ann Arbor, Michigan; Constance Sancetta, Lamont-Doherty Geological Observatory, Palisades, New York; William Sayre, Department of Oceanography, University of Southampton, Southampton, United Kingdom (present address: Department of Earth Sciences, Iowa State University of Science and Technology, Ames, Iowa); André Schaaf, Institut de Géologie, Strasbourg, France; Ronald R. Schmidt, Institute of Earth Sciences, University of Utrecht, Utrecht, The Netherlands; Karl E. Seifert, Department of Earth Sciences, Iowa State University of Science and Technology, Ames, Iowa; Edith Vincent, Geological Research Division, Scripps Institution of Oceanography, La Jolla, California; Kenneth E. Windom, Department of Earth Sciences, Iowa State University of Science and Technology, Ames, Iowa.

Hole 465A was spudded in to 39 meters, and coring was continuous from that depth to the base of the hole. The Albian to Pleistocene sediments reflect the transition of the southern Hess Rise depositional paleoenvironment from tropical to temperate latitudes—because of horizontal movement of the Pacific Plate—and from shallow to intermediate water depth, because of subsidence of this aseismic rise. The trachyte (Unit III) is highly altered and has some vesicles greater than 5 mm in diameter, suggesting shallow water, or possibly even subaerial extrusion. Textures show flow orientation of feldspar laths and microlites. Oldest sediments (Unit II) consist of olive-gray, laminated upper Albian to Cenomanian limestone, in a unit 136 meters thick, which shows many indications of current activity and redeposition along the former sea floor. High organic-carbon contents indicate anoxic conditions, probably related to a mid-water oxygen-minimum zone along the submarine slopes of an archipelago. The overlying sediment (Unit I) is 276 meters thick and consists of Coniacian to Pleistocene nannofossil ooze and foraminifer nannofossil ooze, with intercalated chert. This unit reflects a slowly deepening, relatively quiet depositional environment within an intermediate-depth water mass. Significant hiatuses occur from early Cenomanian to late Coniacian, from Santonian to late Campanian, and from late Paleocene to Pliocene. Calcareous oozes of Lithologic Unit I show signs of intense dissolution, despite their shallow-water depth of deposition. A highlight of this hole was the recovery of an apparently complete sedimentary sequence across the Cretaceous/Tertiary boundary, with well-preserved sediments of the *G. eugubina* Zone in Core 3 of Hole 465A. A heat flow of 1.36 HFU is similar to that of averaged North Pacific heat flow for crust of this age.

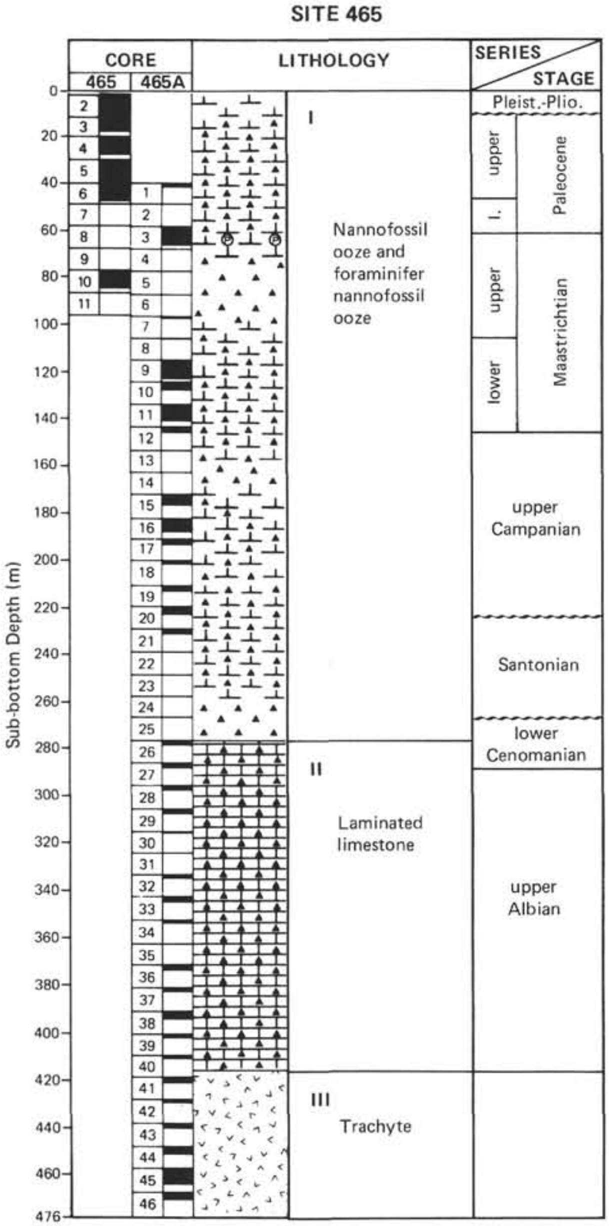

Figure 2. Stratigraphy of Site 465.

BACKGROUND AND OBJECTIVES

Hess Rise is one of the major structural features of the central North Pacific. It is bounded on the west by the moat that lies east of the Emperor Seamounts, on the northeast by the Emperor Trough, and on the south by the Mendocino Fracture Zone. These three structural lineaments outline a triangular, elevated, aseismic high that lies above abyssal regions of the Pacific Plate which are characterized as normal oceanic crust by Mesozoic linear magnetic anomalies. Previous attempts to drill Hess Rise during DSDP Leg 32 (Larson, Moberly, et al., 1975) failed to reach basement, and the early origin of Hess Rise has remained largely unknown. The oldest sediments cored at Site 310 are of early Cenomanian to late Albian age. Volcanic rocks reached at the bottom of Hole 464 are overlain by sediments of early Albian (or Aptian) age, suggesting a minimum age of northern Hess Rise of approximately 110 m.y. However, age data on the bottom sediment cores from Hole 464 are very poor.

Previous coring on Hess Rise sampled sediments from water depths >3.5 km (Site 310) and >4.5 km (Site 464). Because hiatuses and, at least in part, unfossiliferous pelagic-clay sequences were found at both previous sites, the location of Site 465 (Figs. 3 and 4) had been planned where a well-stratified, 400- to 500-meter-thick sedimentary sequence above an apparently volcanic basement could be sampled in relatively shallow water. There are several reasons for the choice of such a location:

1) Southern Hess Rise is close to the northern boundary of modern subtropical planktonic-foraminifer faunas (Vincent, 1975). Well-documented sediment sections from Hess Rise could allow a close correlation between high- and low-latitude biostratigraphies elsewhere in the central Pacific.

2) We expected the shallow water depth to provide us with pelagic sediments containing well-preserved calcareous fossils.

3) The location close to the crest of Hess Rise (Fig. 4)—yet on a gently sloping plateau underlain by a clearly stratified sedimentary sequence—may have been protected from reworking of older sediments, such as that caused by slumping.

4) Because of the recognition of important and long-lasting hiatuses in the Cenozoic section penetrated at Sites 310 and 464, a shallow location might provide us with an optimal chance to avoid a depth level which had been affected by the current regime generating the hiatuses.

5) Common chert layers in the Cretaceous section of Sites 310 and 464 had resulted in a very poor recovery of

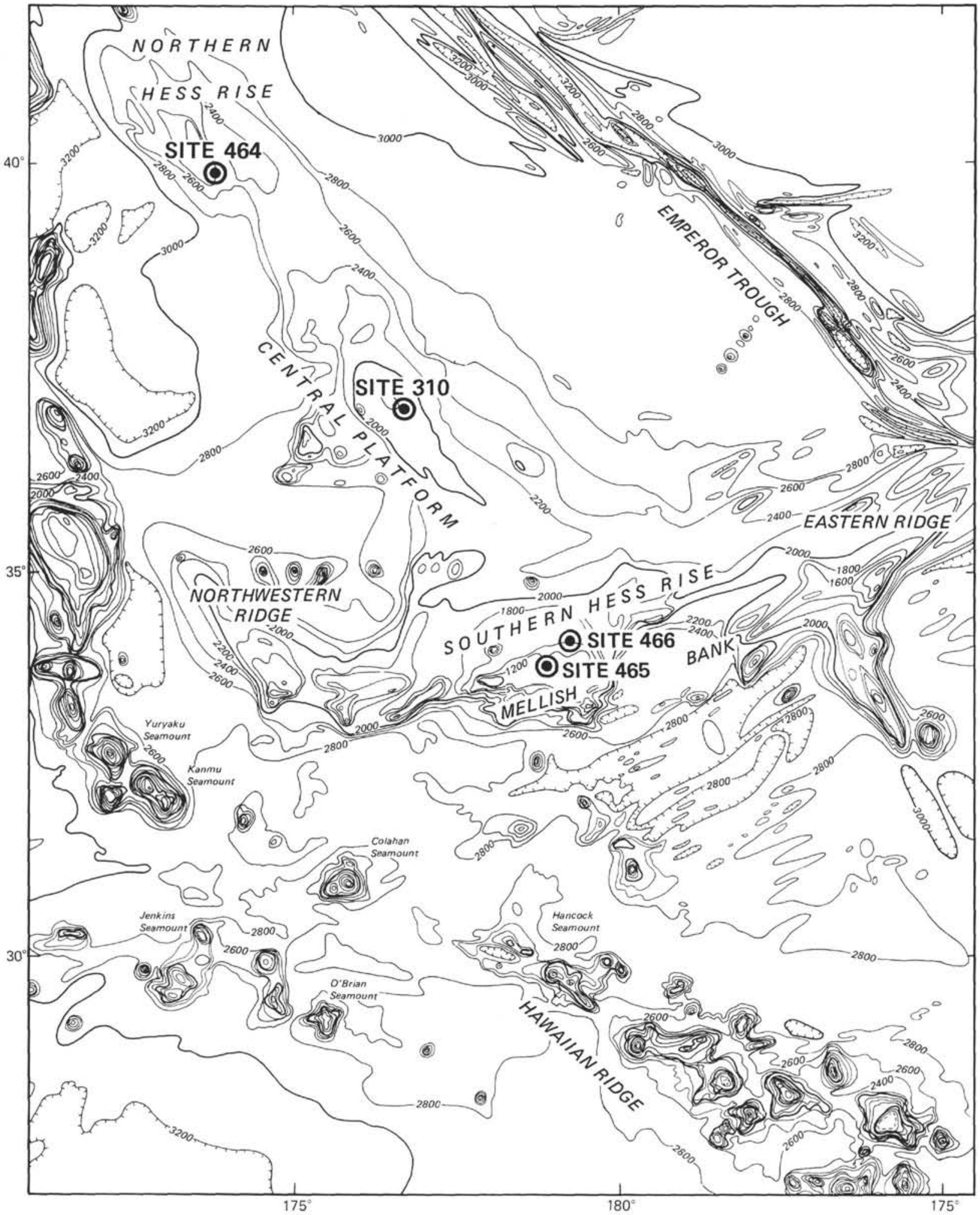

Figure 3. Location map for sites drilled on Hess Rise. Site 310 was drilled during Leg 32 (Larson, Moberly, et al., 1975). Bathymetry in fathoms (from Chase et al., 1971).

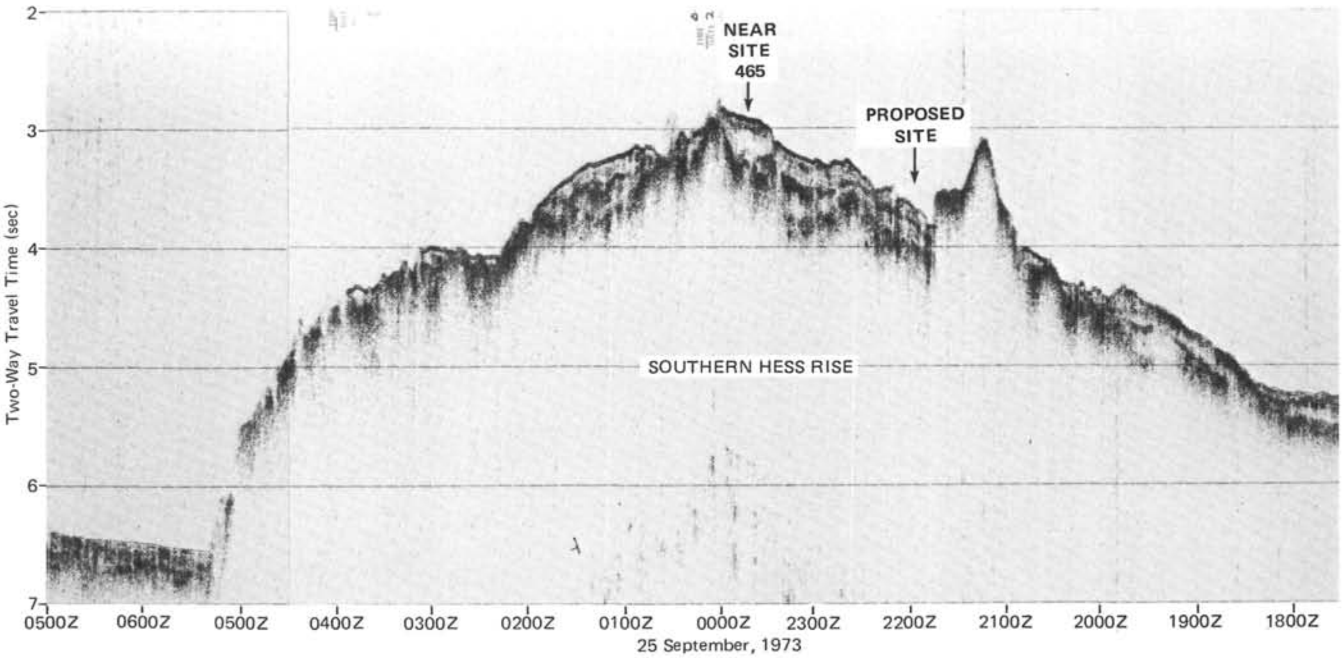

Figure 4. *Glomar Challenger* Leg 32 track line (Larson et al., 1975) across southern Hess Rise. Speed was about 10.5 knots, and course almost 150°, from right to left.

the relatively soft chalks, claystones, marlstones, and limestones. Both of the previously sampled sections are therefore of limited value in reconstruction of the late Mesozoic central Pacific paleoenvironment. By selecting a shallow site, we hoped to avoid lithofacies rich in silica and therefore unaffected by chert formation.

6) Although none of the previously drilled sites on Hess Rise had revealed evidence for a shallow-water depositional environment during its early history, we hoped to penetrate reef deposits or other shallow-water sediments before reaching volcanic basement rocks.

7) We hoped that the location close to the rise crest and the pinnacle-shaped configuration of the acoustic basement would allow us not only to reach rocks of the supposed volcanic edifice under the sediment cover of Hess Rise, but also to penetrate any igneous basement rocks to considerable depth.

We expected that, because of the continuous northward horizontal movement of the Pacific Plate from a position well south of the equator during mid-Cretaceous time to its present location under the oligotrophic subtropical central North Pacific water masses (Lancelot and Larson, 1975), the sediments on southern Hess Rise would show large variations in composition, as well as in thickness, despite the shallow water depth. Moreover, by combining the results of Site 310 on central Hess Rise, 464 on northern Hess Rise, and 465 on southern Hess Rise, we planned to recover Upper Cretaceous sedimentary sequences that could document the time when this region crossed under the fertile equatorial surface-current regime. Expanded stratigraphic sequences caused by high biogenic-sedimentation rates were expected to provide an opportunity to study the timing of the evolution of the mid- and Late Cretaceous calcareous and siliceous planktonic communities. The three sites on Hess Rise are spread over a depth range of approximately 3 km, which could provide us with clues to the position of the late Mesozoic CCD.

A position for Site 465 on southern Hess Rise which seemed suitable to achieve the above-listed goals had been selected along the *Glomar Challenger* Leg 32 seismic-reflection profile across southern Hess Rise (Fig. 4) (Larson, Moberly, et al., 1975).

OPERATIONS

We completed a short seismic-reflection survey of Site 464 and steamed toward Site 465 on southern Hess Rise, where a drill site had been chosen on the *Glomar Challenger* Leg 32 air-gun profile. About 50 miles from the proposed site, we intersected the *Glomar Challenger* Leg 32 track line (1700Z, 24 September 1973) and steamed along that profile to the site. We did not drop a beacon on the proposed site (Fig. 4), but continued another 15 miles along the GL32 profile to a more promising location. At 2045Z on 23 August, we dropped the beacon and continued on course until 2145Z. After pulling in the gear, we returned to the beacon (Fig. 5).

Site 465 is located in 2161 meters (corrected from PDR) of water. This depth was chosen, rather than the length of drill pipe, because of some difficulty in establishing the mud line. Several reflectors are apparent on the air-gun seismic-reflection profile across the site (Fig. 6). Hole 465 was spudded in, and the first core was on deck at 0715Z, August 24. After 11 cores had been cut to a depth of 96 meters, the ship drifted off the beacon, and the drill string was pulled above the mud line at 1800Z. We repositioned over the beacon until 1955Z, when a second hole (Hole 465A) was spudded in, drilled to a depth of 39 meters, and subsequently cored contin-

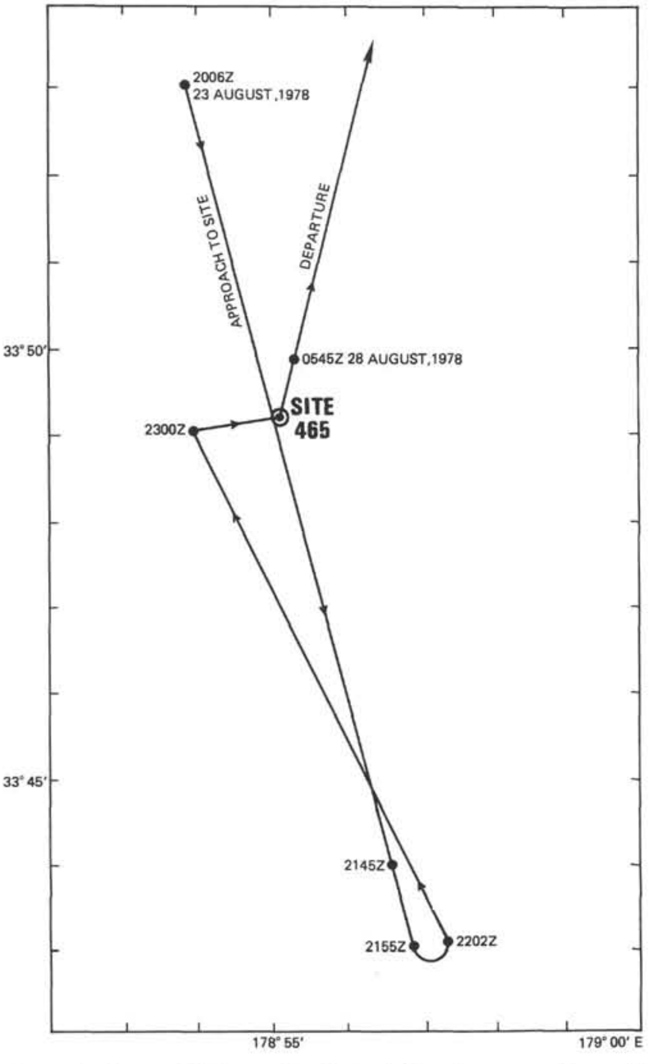

Figure 5. *Glomar Challenger* Leg 62 track lines for approach to and departure from Site 465.

uously to a sub-bottom depth of 476 meters (Table 1). We began coring at 39 meters in Hole 465A, well above the base of Hole 465, in order to sample the Cretaceous/Tertiary boundary, which had not been sampled adequately in Hole 465.

A hole-inclination test was made as we took Core 40, which indicated that the hole was inclined about 4° from the vertical. Heat-flow measurements were attempted between Cores 10 and 11 in Hole 465, and between Cores 6 and 7, 8 and 9, and 14 and 15 in Hole 465A.

The bit reached igneous basement at 411.7 meters in Core 40. Coring was continued in the basement to a depth of 476 meters (Core 46). When the core barrel was dropped for Core 47, the drill string had become stuck (August 27, 1300Z), and we were unable to circulate or to loosen the string. An attempt was made to shoot off the bottom-hole assembly, but the explosive charge fortunately failed to detonate. Subsequently, while raising the drill string a small amount, it was apparent that the drill string somehow had loosened. Thereafter, we pulled out the drill string with no further problems.

Site 465 was abandoned at 0512Z on August 28, and we departed for Site 466 (Fig. 5). Gear was streamed by 0530Z, and we were under way for Site 466.

LITHOLOGIC SUMMARY

Lithologic Subdivision

The section recovered at Site 465 on southern Hess Rise was subdivided into three lithologic units, on the basis of composition, degree of lithification, and sedimentary structures (Table 2; Fig. 2).

Unit I: Nannofossil Ooze and Foraminifer Nannofossil Ooze (0–276 m)

Unit I consists of homogeneous, white (N9 and lighter), moderately to highly disturbed nannofossil ooze. The main variability within the unit is in the rela-

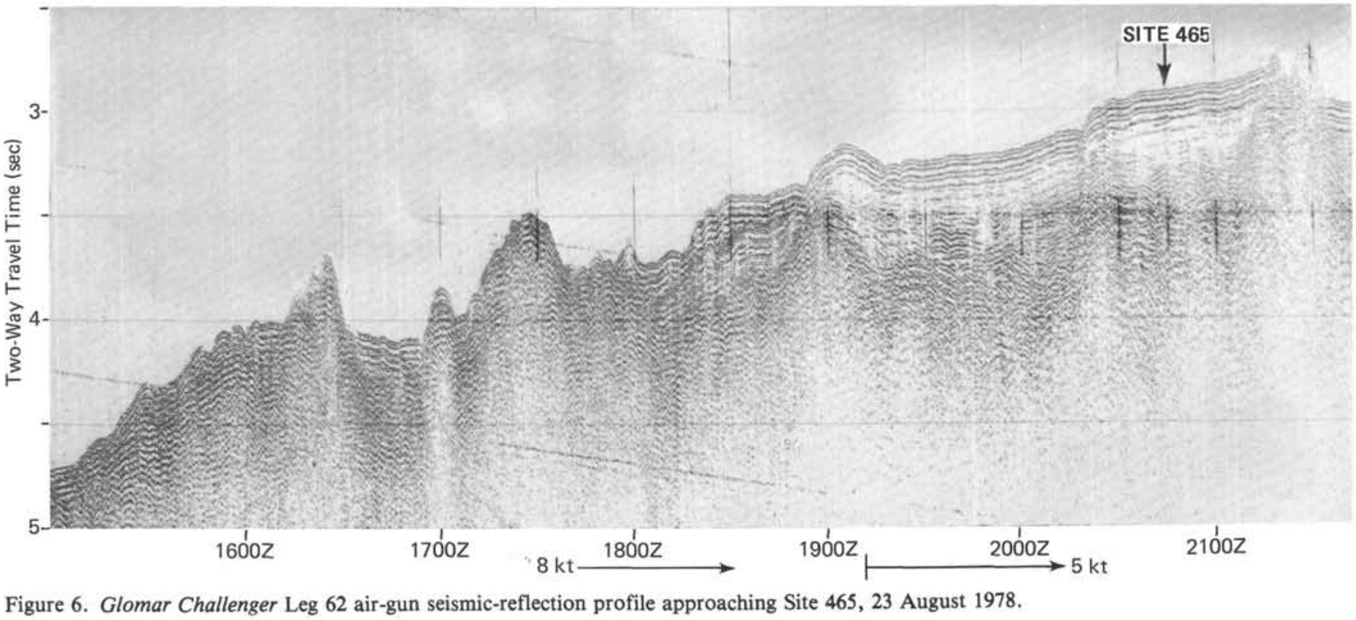

Figure 6. *Glomar Challenger* Leg 62 air-gun seismic-reflection profile approaching Site 465, 23 August 1978.

Table 1. Site 465 coring summary.

Core No.	Date (August 1978)	Time (L)	Depth From Drill Floor (m) Top Bottom	Depth Below Sea Floor (m) Top Bottom	Length Cored (m)	Length Recovered (m)	Percent Recovery
465-1	24	1915	2165.5-2166.5	0.0-1.0	1.0	0.89	89
2	24	1956	2166.5-2176.0	1.0-10.5	9.5	8.31	87.5
3	24	2036	2176.0-2185.5	10.5-20.0	9.5	5.98	62.9
4	24	2127	2185.5-2195.0	20.0-29.5	9.5	5.56	58.5
5	24	2218	2195.0-2204.5	29.5-39.0	9.5	8.57	90.2
6	24	2257	2204.5-2214.0	39.0-48.5	9.5	6.96	73.3
7	25	0011	2214.0-2223.5	48.5-58.0	9.5	0.07	0.8
8	25	0113	2223.5-2233.0	58.0-67.5	9.5	0.04	0.4
9	25	0205	2233.0-2242.5	67.5-77.0	9.5	0.06	0.7
10	25	0300	2242.5-2252.0	77.0-86.5	9.5	7.42	78.1
11	25	0535	2252.0-2261.5	86.5-96.0	9.5	0.03	3.2
465A-1	25	0934	2204.5-2214.0	39.0-48.5	9.5	1.5	15.8
2	25	1020	2214.0-2223.5	48.5-58.0	9.5	0.02	0.2
3	25	1106	2223.5-2233.0	58.0-67.5	9.5	8.27	87.0
4	25	1204	2233.0-2242.5	67.5-77.0	9.5	0.12	1.3
5	25	1250	2242.5-2252.0	77.0-86.3	9.5	0	0
6	25	1347	2252.0-2261.5	86.5-96.0	9.5	0.06	0.6
7	25	1655	2261.5-2271.0	96.0-105.5	9.5	0.80	8.4
8	25	1741	2271.0-2280.5	105.5-115.0	9.5	0.64	6.7
9	25	2032	2280.5-2290.0	115.0-124.5	9.5	8.03	84.5
10	25	2128	2290.0-2299.5	124.5-134.0	9.5	3.85	40.3
11	25	2215	2299.5-2309.0	134.0-143.5	9.5	6.33	66.6
12	25	2300	2309.0-2318.5	143.5-153.0	9.5	2.38	25.1
13	25	2348	2318.5-2328.0	153.0-162.5	9.5	0.3	3.2
14	26	0048	2328.0-2337.5	162.5-172.0	9.5	0.05	0.5
15	26	0342	2337.5-2347.0	172.0-181.5	9.5	4.53	47.7
16	26	0436	2347.0-2356.5	181.5-191.0	9.5	5.74	60.4
17	26	0532	2356.5-2366.0	191.0-200.5	9.5	2.38	25.1
18	26	0623	2366.0-2375.5	200.5-210.0	9.5	1.95	20.5
19	26	0715	2375.5-2385.0	210.0-219.5	9.5	2.72	28.6
20	26	0806	2385.0-2394.5	219.5-229.0	9.5	3.48	36.6
21	26	0855	2394.5-2404.0	229.0-238.5	9.5	2.30	24.2
22	26	0946	2404.0-2413.5	238.5-248.0	9.5	0.10	1.1
23	26	1038	2413.5-2423.0	248.0-257.5	9.5	0.15	1.6
24	26	1130	2423.0-2432.5	257.5-267.0	9.5	0.11	1.2
25	26	1246	2432.5-2442.0	267.0-276.5	9.5	0.06	0.6
26	26	1436	2442.0-2451.5	276.5-286.0	9.5	1.20	12.6
27	26	1620	2451.5-2461.0	286.0-295.5	9.5	2.54	27.1
28	26	1814	2461.0-2470.5	295.5-305.0	9.5	2.06	21.7
29	26	1949	2470.5-2480.0	305.0-314.5	9.5	2.38	25.1
30	26	2050	2480.0-2489.5	314.5-324.0	9.5	0.58	6.1
31	26	2205	2489.5-2499.0	324.0-333.5	9.5	0.35	3.7
32	26	2315	2499.0-2508.5	333.5-343.0	9.5	1.50	15.8
33	27	0031	2508.5-2518.0	343.0-352.5	9.5	2.99	31.5
34	27	0149	2518.0-2527.5	352.5-362.0	9.5	2.15	22.6
35	27	0336	2527.5-2537.0	362.0-271.5	9.5	0.59	6.2
36	27	0457	2537.0-2546.5	371.5-381.0	9.5	3.25	34.2
37	27	0626	2546.5-2556.0	381.0-390.5	9.5	2.38	25.1
38	27	0751	2556.0-2565.0	390.5-400.0	9.5	3.77	40.0
39	27	0916	2565.0-2575.0	400.0-409.5	9.5	2.42	25.5
40	27	1137	2575.0-2584.5	409.5-419.0	9.5	3.0	31.6
41	27	1346	2584.5-2594.0	419.0-428.5	9.5	3.07	32.3
42	27	1529	2594.0-2603.5	428.5-438.0	9.5	2.04	38.1
43	27	1658	2603.5-2613.0	438.0-447.5	9.5	2.04	21.4
44	27	1854	2613.0-2622.5	447.5-457.0	9.5	3.45	36.6
45	27	2250	2622.5-2632.0	457.0-466.5	9.5	6.0	63.2
46	28	0044	2632.0-2641.5	466.5-476.0	9.5	3.29	34.6

tive proportions of foraminifers and nannofossils. On the basis of smear-slide descriptions (Appendix A), foraminifers generally constitute less than 30% of the sediment, and nannofossils more than 50%. Therefore, most sediments in Unit I are classified as nannofossil ooze (foraminifers < 10%) or foraminifer nannofossil ooze (foraminifers 10–30%). Calcareous microfossils are very well preserved throughout Unit I. Clay mineralogy is given in Appendix B (see also Nagel and Schumann, this volume).

The only observed macrofossils were large fragments of *Inoceramus*, up to 3.5 cm in length and 1 cm thick, in Cores 9A and 13A.

Most of the sediment recovered from Unit I is soupy to stiff ooze; sediment firm enough and coherent enough to be called chalk is rare, and was encountered only in Cores 18A and 21A. Undoubtedly, the *in situ* abundance of chalk is much greater, but, because of high pump pressures required to core chert, much of the chalk was lost.

Chert was first encountered in the core catcher of Core 2, and is a common constituent throughout the unit. With few exceptions, the chert is medium to light gray in color (N4 to N7).

Pyrite occurs as black blebs up to 1 cm in diameter in Sections 3 and 4 of Core 3A. Smearing of black pyrite with white ooze during the drilling process imparted a gray color to the sediment in Section 3 of Core 3A. Pyrite also occurs in trace amounts throughout the section (Appendix A). Additional evidence for sulfate reduction within the sediments of Unit I was the odor of H_2S from all cores when first opened. Also, chert fragments from Unit I gave off a strong odor when cut.

Crystals and crystal aggregates of carbonate are common in the sediments throughout Unit I. Individual crystals occur as "needles" (~2–4 μm wide and 10–15 μm long), as subangular to subrounded, equant grains (~10–20 μm in diameter), and as a matrix of fine crystals (<1 μm).

The boundary between Units I and II is placed at the bottom of Core 25A. Unfortunately, Cores 24A and 25A recovered only chert, so that the actual contact between ooze (chalk?) of Unit I and limestone of Unit II was not observed. It is unlikely that any limestone of Unit II occurs above Core 26A (276 m sub-bottom), although some ooze (chalk?) of Unit I may have extended into Core 26A and may have been washed out by the high pump pressures that are required to cut the chert and limestone.

Unit II: Laminated Limestone (276–411.7 m)

The dominant lithology of Unit II is limestone, laminated on a scale of less than 1 mm, and colored various shades of olive-gray (mostly olive-gray, 5Y 5/2 and 5Y 4/2, with some dark olive-gray, 5Y 3/2, and light olive-gray, 5Y 6/2) (Fig. 7). The laminated limestone is pelagic and similar in general petrographic characteristics to the pelagic limestones of Lithologic Units II, III, and IV at Site 463, in that it consists of silicified radiolarians and foraminifers in a micritic matrix. The

Table 2. Lithologic units at Site 465.

Unit	Lithology	Cores	Sub-bottom Depth (m)	Thickness (m)	Age (m.y.)
I	Nannofossil ooze and foraminifer nannofossil ooze	1–11 1A–25A	0–276	276	Pleistocene to late Turonian (0–86 m.y.)
II	Laminated limestone	26A–40A	276–411.7	135.7	Early Cenomanian to late Albian (98–103 m.y.)
III	Trachyte	40A–46A	411.7–476.0	64.3	Late Albian or older (103+ m.y.)

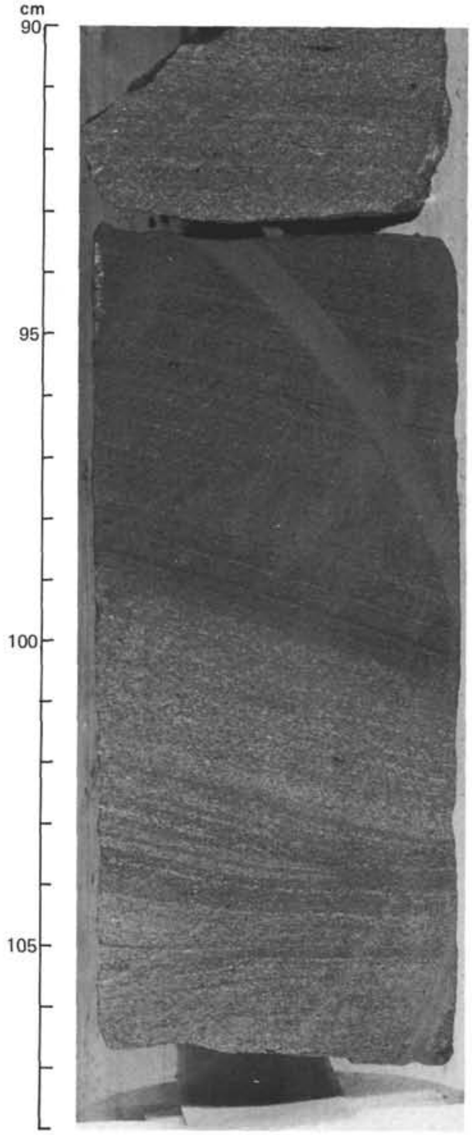

Figure 7. Core photograph of typical laminated olive-gray limestone of Unit II, but with laminae showing a change in dip, 465A-40-1, 90–108 cm.

main differences are the laminated appearance of the limestone at Site 465 and the much greater degree of silicification of the pelagic limestones at Site 463. The laminated appearance of the limestone at Site 465 is mainly the result of wispy, discontinuous, flaser-like laminae of dark (organic?) matter (Fig. 8A, B), differences in the degree of silicification (Fig. 8C), and concentrations of radiolarians and foraminifers into layers (Fig. 8D). The discontinuous laminae are distorted around radiolarians and foraminifers, giving the laminae a lens-shaped or "birds-eye" appearance in thin section (Fig. 8B). The internal structure of radiolarians and walls of foraminifers mostly has been destroyed by silicification, but these features are preserved in some samples.

Thin beds of gray (mostly N4 with some beds of N5 and N6), finely-crystalline limestone commonly occur interbedded with olive-gray limestone throughout the unit. They usually are less than 2 cm thick (Fig. 9), with a maximum thickness of 22 cm in Core 29A, Section 1, 76–98 cm. About 5% of the rocks recovered from Unit II are gray limestone, with a maximum of 30% in Core 29A. The massive gray limestone beds mostly consist of micrite that has been silicified more than the laminated limestone (Fig. 9). The laminated limestone generally contains less than 5% SiO_2, whereas the gray limestone beds generally contain more than 15% SiO_2 (see Dean, this volume). The contact between a gray limestone bed and an underlying laminated olive-gray limestone bed is always sharp. The upper contact of a gray limestone bed is usually gradational with the overlying olive-gray limestone, but may be sharp, and commonly exhibits evidence of scour and erosion (Fig. 10).

The dip of laminae in the olive-gray limestone beds appears to increase with depth in the hole, deviating from the horizontal by as much as 15°. Some of this dip change may be only apparent, caused by deviation of the hole from vertical (an inclination test during collection of Core 40 showed a 4° deviation from vertical), but most dip is real. Dips of laminae within any one piece of limestone are usually the same, although changes in dip of laminae of about 10° within a single piece were observed (Fig. 7). Graded bedding was observed only at the top of Unit II. Truncation of ripple(?) lamination by overlying horizontal laminae also was observed in several places within Unit II.

Chert is a common and persistent minor lithology throughout Unit II. The color of the chert varies only slightly and is mostly black (N1 and N2). The chert of Unit II, like the chert of Unit I, gave off a strong sulfur odor when cut. At several places within Unit II, chert encloses a thin bed of what appears to be typical laminated olive-gray limestone; however, thin-sections reveal that the chert has preserved the laminated fabric of the original radiolarian- and organic-carbon-rich sediment, and that the limestone in the center of the chert also has been silicified (Fig. 11). Radiolarians apparently were a common constituent of the original sediment throughout Unit II, but they almost all have been replaced by $CaCO_3$ (Fig. 8B, C). As a result, very few recognizable radiolarians were recovered from Unit II. Veins filled with coarsely crystalline calcite and quartz were observed at a number of places cutting across beds of laminated olive-gray limestone.

The base of Unit II from 110 cm in Section 1, Core 40A, to the top of the trachyte (Unit III) at 65 cm in Section 2, Core 40A, exhibits considerable lithologic variation. The first of several beds of massive clastic limestone was observed from 110 to 115 cm in Section 1, Core 40A. Many of the clasts in the clastic limestone beds are of altered trachyte. The beds of clastic limestone are usually intercalated between beds of olive-gray limestone with abundant organic-carbon-rich laminae.

Volcanic ash was first observed from 143 to 148 cm in Section 1, Core 40A, where it is intercalated with olive-gray limestone, dolomite, organic-rich layers, and pyrite. Beds and laminae of water-laid ash are common in Section 2, Core 40A (Fig. 12). The trachyte of Unit III is overlain immediately by a bed of horizontal and cross

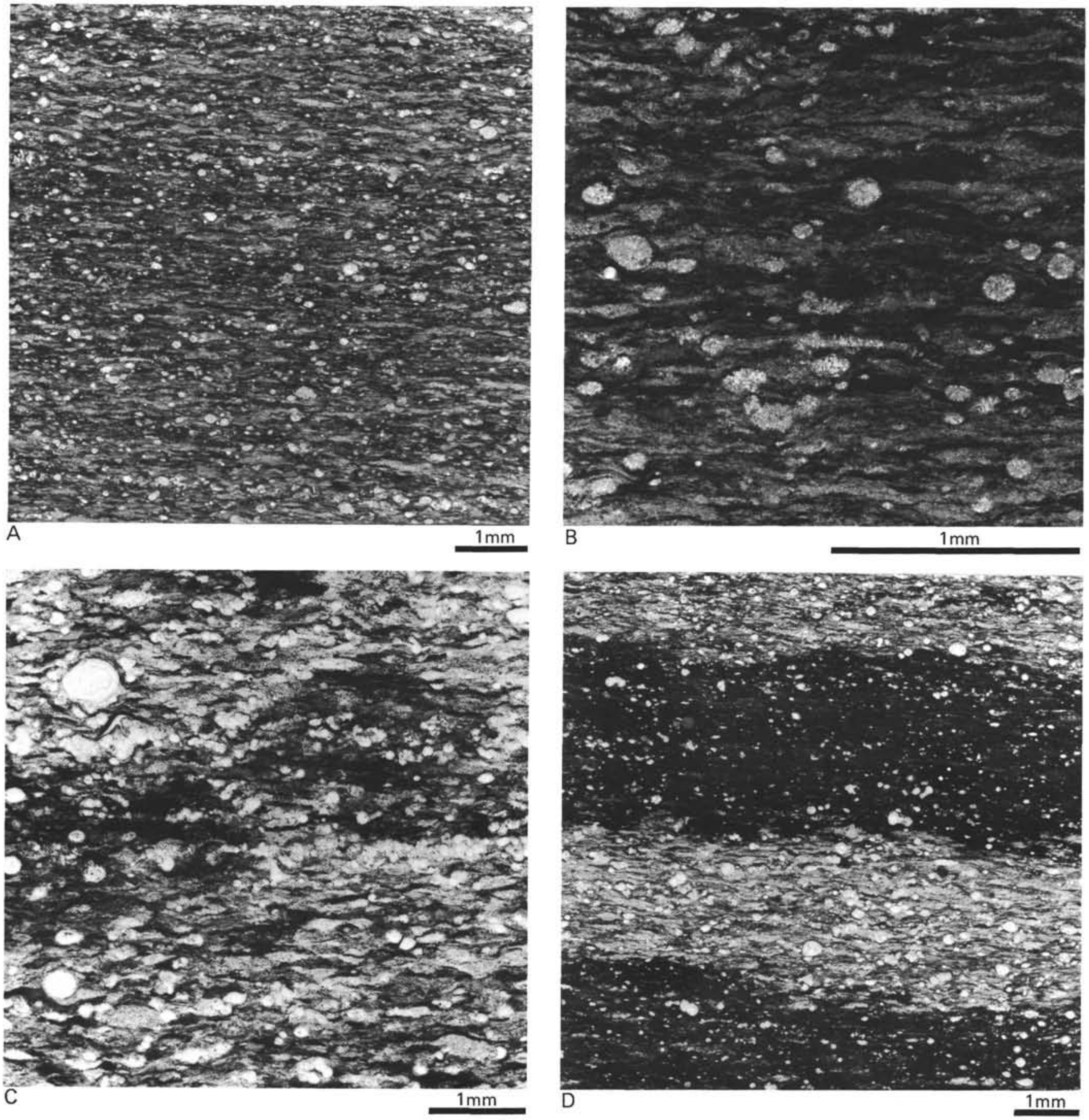

Figure 8. Photomicrographs of the laminated olive-gray limestone of Unit II. All bar scales equal 1 mm. A. 465A-28-2, 53 cm; cross-polarized light; typical laminated limestone. B. 465A-28-2, 53 cm; cross-polarized light; enlargement of Figure 8A, showing partly to completely replaced radiolarians and foraminifers, with discontinuous laminae of dark organic material which is distorted, giving a lens-shaped or "bird's-eye" appearance to the laminae. C. 465A-37-1, 134 cm; plane light; laminated gray limestone, illustrating the concentration of radiolarians and foraminifers into layers. D. 465A-28-2, 53 cm; cross-polarized light; darker silicified layers of olive-gray limestones and lighter layers of limestone only partly replaced by silica.

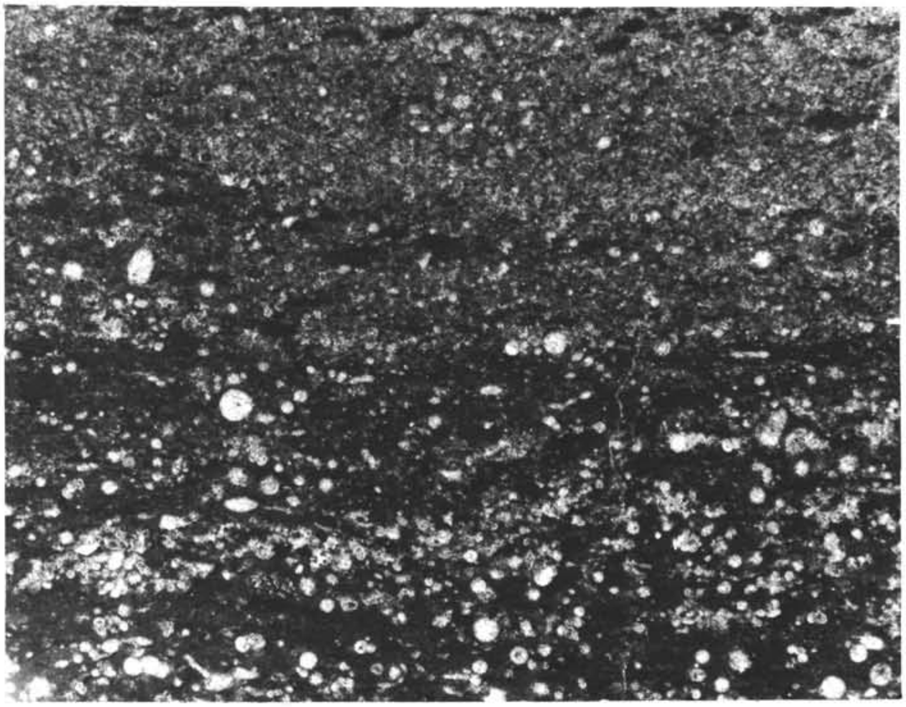

Figure 9. 465A-37-1, 126 cm. Contact between laminated olive-gray limestone (bottom) and massive gray limestone (top).

laminated ash (Fig. 13). Between 17 and 34 cm in Section 2, Core 40A, is a bed of clastic dolomite containing veins of large (~ 1 cm long), bladed crystals of dolomite and large (up to 5 mm) crystal aggregates of pyrite.

Unit III: Trachyte (411.7–476 m)

The trachyte (see additional information in the next section of this chapter) at the top of Unit III is brecciated. The fragments of trachyte are held together by a cement of calcite, dolomite, and barite. The trachyte fragments in the breccia near the top of Unit III are fairly well rounded and are usually "floating" in calcite, dolomite, and barite cement. With depth, the trachyte fragments become more angular. The amount of cement decreases with depth until the cement is simply vein-filling in fractures in the trachyte. At a depth of about 429 meters sub-bottom, obvious trachyte breccia ends and vesicular trachyte typical of Unit III begins.

Discussion

The sediments and rocks recovered at Site 465 contain an incomplete record of carbonate sedimentation on top of trachyte that apparently forms the volcanic base of southern Hess Rise. Missing from the record are sediments of early Cenomanian to middle Turonian age, late Coniacian age, and early Campanian age.

The basement at Site 465 consists of trachyte flows that apparently crystallized under relatively low hydrostatic pressure (<200 m). The first ash beds above the trachyte are water-laid, with cross-lamination suggesting deposition by lateral current flow (Fig. 12). Deposition of abundant organic matter and carbonate along with ash is first recorded in the sediments from 0 to 4 cm in Section 2, Core 40A. Graded beds of clastic limestone with abundant organic matter occur in Core 40A, Section 1, 116–135 cm. The dominant clasts in the clastic limestone beds are of altered trachyte, and large mollusk fragments are common. We interpret these beds to represent unit A of a theoretical Bouma turbidite sequence; they probably are more-proximal (landward) portions of turbidites. These few bits of evidence—shallow-water or subaerial cooling of the trachyte, current deposition of the ash, high content of organic matter, and graded clastic limestones with clasts of trachyte and abundant mollusk debris—suggest that the first sediments deposited on volcanic basement at Site 465 during the late Albian time were deposited in relatively shallow water (on the order of several hundreds of meters or less). Shipboard data on benthic foraminifers suggest slope water depths in the Albian, deepening to upper bathyal by early Cenomanian.

Sometime after (and perhaps during) the deposition of the first meter of sediment, the sediments were subjected to mineralization. The main manifestations of this mineralization are (1) the abundance of pyrite as disseminated crystals, crystalline masses, thin beds, laminae, lenses, and stringers, (Fig. 14); and (2) the abundance of dolomite as large crystal aggregates and as rhombs replacing the limestone matrix and most of the constituent particles. Typical laminated olive-gray limestone of Unit II begins at about 105-cm in Section 1, Core 40A.

We believe that the most likely mechanism for deposition of the typical laminated limestone of Unit II is turbidity currents. The main types of lamination are concentrations of radiolarians and flaser lamination of

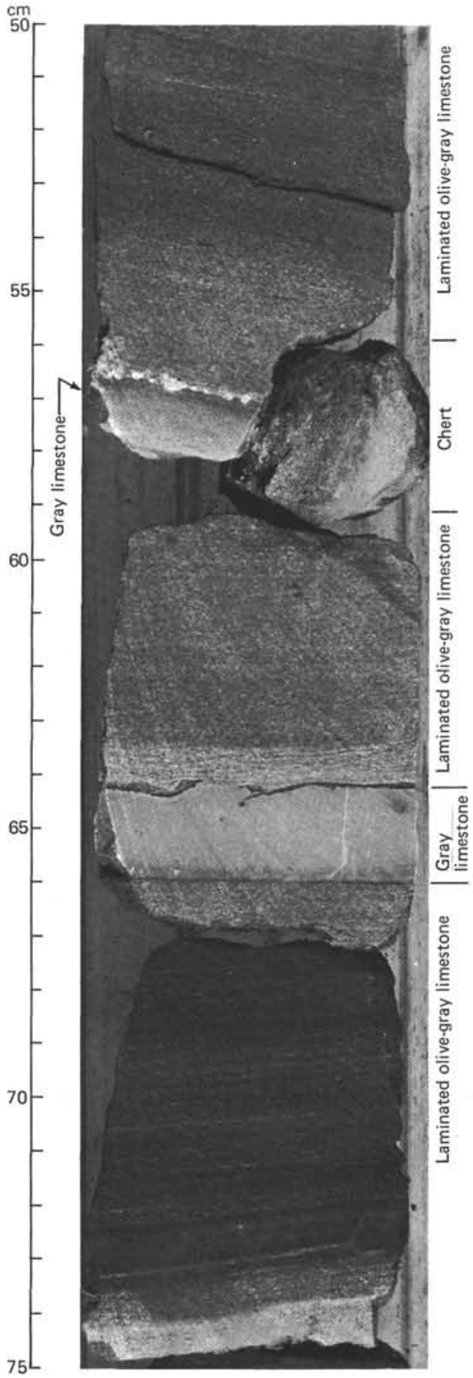

Figure 10. Gray limestone and laminated olive-gray limestone interbeds in Unit II, 465A-36-2, 50–75 cm. A chert fragment occurs at 56 to 60 cm.

dark organic material in a micritic calcite matrix. The laminae would be equivalent to upper parallel lamination (unit D) and(or) interturbidites (unit E) of a theoretical Bouma turbidite sequence, interpreted as representing deposition by low-density turbidity currents mixed with pelagic sediments. We conclude that laminated limestone of Unit II represents turbidites that originated up-slope on Mellish Bank. Because of recrystallization, we have no way of knowing how much of the $CaCO_3$ was contributed as pelagic rain and how much was brought in by turbidity currents. However, the abundance of organic material reorganized into flaser laminae, together with redeposited mollusk fragments and shelf benthic foraminifers, suggests downslope movement. The reworking of radiolarians into laminae (Fig. 7) is further evidence of current reworking of pelagic components. The relatively high linear sedimentation rate of the laminated limestone (48 m/m.y.) also supports transport of additional sediment to Site 465 by turbidity currents.

Interpretation of the finely crystalline gray limestones intercalated with laminated olive-gray limestone is a greater problem. These limestone interbeds generally consist of very fine (< 1 μm) calcite crystals, and exhibit only faint hints of bedding or lamination. They are more silicified than beds of olive-gray limestones. We have discounted the possibility that the fine-grained limestone represents the pelagic component that follows a theoretical Bouma sequence, because if this were the case we would expect the fine-grained limestone to have a gradational and possibly bioturbated lower contact with the underlying laminated limestone, and a sharp erosional upper contact with the overlying laminated limestone. Usually, however, the opposite is observed: the lower contact is sharp and the upper contact is either gradational or sharp (Fig. 9). That the lower contact of the beds of fine-grained gray limestone are sharp and often scoured suggests lateral implacement by currents. One possibility is that the gray limestone was derived from a different, finer-grained source than the olive-gray limestone.

A lacuna (early Cenomanian to Santonian), occurs between the limestone of Unit II and nannofossil ooze of Unit I. This is a relatively short hiatus, considering the marked differences in degree of diagenesis and composition between the olive-gray laminated limestone of Unit II and the stark-white, almost structureless nannofossil ooze of Unit I. Unfortunately, the nature of the unconformity between Unit I and Unit II is not known even approximately, because the bottom two cores of Unit II recovered only fragments of chert. However, it is unlikely that the ooze (chalk?), undoubtedly interbedded with chert at depths of 258 to 276 meters subbottom, is much more lithified than the ooze recovered above 258 meters; otherwise, some of the more-lithified sediments would have been recovered. Furthermore, the marked difference in degree of lithification between Units I and II suggests that a considerable amount of material was eroded.

Unit I is a record of normal pelagic carbonate deposition that lasted 80 m.y. in waters that probably were never deeper than at present and that were always above the CCD. This carbonate record is interrupted by two significant lacunas representing an unknown portion of the early Cenomanian to Santonian and Santonian to late Campanian. In addition, there is a major lacuna between the late Paleocene and early Pliocene. Linear sedimentation rates for sediments in Unit I range from 3 to 40 m/m.y. (late Campanian to early Maastrichtian), but most are <10 m/m.y. and are low to normal for

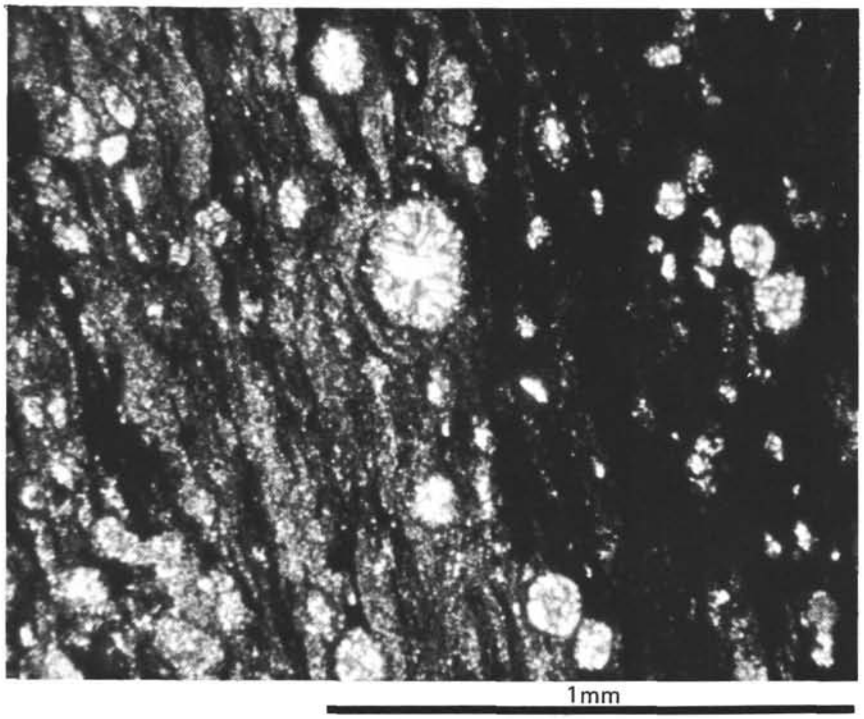

Figure 11. Photomicrograph of contact between chert (right) and silicified limestone in Unit II. Both lithologies contain recrystallized radiolarians and flaser laminations of dark organic matter. Sample 465A-28-2, 53–55 cm (cross-polarized light).

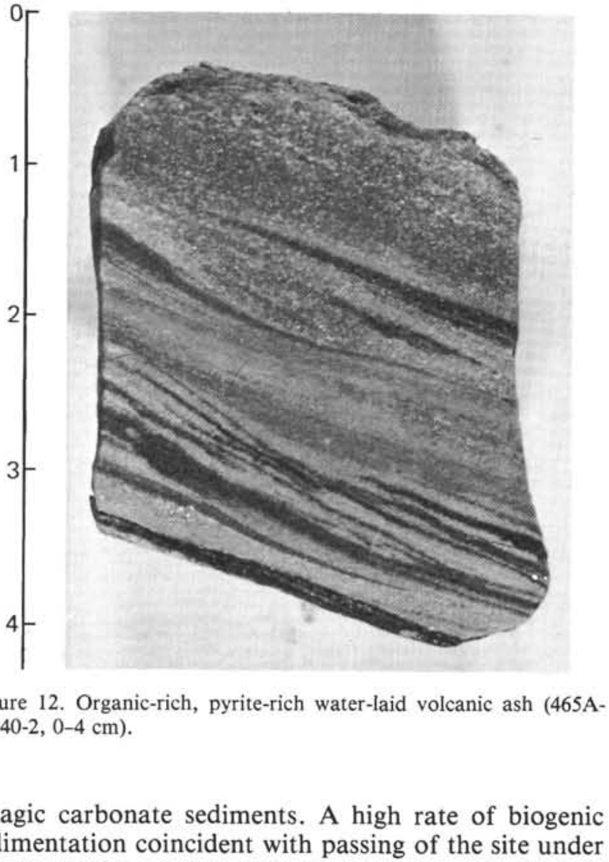

Figure 12. Organic-rich, pyrite-rich water-laid volcanic ash (465A-40-2, 0–4 cm).

pelagic carbonate sediments. A high rate of biogenic sedimentation coincident with passing of the site under the equatorial zone of high productivity apparently is not represented in the sediments recovered at Site 465. Backtracking of the site using the plate-rotation model of Lancelot and Larson (1975) and Lancelot (1978) places the time of equatorial crossing of Site 465 at approximately 90 m.y. ago, during the Turonian. As discussed above, the difference in degree of lithification between Units I and II suggests that a large amount of sediment above the limestones of Unit II was eroded. This sediment, now represented by a lacuna, would have been early Cenomanian to Santonian in age and probably would have been thick as a result of the increased sedimentation rate under the equatorial high-productivity zone. Assuming a linear sedimentation rate of about 48 m/m.y. over a period of about 12 m.y., as much as 600 meters of sediment may have been present and later eroded. Thus, we have two independent lines of evidence that a considerable amount of sediment may have been eroded between early Cenomanian and late Coniacian time.

About 270 meters of remarkably uniform pelagic carbonate ooze were deposited at Site 465 between late Coniacian and late Paleocene time, with only small lacunas within that time (see biostratigraphy section, this chapter). After about 55 m.y. of non-deposition, and possibly some periods of erosion (late Paleocene to Pliocene), the last events recorded at Site 465 is the deposition of a little over 2 meters of nannofossil ooze and foraminifer nannofossil ooze of Plio–Pleistocene age.

IGNEOUS ROCKS

Introduction

Igneous rock representing acoustic basement was recovered between 411.7 and 476.0 meters in Hole 465A. Recovery of these igneous rocks averaged 37.1% (23.9

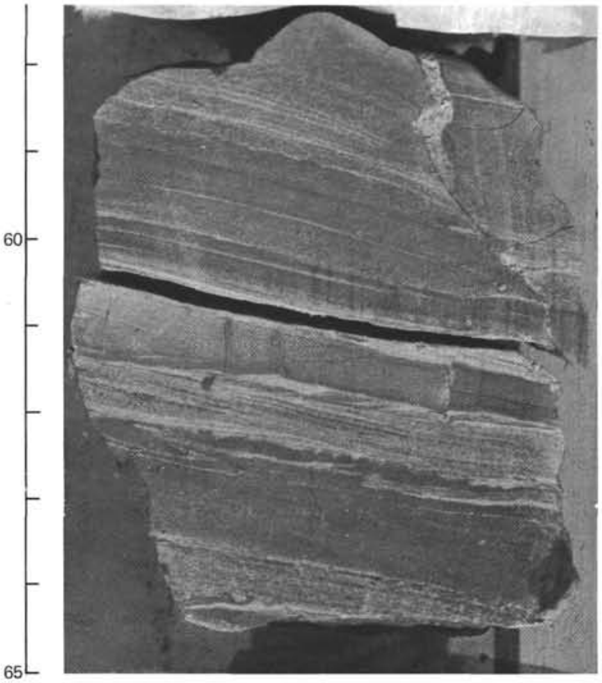

Figure 13. Horizontal and cross-laminated volcanic ash in Unit II, directly above trachyte (465A-40-2, 57–65 cm).

out of 64.3 meters drilled). The upper portion, from 411.7 to 429.0 meters, is breccia composed of bluish-gray fragments cemented largely by calcite. Below the breccia, from 429.0 meters to the bottom of the hole at 476.0 meters, the cores consist of highly altered, dominantly fine-grained, vesicular trachyte with feldspar microphenocrysts. The abundant feldspar is surrounded by altered glass and shows varying degrees of flow alignment. Many of the rocks exhibit trachytic texture, although flow orientation ranges from virtually none to highly aligned. Abundant smectite and random mixed-layer clay in all trachyte appears to be derived from alteration of glass and some feldspar. Pyrite decreases with depth; it occurs as disseminated crystals and as fine veins in the trachyte. Numerous clots of greenish-brown clay were observed in thin section; these may represent altered mineral grains (perhaps pyroxene), or simply aggregates of clay. No fresh mafic minerals were observed.

Lithology

The trachytes are divided into 30 layers that can be grouped roughly into five units (Fig. 15). Some layers display central regions with relatively coarse crystal size and low abundance of vesicles; these regions grade both up and down into regions with finer crystal sizes and higher abundances of vesicles; these are termed flow layers in this report. The remaining layers do not show this kind of variation and are merely designated as layers. Layers are characteristically fine grained and highly vesicular throughout. Because recovery averages 37.1%, only an estimate of the minimum number of layers penetrated is possible. Also, because no continuous core was taken across an entire flow layer, layers listed as flows are probably parts of several different flow layers. It does seem likely, however, that the dominance of fine-grained vesicular trachyte indicates that the section consists dominantly of thin flows.

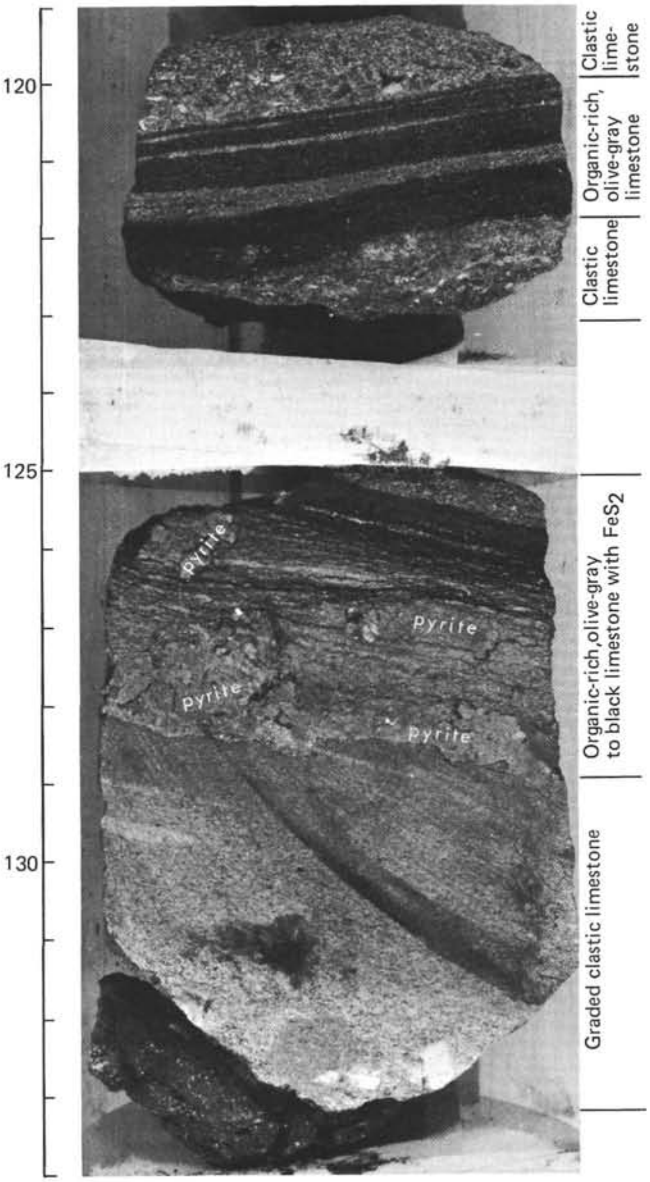

Figure 14. Graded clastic limestone and organic-carbon-rich olive-gray limestone, with pyrite as disseminated crystals, thin beds, and lenses. Sample 465A-40-1, 119–134 cm.

Unit 1: Brecciated Trachyte

This unit extends from 411.7 to 429.0 meters and includes brecciated and fractured trachyte in layers 1 through 5. Individual fragments are blue-gray, grading downward to gray, and may be either massive or layered. The layering is sometimes highly contorted. All groundmass is highly altered to smectite. The dominant cement holding fragments together is calcite covered with a greenish coating, although a barite vein occurs in one fragment. Pyrite is a common accessory mineral in both cement and trachyte. Clasts range from angular to well rounded, the degree of angularity increasing downward. The angular shape of most fragments indicates very little transport, and suggests that brecciation may have been caused by explosive release of trapped volcanic gases.

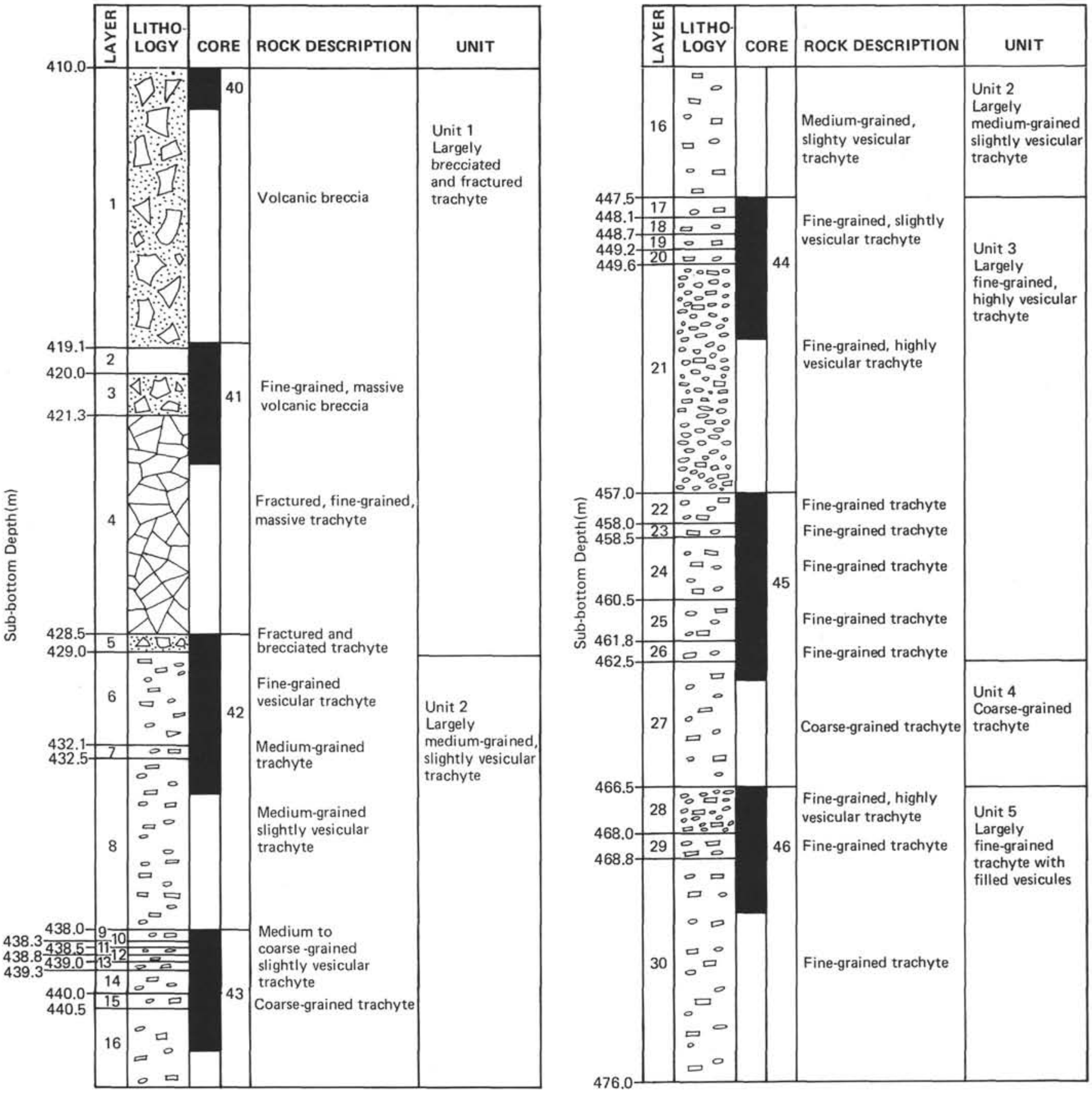

Figure 15. Major units and layers in trachyte from Hole 465A.

Unit 2: Medium-Grained Vesicular Trachyte

This unit extends from 429.0 to 447.5 meters and includes layers 6 to 16. Layer 6 is fine-grained, but layers 7 through 14 and layer 16 are medium-grained, and layer 15 is coarse-grained. The trachyte is light gray and vesicular, the abundant feldspar microphenocrysts showing varying degrees of flow layering. Pyrite occurs both as disseminated crystals and as thin veins. Layers 7 through 16 have the characteristics attributed to flows: increasing vesicularity and decreasing crystal size away from a central region with few or no vesicles and coarser crystal size. Layer 6 does not show these characteristics and cannot be interpreted as a flow on the available evidence. Vesicle size is generally less than or near 1 mm, but some vesicles reach 5 mm. Many vesicles are filled with a lining of smectite and a center of calcite.

Unit 3: Fine-Grained, Highly Vesicular Trachyte

Unit 3 extends from 447.5 to 462.5 meters and includes layers 17 through 26. These trachytes are dominantly light gray, fine grained, and vesicular to highly vesicular. The abundant lath-shaped feldspar microphenocrysts and microlites frequently show well-developed trachytic texture. Pyrite occurs as finely disseminated crystals and veins. The vast majority of vesicles are 1 mm or less in diameter, although they range up to about 5 mm, indicating a shallow-water or possibly a subaerial origin. Some vesicles are flattened perpendicular to the length of the core. Layers 17 through 20, and layers 22, 23, 25, and 26 have the characteristics of flows (vesicle abundance and mineral-size variations). Units 21 and 24 represent regions of fine-grained, highly vesicular trachyte that do not show the variations expected of flows. A reddish color was noted in some cores.

Unit 4: Coarse-Grained Trachyte

Unit 4 includes only layer 27; it extends from 462.5 to 466.5 meters, but there was little recovery in this region. As usual, the trachyte is highly altered to soft smectite and random mixed-layer clays; it is light gray in color. Oriented feldspar microphenocrysts are present. Layer 27 appears to be a flow and has a significantly coarser crystal size than do adjacent layers; consequently, it has been designated as a separate unit.

Unit 5: Fine-Grained, Amygdaloidal Trachyte

Unit 5 extends from 466.5 meters to the bottom of the hole at 476.0 meters; it includes layers 28 through 30. Layer 29 has the characteristics of a flow, but layers 28 and 30 do not. This light-gray trachyte is highly altered and contains abundant flow-oriented feldspar microphenocrysts and microlites. Occasionally an unidentified bright-green mineral (smectite?) is observed, and small amounts of pyrite are disseminated throughout the trachyte. Most vesicles are filled with either a green smectite or white carbonate material, although some pieces of trachyte have little or no vesicle filling. Vesicle size remains the same as in overlying trachyte, being generally near or less than 1 mm, but ranging up to approximately 5 mm.

Petrography

Petrographic studies of igneous rocks from Hole 465A reveal a dominant trachytic texture throughout the cored section. Pervasive alteration has affected all of the rock; the original glass and whatever mafic materials may have been present are altered to brown or greenish-brown smectite and random mixed-layer clay. Alteration of feldspar has also occurred, but to a much smaller degree than alteration of glass.

All studied rocks contain at least one microphenocryst phase. The original phenocryst assemblage consisted of feldspar, and perhaps a mafic mineral; feldspar is by far the dominant phase, accounting for 4 to 8% of the total rock. Feldspar phenocrysts occur in two distinct sizes: large (0.5–1.0 mm), euhedral to rhombic crystals, and smaller (0.04–0.3 mm) laths. The smaller crystals are rarely zoned, but commonly show skeletal growth.

The groundmasses of all studied samples consist of altered glass and feldspar microlites which are usually potash feldspar (Lee-Wong, this volume). Glass was the dominant phase, accounting for 60 to 75% of the rocks. The feldspar microlites range in volume from 12 to 30% of the rock.

All samples can be described as having trachytic texture, with varying degrees of flow layering of lath-shaped feldspar microphenocrysts. Three are vesicular, with 2 to 9% irregularly shaped vesicles. Most vesicles are empty, but some are lined with smectite and filled with calcite. Feldspar microlites commonly are concentrated around vesicle walls.

Chemistry

Despite the extensive alteration of these rocks, it is possible to determine chemically that they are trachytes (Seifert et al., this volume). The major-element chemistry shows a considerable range for several oxides—such as K_2O and MgO—as well as considerable addition of H_2O and oxidation. Variations in SiO_2, K_2O, and MgO correlate well with H_2O, indicating that these variations are the result of alteration. Nevertheless, the least-altered sample, with the lowest H_2O content, has the composition of trachyte and is comparable to trachytes from other oceanic regions.

The average percentage values for the trachytes are as follows (compared to the freshest sample, 465A-43-2, 65–68 cm, values of which are in parentheses): SiO_2, 59.50 (60.81); TiO_2, 1.02 (1.02); Al_2O_3, 18.73 (18.80); Fe_2O_3, 2.98 (1.98); FeO, 0.67 (0.26); MnO, 0.034 (0.02); MgO, 1.00 (0.31); CaO, 2.44 (1.94); Na_2O, 5.10 (5.32); K_2O, 4.88 (6.27); P_2O_5, 0.36 (0.35); H_2O^+, 2.23 (0.86); H_2O^-, 2.23 (0.64); CO_2, 0.60 (0.59) (see Seifert et al., this volume).

In general, trace elements do not appear to be affected by the alteration, and the rare-earth patterns are very consistent, with strong LREE to HREE enrichment and no significant Eu anomalies. The most interesting feature of alteration in these rocks is the rough correlation between Lu and H_2O content; this has not been observed before, to the authors' knowledge.

Average values (ppm) for trace-element concentrations, compared to the least-altered sample (in parentheses), are: Zr, 715 (475); Sr, 308 (256); Ba, 631 (656); Co, 16.6 (19.3); Th, 10.6 (10.2); Hf, 16.9 (15.0); Ta, 9.53 (9.38); Rb, 35.6 (34.3); Sc, 3.06 (2.85); Ce, 170 (167); La, 82.2 (89.1); Sm, 10.5 (9.32); Eu, 3.01 (2.98); and Yb, 2.97 (2.24). Cr and Ni have concentrations of less than 10 ppm in all samples.

Summary

Petrographic, X-ray-diffraction, and chemical studies reveal that the igneous rocks recovered from Hole 465A are altered trachytes. All of the original groundmass phases, and some feldspar laths, have been completely altered to one or more smectite minerals and random mixed-layer clays; secondary carbonate minerals are also present in these rocks. Vesicle fillings are complex, with a rim of smectite and a central filling of calcite and perhaps other minerals.

Chemical variations in these rocks correlate with H_2O content, indicating that the variations result from alteration, not differentiation. Nevertheless, the least-altered sample is chemically similar to trachytes from many oceanic islands. Judging from this, and the trachytic texture, we interpret these rocks as trachytes which probably represent late stage differentiates of alkalic basalt magma.

The abundance and size of vesicles, and the red oxide staining and lack of any glassy flow margins, indicate shallow subaqueous or subaerial volcanism. This implies that at least parts of Hess Rise were near or above sea level prior to late Albian time.

INTERSTITIAL-WATER GEOCHEMISTRY

Results of shipboard measurements of *p*H, alkalinity, salinity, calcium, magnesium, and chlorinity in interstitial water from six whole-core sediment samples are presented in Figure 16. The surprising feature of these profiles is that none exhibit significant variation with depth within the 235 meters of nannofossil ooze. There is a slight tendency for calcium to increase with depth (from 10.6 to 13.6 m*M*/l), and for magnesium to decrease with depth (from 54.0 to 49.6 m*M*/l). An increase in calcium concentration in interstitial waters is commonly observed in carbonate-rich deep-sea sediments, and this is usually matched by a 1:1 molar decrease in concentration of magnesium (see interstitial-water geochemistry for Site 463, this volume).

This marked inverse relationship between calcium and magnesium concentrations is usually explained by dissolution of $CaCO_3$ and formation of dolomite at depth. The lack of any trends at Site 465 implies that little if any dolomite is forming within the upper 235 meters of sediment, and that either no dissolution of $CaCO_3$ is occurring, or dissolution and reprecipitation are occurring at about equal rates. That nannofossils and foraminifers are moderately well-preserved, and that recrystallized carbonate was commonly observed in smear slides (Appendix A), suggests that both dissolution and reprecipitation indeed are occurring. However, the lack of significant variation in calcium concentration with depth (Fig. 16) suggests that the rate of carbonate dissolution is about matched by the rate of carbonate precipitation.

PHYSICAL PROPERTIES

Wet-Bulk Density and Sound Velocity

For unconsolidated sediments of nannofossil ooze and foraminifer nannofossil ooze (Cores 1-10 and 3A-21A), wet-bulk density was measured by analog GRAPE method, and sound-velocity measurement was made occasionally on the sample embedded in the liner tube (Fig. 17). For limestone in Cores 26A to 46A, wet-bulk density was measured at a few points per section for whole core-size specimens by using the 2-minute GRAPE method, before the sample was split.

Minicore samples were taken one or two per section for Cores 26A to 46A, and 2-minute GRAPE and gravimetric wet-bulk density and sound velocities in horizontal and vertical directions were measured. All of the measured values of sound velocity, wet-bulk density, porosity, water content, and thermal conductivity at room temperature are shown in Appendix C.

The section recovered at Site 465 has been divided into three major and two minor acoustic units. The major acoustic units correspond well to the lithologic units. The values of wet-bulk density and interval velocity are averaged for each acoustic unit and listed in Table 3.

The least-squares fits to the minicore data of wet-bulk density and velocity in Unit II show decrease of values with sub-bottom depth (-0.53 g/cm^3/100 m for density, and -2.09 km/s/100 m for velocity), although we cannot specify the cause of this decrease.

Thermal Conductivity and Sub-bottom Temperature

To estimate the terrestrial heat flow at Site 465, thermal conductivity of recovered samples and four down-hole temperature measurements were made. Thermal conductivity was measured for each core by using QTM (Quick Thermal Conductivity Meter, Showa Denko Co., Ltd.). Down-hole temperatures, calculated by the Tokyo T-probe technique (Uyeda and Horai, 1979; Yokota et al., 1979), are 6.5 ± 0.3°C at 86.5 meters sub-bottom depth in Hole 465, and 10.0°C at 172 meters in Hole 456A. The average value of the *in situ* thermal conductivity of sediments is 3.32 mcal/cm•s•°C, and the heat flow value of 1.36 HFU is obtained by the method discussed in detail by Fujii (this volume).

PALEOMAGNETISM

Twenty-six samples of upper Albian limestone and 26 trachyte samples were taken for paleomagnetic measurements (Sayre, this volume). Although most samples carry stable components of magnetization, it is not possible to construct an unambiguous reversal stratigraphy, because magnetic inclinations in both the limestone and trachyte are very low. Variations in susceptibility, the intensity of natural remanence, and Curie temperature indicate that trachyte Units 1 and 2 are highly oxidized and probably have acquired a secondary chemical remanence. In addition, low-titanium titanomagnetites and(or) large magnetic-grain sizes may characterize the center of Unit 3. A paleolatitude estimate indicates that the site was close to the equator during formation of the trachytes.

CORRELATION OF SEISMIC-REFLECTION PROFILES AND DRILLING RESULTS

Three major lithologic units at Site 465 correspond to the acoustic units. The top unit consists of nannofossil ooze and is 276 meters (0–276 m) thick. The second unit is limestone, 136 meters (276–411.7 m) thick, and the third is trachyte, encountered at a depth of 411.7 meters. Two major reflectors are apparent on the air-gun seismic-reflection profile (Fig. 18). One is at 0.36 seconds two-way time, and the other is at 0.47 seconds. These reflectors mark the boundaries between lithologic units. Reflectors near the top of Unit I probably correspond to acoustic interference caused by the air-gun bubble pulse, but the remaining faint reflectors in that unit are chert layers. The interval velocity (V_p) calculated for Unit I is about 1.53 km/s, whereas that calculated for Unit II is about 2.45 km/s. Velocities measured on small samples in the shipboard laboratory are an

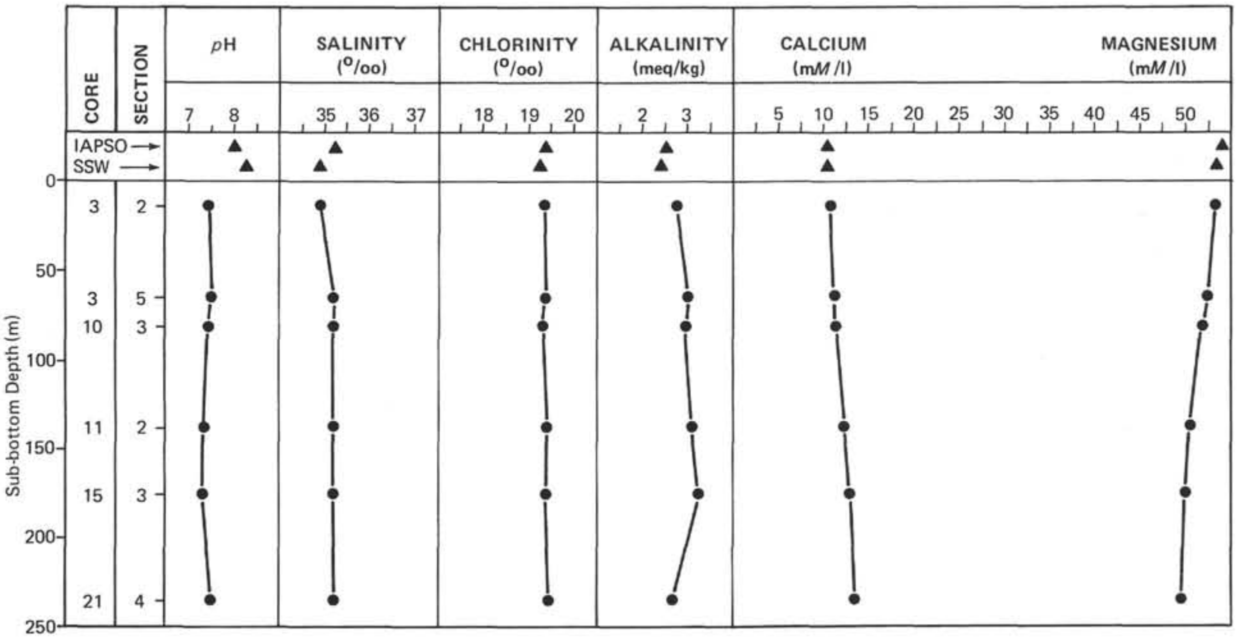

Figure 16. Interstitial-water geochemistry, Site 465.

average of 1.58 km/s for Unit I (range 1.55–1.63 km/s), an average of 2.89 km/s for Unit II (range 1.88–4.40 km/s), and 3.60 km/s for the trachyte. These values agree well with those that were calculated from the acoustic profile.

BIOSTRATIGRAPHY

Biostratigraphic Summary

Sediments of Pleistocene to late Albian age were recovered from two holes at Site 465 on Hess Rise. Most samples contained planktonic foraminifers and nannofossils; benthic foraminifers occurred throughout the section to the upper Albian, but were absent from the last four cores of the hole. Radiolarians occurred infrequently in the Cretaceous, in one sample from the Santonian, and in discrete layers in the Albian limestone.

A summary of the biostratigraphy of this site, based primarily on nannofossils and planktonic foraminifers, is shown in Figure 19.

Pliocene and Pleistocene sediments were recovered in Cores 1 to 2, 0 to 10.5-meters in Hole 465. The lower Pleistocene and Pliocene down to the middle lower Pliocene are present. Rare diatoms occur in Section 1-1 and belong to the *P. doliolus* Zone of the Quaternary. Below the lower Pliocene sediments there is a mixed interval (Section 2-3, 46 cm to 2-6, 45 cm) containing lower Eocene, upper Paleocene, and lower Pliocene materials mixed into upper Pliocene sediments. Foraminifers are very badly dissolved throughout the Pleistocene–Pliocene section.

The Paleogene section contains only Paleocene sediments (465-2,CC to 8,CC, 10.5 to 67.5 m; and 465A-1,CC to 3-3, 144 cm, 39 to 62.4 m). The Paleocene section includes all zones. The equivalent of the type Danian is about 11 meters in length (465A, Core 3) and the basal Tertiary "*Globigerina*" *eugubina* Zone occurs from 465A-3-3, 40 cm to 3-3, 144 cm. This is the thickest "*G.*" *eugubina* Zone yet recorded from DSDP cores. Paleocene nannofossils and foraminifers are very well preserved.

Cretaceous sediments were cored at 465-8 to 11,CC and 465A-3-3, 146 cm to 40-1, 138 cm (39–411 m). This section includes sediments of the Maastrichtian, upper Campanian, Santonian, lower Cenomanian, and upper Albian. The Cretaceous/Tertiary boundary was recovered and is considered nearly continuous. Microfossils from the Upper Cretaceous sediments are generally well preserved, except in horizons where intense dissolution has occurred. The middle and Lower Cretaceous fossils are only moderately well to poorly preserved; recrystallization of foraminifers is common, and nannofossils are badly etched in the Cenomanian–Albian limestones at the bottom of this hole.

Redeposition

Redeposited materials such as plant fibers, mollusk fragments, shelf benthic foraminifers, brown clay, and possibly glauconite, occur at several levels in the Cretaceous section. Redeposited materials are commonly found in the upper Maastrichtian *M. mura* Zone, the upper Campanian *T. trifidus* Zone, the *G. concavata*-*G. elevata* Zone of the Santonian, and throughout the lower Cenomanian to upper Albian limestone sequence. Redeposited radiolarians are most common in the upper Albian limestones.

Whereas the redeposited materials from the Albian to the Coniacian can be attributed to the location downslope from a topographic high, the redeposition later in the Cretaceous probably requires another explanation.

Dissolution Intervals

Dissolution, in the absence of diagenetic recrystallization, is common in the Upper Cretaceous sediments

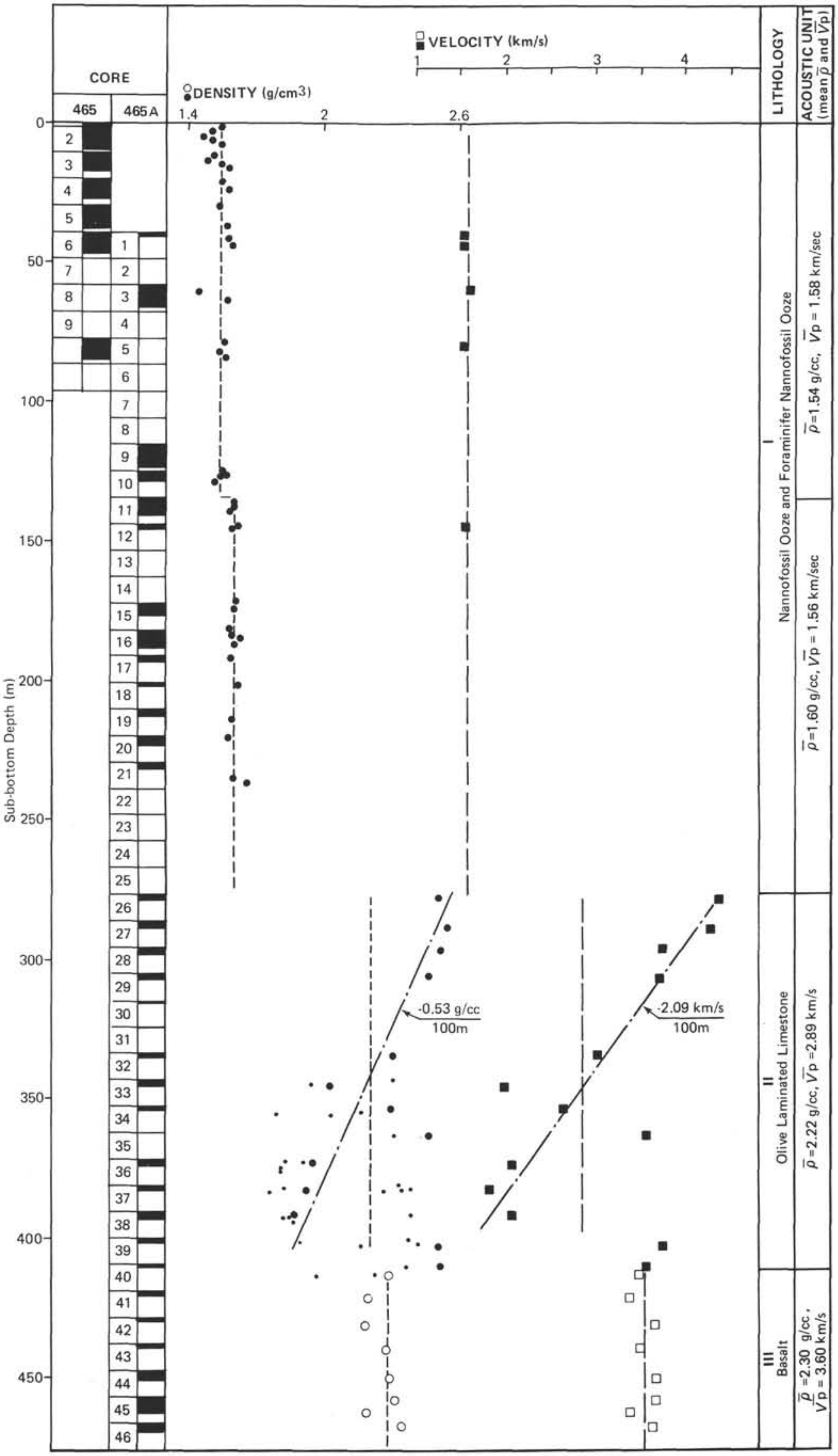

Figure 17. Wet-bulk density and compensated velocity, Site 465.

Table 3. Physical properties of acoustic units at Site 465.

Unit	Sub-bottom Depth (m)	Density[a] (g/cm^3)	Velocity[a] (km/s)	DT (sec)	Thermal Conductivity[a] (mcal/cm•s•°C)	Lithologic Unit
I	0–276	—	—	—	—	I
IA	0–135	1.54	1.58 (4)	0.17	3.50 (9)	
IB	135–276	1.60	1.56 (1)	0.18	3.56 (5)	
II	276–412	2.26[b] (11)	3.06[b] (11)	0.09	4.41 (10)	II
III	412–	2.30 (8)	3.60 (7)	—	3.38 (7)	III

[a] Number of samples averaged in parentheses.

[b] Averages neglecting data from Cores 39 and 40.

at Site 465. Undissolved foraminifers and coccoliths are moderately well preserved. There are, however, discrete levels where dissolution is so intense as to badly etch the nannofossils and dissolve most of the globotruncanids. In the upper Maastrichtian, there are even dissolution levels where all planktonic foraminifers are removed. Intervals intense dissolution include the upper Maastrichtian (*M. mura* Zone), the Maastrichtian to upper Campanian (*T. trifidus* Zone), the lower Santonian, and the upper Albian.

Nannoplankton

Nannofossils are present in the 11 cores of Hole 465, and in all cores of Hole 465A to the trachyte (465A-40). In the nannofossil and foraminifer nannofossil oozes of Unit I, nannofossil assemblages of Pliocene to Pleistocene age, of early Paleocene to late Campanian age, and of Santonian to late Turonian age were recovered. In the olive-gray laminated limestones of Unit II, nannofossil assemblages are readily assignable to two zones of late Albian to Cenomanian age. Samples from Section 465A-40-1, just above the trachyte, belong to the late Albian *Eiffellithus turriseiffeli* Zone (100–104 m.y.).

Cenozoic

In samples from Core 1 and the top of Core 2 (to 2-1, 125 cm), well-preserved assemblages of the *Pseudoemiliania lacunosa* (NN19) Zone of early Pleistocene age are present. Reworked Pliocene discoasters are present in some of these samples. In samples from 2-1, 147 cm to 2-3, 41 cm, a diverse assemblage of discoasters, abundant *Pseudoemiliania lacunosa*, and rare *Reticulofenestra pseudoumbilica* are found. The joint occurrences of these species, without considering complications of possible reworking, place these samples in the zonal interval NN14 to NN18. It is plausible that lower Pliocene species such as *Reticulofenestra pseudoumbilica* and *Discoaster asymmetricus* could be reworked into upper Pliocene assemblages (NN16–NN18).

In samples from the interval 2-3, 46 cm to 2-6, 45 cm, the nannofloras show a mixing of components of three different ages in a random fashion (one of the following, two of the following, all of the following): Pliocene (NN14–NN18), early Eocene (NP13), and late Paleocene (NP9). One set of samples in the interval 2-3, 46 cm to 2-3, 147 cm includes an unmixed flora of late Eocene age. Moderately well-preserved assemblages of the *Discoaster lodoensis* (NP13) Zone are recognized. It is not known whether this mixing occurs naturally or represents drilling disturbance. Natural mixing is considered more likely, and the lower Eocene sediment is interpreted as displaced into the Pliocene.

A sequence of zones spanning the entire Paleocene is recognized in Holes 465 and 465A. Most nannofloras are moderately well preserved, often showing a combination of etching and overgrowth. This makes it difficult to make a definite age determination in some inter-

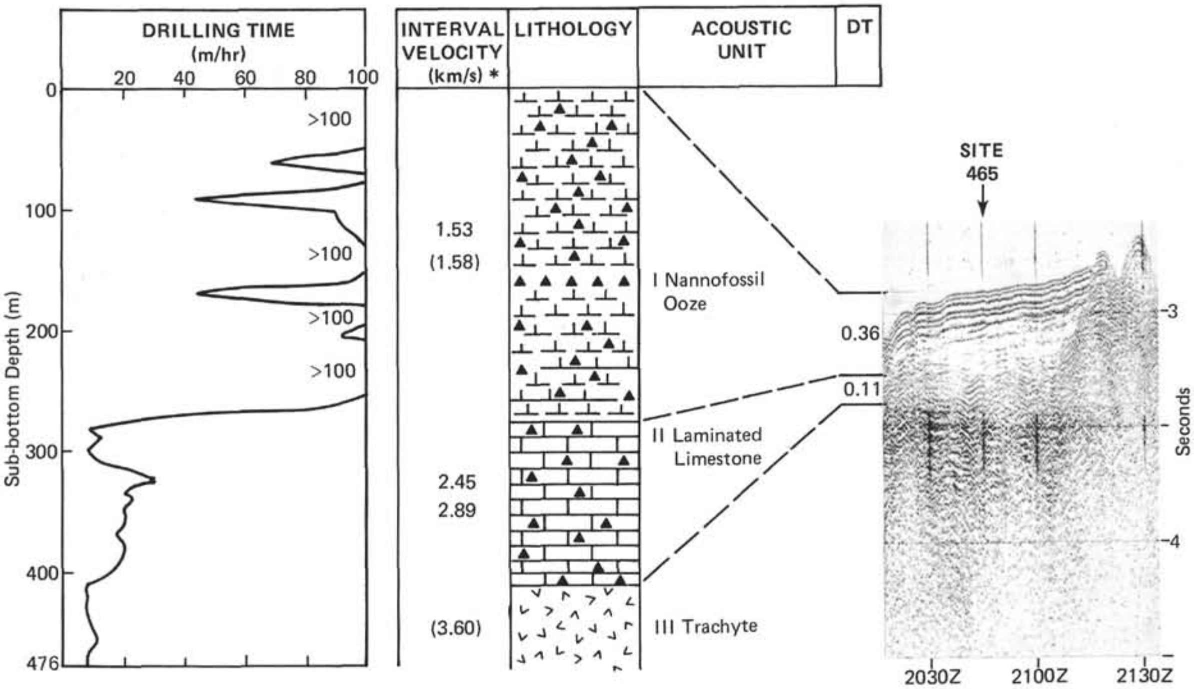

Figure 18. Correlation of seismic-reflection profiles and drilling results, Site 465. Values from laboratory measurements are shown in parentheses.

vals. Sample 2,CC contains a diverse nannoflora of the *Discoaster multiradiatus* Zone of late Paleocene age. Samples 3,CC and 4,CC are assigned to the *Discoaster mohleri* (NP7)/*Heliolithus riedelli* (NP8) zonal interval of late Paleocene age. Samples 5,CC and 1A,CC belong to the *Heliolithus kleinpellii* (NP6) Zone of early Paleocene age.

Sample 6,CC contains a poorly preserved nannoflora of the *Fasciculithus tympaniformis* (NP5) Zone. Because of bad preservation, Sample 7,CC is assignable only to the *Chiasmolithus danicus* (NP3)/*Ellipsolithus macellus* (NP4) zonal interval. Sample 2A,CC, a better-preserved sample, has a nannoflora indicative of the *Chiasmolithus danicus* (NP3) Zone of early Paleocene age. In Sample 8,CC, most coccoliths have etched centers, but specimens transitional from *Cruciplacolithus* to *Chiasmolithus* are present. This sample is tentatively assigned to the *Cruciplacolithus tenuis* (NP2)/*Chiasmolithus danicus* (NP3) zonal interval.

In samples from 3A-1 to 3A-3, 128 cm, exceptionally well-preserved nannofloras were observed. They are characterized by an abundance of *Thoracosphaera* fragments. Very small coccoliths (1-2 μm) are also present, indicating that almost no dissolution of the coccolith assemblages has occurred. Rare to few *Markalius inversus* and very rare *Biantholitus sparsus* are found in some sample intervals. No specimens of *Cruciplacolithus tenuis* or *Chiasmolithus* spp. were found; these samples are assigned to the *Markalius inversus* (NP1) Zone of earliest Paleocene age.

Mesozoic

Predominantly abundant and moderately well-preserved nannofossils are found throughout the Upper Cretaceous section. Poorly preserved calcareous nannofossils were commonly recovered from the Lower Cretaceous. A sequence of nine nannofossil zones or zonal intervals has been recognized:

1) Upper Maastrichtian (3A-3, 120 cm to 3A,CC); *Micula mura* Zone.

2) Middle to Upper Maastrichtian (9,CC to 11,CC; 4A,CC); *Lithraphidites quadratus* Zone.

3) Lower Maastrichtian (6A,CC to 11A-5, 8-9 cm); *Arkhangelskiella cymbiformis* Zone.

4) Upper Campanian to Lower Maastrichtian (11A, CC to 19A,CC); *Tetralithus trifidus* Zone.

5) Upper Campanian (20A-1, 33-34 cm to 20A,CC); *Tetralithus gothicus* Zone.

6) Lower to middle Campanian (21A-3, 135-136 cm to 21A-4, 43-44 cm); *Broinsonia parca* Zone.

7) Coniacian to Santonian (21A,CC to 23A,CC); the abundant assemblages in this interval are characterized by the absence of certain index species important to the zonation; the upper limit of this zonal interval is determined by the first occurrence of *Broinsonia parca*, and the lower limit by the last occurrence of *Lithraphidites acutum*, and by the first occurrence of *Eiffellithus eximius, Micula staurophora*, and *Lithastrinus grilli*.

8) Uppermost Albian to Cenomanian (26A-1, 14-15 cm to 27A,CC); *Lithraphidites alatus* Zone.

9) Upper Albian (28A-1, 58-59 cm to 40A-1, 139-140 cm); *Eiffellithus turriseiffeli* Zone.

Foraminifers

Neogene

Neogene sediments were recovered only in Core 465-1 and part of Core 465-2. Core 465-1,CC is of Pleistocene age (N22), judging from the presence of *Globorotalia truncatulinoides*. The foraminifer fauna is poorly preserved, as indicated by a very large amount of fragmentation. The planktonic assemblage is typical of temperate water. *Globorotalia inflata* is abundant and dominates the assemblage; *Globigerina bulloides* is common. Rare species include *Globigerinoides ruber, Globorotalia scitula, G. crassaformis*, and *G. truncatulinoides*. At nearby DSDP Site 310, the two temperate species *G. inflata* and *G. bulloides* are also among the main components of the Pleistocene planktonic fauna. *Neogloboquadrina pachyderma*, however, which constitutes 40% of the fauna in the uppermost sediments (upper part of Core 1) at the latter site, is very rare at Site 465. *Uvigerina peregrina disrupta* is the most common benthic-foraminifer species, as is often the case in Pacific benthic-foraminifer assemblages at this water depth.

Paleogene

A nearly complete section of Paleocene sediments can be assembled by the combination of the sections of Holes 465 and 465A. Planktonic foraminifers are well preserved throughout the section, particularly in the Danian, which is about 11 meters thick in Hole 465A. The controversial basal Tertiary "*Globigerina*" *eugubina* Zone occurs at 465A 3-3, 40 cm to 3-3, 144 cm. This is the thickest "*G.*" *eugubina* Zone recorded in the deep sea.

At the top of the Paleocene section, planktonic foraminifers occur in diverse assemblages typical of tropical waters. *Morozovella velascoensis* is large, with wide, open umbilici and almost cantilevered chambers. Morozovellids and acarinids are very diverse; subbotinids in Zone P4 are very large; chiloguembelinids are rare and flat.

Foraminifer populations change in Zone P3b (465-5 to 6,CC), not only in species content, but also in morphotypic expression. Morozovellids become tightly coiled, with closed umbilici, and benthic forms are more abundant (6,CC).

The planktonic-foraminifer association in Zone P1 is unusual (465-8,CC; 465A-2-3, 144 cm). Chiloguembelinids dominate all faunas, while other species are very rare. *Guembelitria cretacea* dominates the *G. eugubina* faunas at lower levels, but it is replaced by *G. eugubina* at higher levels. Little or no reworking of Cretaceous material is found in samples from 3-3, 40 cm to 3-3, 100 cm; this lack of admixed Cretaceous is unique. Mixing of Cretaceous and the "*G.*" *eugubina* fauna progressively increases below 3-3, 110 cm to 3-3, 142 cm, presumably because of the disturbance of coring.

Cretaceous/Tertiary Boundary

The Cretaceous/Tertiary boundary is at 465A-3, 144 cm. The boundary is actually spread through a mixed zone approximately 30 cm in length. Well-preserved

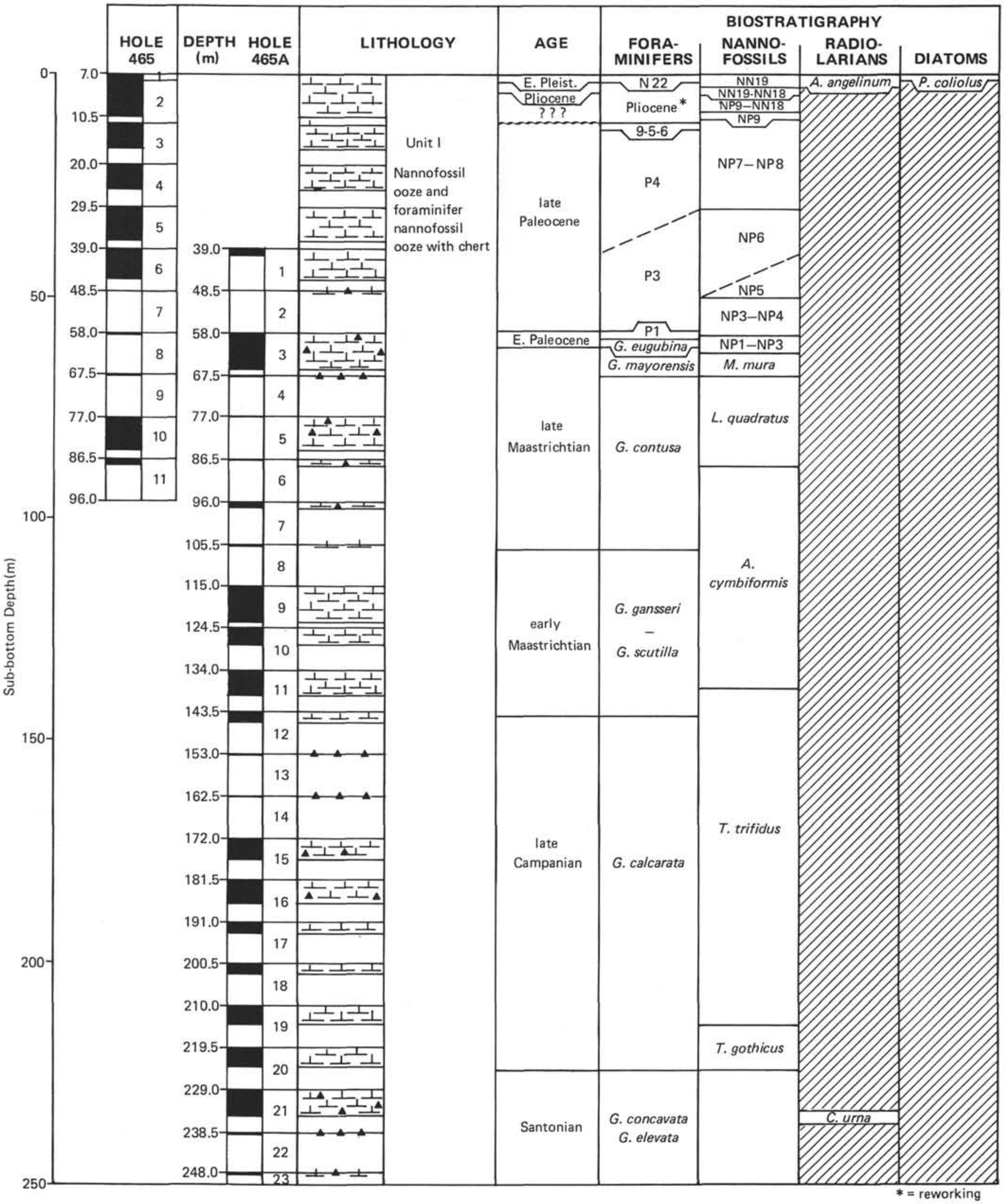

Figure 19. Biostratigraphy of Site 465.

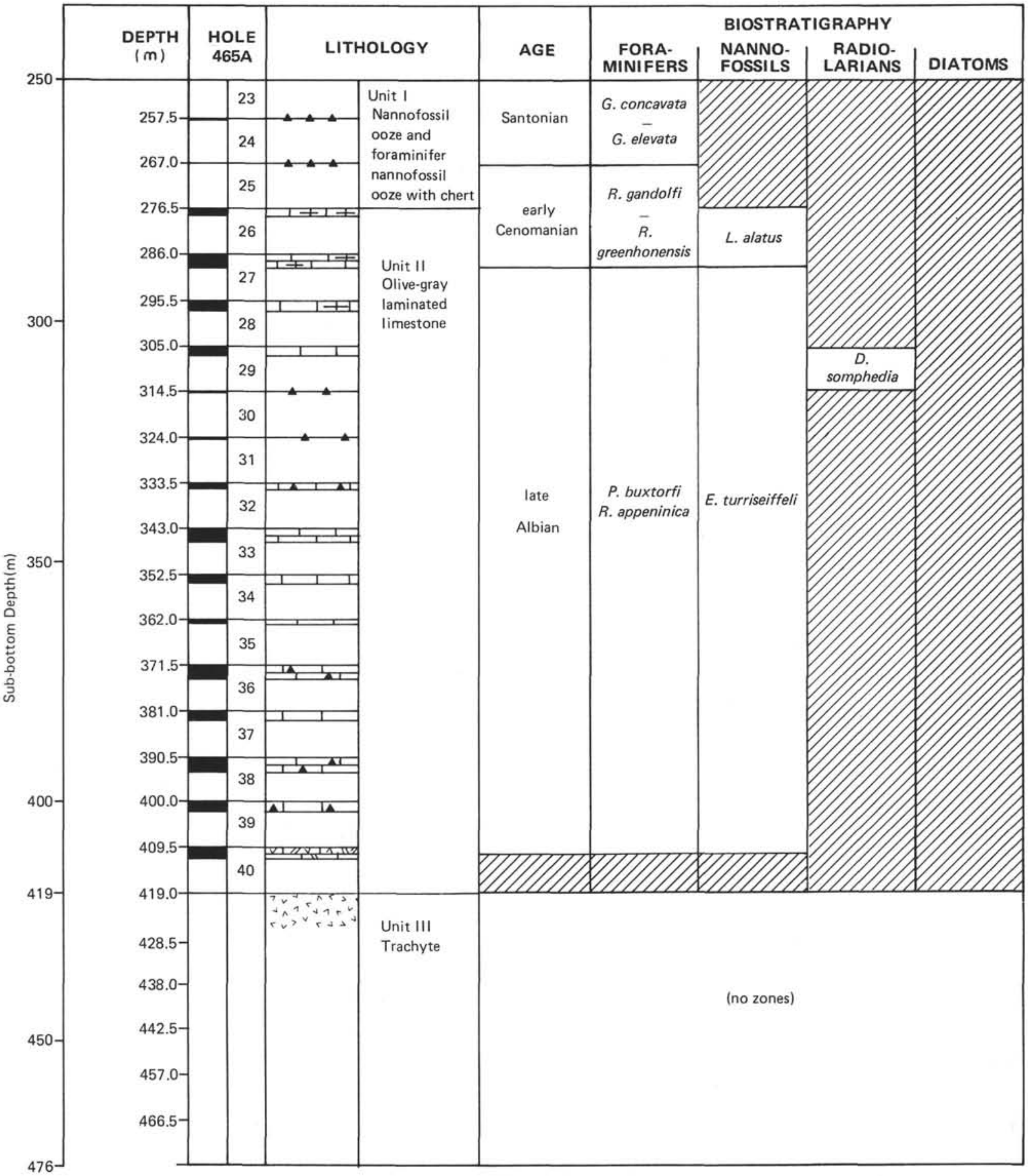

Figure 19. (Continued).

latest Cretaceous fossils occur in discrete white stringers through light-gray Tertiary sediments.

Cretaceous

Cretaceous sediments were recovered from Cores 9 to 11,CC in Hole 465 and 3-3, 146 cm to 4-2 in Hole 465A.

Maastrichtian. The *A. mayaroensis* (465A-9 to 11,CC; 3-3 to 3-5), *G. gausseri* (9-2 to 10-1), and *G. scutilla* (10-2 to 14,CC) zones were recognized. Aside from several levels (465-9,CC; 465A-12,CC; 465A-3-6, 50 cm) where most of the planktonic foraminifers are dissolved, Maastrichtian planktonic foraminifers are diverse and well preserved. Benthic foraminifers are rare.

Campanian. The *G. calcarata* (14,CC to 20-2) and *G. elevata* (20-3 to 22,CC) zones were recognized. Foraminifers are well preserved; the benthic forms are rather rare.

Santonian. The very short *G. elevata* Zone belongs to the Campanian, according to accompanying nannofossils. Thus, only the early Santonian *G. concavata–G. elevata* Zone (23,CC) was determined. Foraminifers are frequently highly dissolved; some of the benthic foraminifers appear to be redeposited.

Turonian–Coniacian. The *G. rengi–G. sigali* Zone was recognized from 24 to 25,CC. In these samples, dissolution and recrystallization are intense. *Inoceramus* prisms occur in the coarse fraction.

Albian. The *R. apenninica–P. buxtorfi* Zone (28-1 to 40-1) was recognized. The badly recrystallized planktonic faunas were dominated by hedbergellids. Only one specimen of *P. buxtorfi* was found throughout the interval. The few moderately diverse assemblages (34-1) contain *Praeglobotruncana, Ticinella*, and *Rofalipara* species. At several levels, woody fiber and uniform-sized mollusk fragments occur (40-1). Recrystallization and distortion of foraminifers increase toward the bottom, until all are dissolved below 40-1.

Coarse-Fraction (> 63 μm) Components; Abundance and Preservation of Foraminifers

A visual estimate of the relative abundance of the main components of the sediment coarse fraction is presented in Appendix D.

In the Cenozoic and Upper Cretaceous oozes (Lithologic Unit I; Cores 465-1 through 465A-25), planktonic foraminifers are the dominant constituent of the coarse fraction. In these sediments, there are rare occurrences of ostracodes, mollusk, and echinoderm fragments. Radiolarians are rare in the Neogene (Core 465-1), and absent in the remainder of the interval except for one horizon in the Santonian (Core 465A-21), in which they are abundant, dominating the coarse fraction. Chert fragments are rare to common throughout the Paleocene and Upper Cretaceous.

Planktonic foraminifers are poorly preserved in the Neogene (Core 465-1) and greatly fragmented. They are well preserved in the Paleocene and upper Maastrichtian (Cores 465-2 through 10 and 465A-1 and 2), except for one interval with pronounced dissolution in the upper Maastrichtian (Cores 465-10 and 465A-3), in which planktonic foraminifers are rare or absent, so that benthic species dominate the foraminifer assemblages. Foraminifers are moderately well preserved in the lower Maastrichtian to Santonian (Cores 465A-6 through 23), and poorly preserved in the lower Santonian to upper Coniacian (Cores 465A-24 and 25).

In the lower Cenomanian and upper Albian limestones (Lithologic Unit II; Cores 465A-26 through 40, Section 1), the coarse fraction is dominated by limestone chips and planktonic foraminifers, each alternating as the main component. Throughout this interval, planktonic foraminifers are poorly preserved, because of significant recrystallization.

In Cores 465A-27 to 33, limestone chips dominate the coarse fraction, except at one horizon in Core 32, in which quartz grains are the main constituent.

Radiolarians

At Site 465, radiolarians are rare, and preservation is generally poor (see Schaaf, this volume).

Only the first two cores of Hole 465 (up to 2-2, 120 cm) contained common to rare but poorly preserved radiolarians of the *Axoprunum angelinum* Zone (late Pleistocene). By comparison with Site 464, this fauna includes more high-latitude species, although it lies at lower latitudes; *P. murrayana* is the only low-latitude species found in this assemblage. The Cenozoic sections of Hole 465A are barren.

Two cores (21 and 29) contain radiolarians. In Core 21, a poorly preserved association with *A. urna, P. superbus, D. torquata*, and *D. duodecimcostata* can be assigned to the *Artostrobium urna* Zone. Core 29 contains fairly abundant, well-preserved radiolarians such as *L. petila, H. barbui, A. cortinaensis*, and *A. stocki*, from the *Dictyomitra somphedia* Zone. The absence of species of Subfamily Saturnalinae is noteworthy, as these species occur commonly through the Cretaceous at these latitudes.

SEDIMENTATION RATES

Average rates of sedimentation at Site 465 are shown in Figure 20; data for the figure are given in Table 4. Sedimentation commenced in the late Albian to early Cenomanian at a rate at 48 m/m.y. with the accumulation of limestone (Unit II) at this site. This is a very high rate, which may be partly explained by the presence of redeposited material.

Following the early Cenomanian, there is a 15-m.y. hiatus spanning the interval from the lower Cenomanian to the Santonian. Santonian rates are approximately 10 m/m.y. A hiatus of nearly 4 m.y. then precedes the late Campanian, when rates were very high (about 40 m/m.y.), which is reminiscent of the high rates in the Albian, and similar to the rate for the Maastrichtian to late Campanian (52 m/m.y.; 42 m/m.y. for the Maastrichtian alone) at Site 463.

Upper Maastrichtian was recovered in both Holes 465 and 465A. Rates calculated for both holes are slightly higher than for the lower Maastrichtian; for Hole 465, the obtained rates are about 20 m/m.y. and 16 m/m.y., respectively. In the early Paleocene (Zones P1 and P2), sedimentation rates are lower than during the late Maastrichtian, reaching only 4 m/m.y. for Hole 465. Late Paleocene sedimentation rates are again somewhat higher, nearly reaching 8 m/m.y.

After the Paleocene, there is a hiatus of nearly 50 m.y. Sediments after the hiatus consist of a highly mixed zone containing Eocene fossils mixed with *in situ* sediments of early Pliocene age. By Section 3 of Core 2, normal continuous sedimentation of Pliocene fossils is recorded, the rate of sedimentation for the early Pliocene through Pleistocene is 1 m/m.y. However, the late Pleistocene is probably missing, so the rate is somewhat higher.

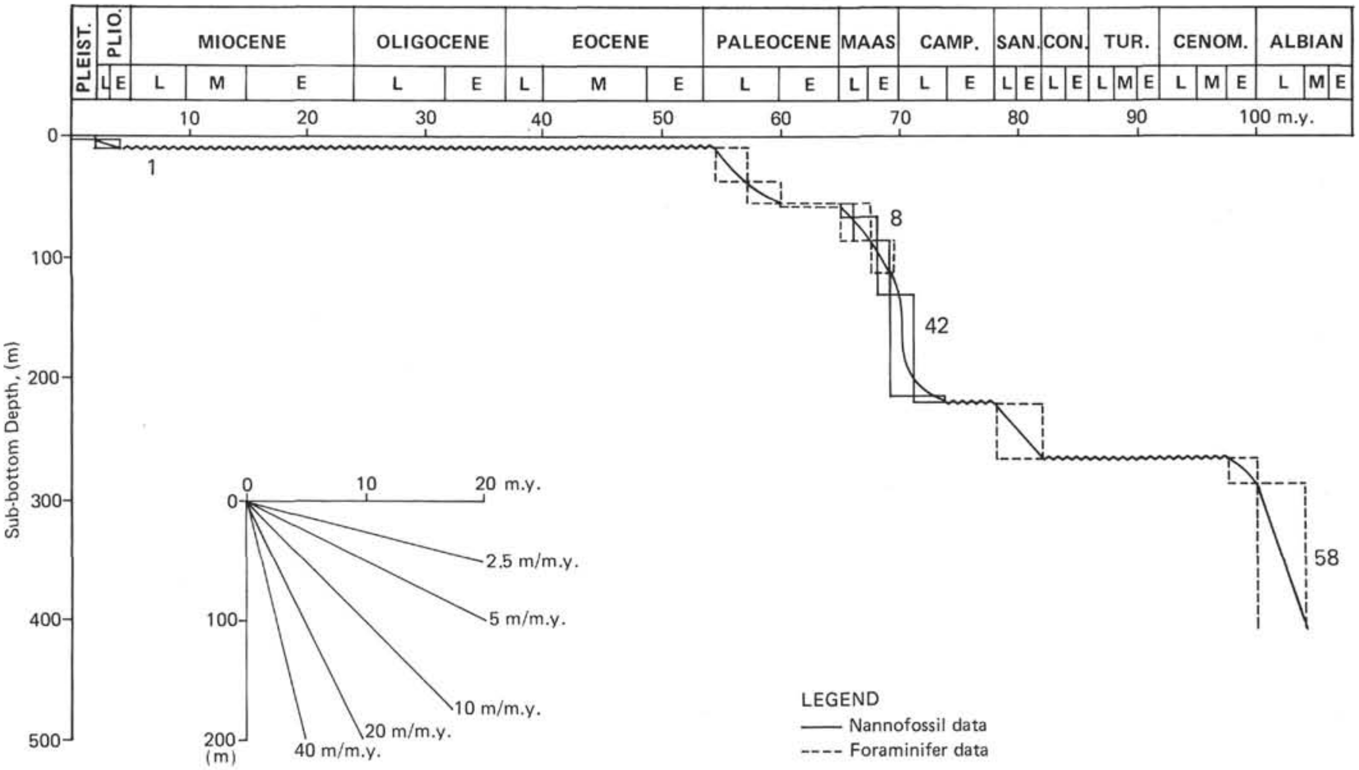

Figure 20. Sedimentation-rate curve for Site 465.

Table 4. Sedimentation rates at Site 465.

Age	Sub-bottom Depth (m)	Thickness (m)	Time (m.y.)	Average Rate (m/m.y.)
Hole 465				
Late Paleocene	10.5–48.5	38	54.5–59	8
Early Paleocene	48.5–67.5	19	60–65	4
Late Maastrichtian	67.5–96	28.5	65–69	7
Hole 465A				
Paleocene (P4–*G. eugubina*)	39–62	23	57–65	3
Late Maastrichtian	62–86.5	24	65–68	8
Early Maastrichtian to late Campanian	134–219.5	85.5	69–71	42
Early Santonian to late Coniacian	250–276.5	26.5	80–84	7
Early Cenomanian to late Albian	276.5–411	134.5	99–102	45
Late Albian	295.5–411	115.5	100–102	58

According to the conclusions of Lancelot and Larson (1975), it is possible to reconstruct the movement of Leg 32 sites by taking into account Pacific Plate motions and magnetic anomalies. Following their assumptions, Sites 465 would have crossed the Equator just after 90 m.y. ago. Table 5 depicts the approximate latitudes versus age of Site 465, according to this model. These authors suggest that two of the criteria indicating that a site has crossed into the equatorial high-productivity zone are high sedimentation rates and(or) increased abundance of radiolarians. At Site 465, the highest sedimentation rates occurred 100 m.y. ago, when the site theoretically had just crossed into the high-productivity area; radiolarians are abundant in sediments of this age.

Table 5. Proposed latitudes of Site 465 and sediment characteristics.

Age (m.y.)	Latitude (Lancelot–Larson model, Leg 32)	Accumulation Rate (m/m.y.)	Radiolarian Zone
60	16°N	4	—
70	11–12°N	42	—
80	6°N	7	*A. urna*
90	1°N	(hiatus)	—
100	4°S	58	*D. somphedia*

At 90 m.y., when this site is supposed to have been just at the Equator, there is a hiatus in the sedimentary succession. At 80 m.y., the site is supposed to have passed out of the high-productivity zone; radiolarians are again preserved at this site. The sedimentation rates at this time were significantly lower, however, because of a hiatus before and age uncertainties after this interval. For this reason, the rate of 7 m/m.y. is only an approximate.

At 70 m.y. accumulation rates were again very high; the site supposedly was at 12°N. It is possible, as suggested earlier, that this was a time of high oceanic fertility. At 60 m.y., in the early Paleocene, the sedimentation rate was relatively low, while the site is assumed to have been close to 16°N.

SUMMARY AND CONCLUSIONS

The volcanic, tectonic, and depositional histories of Site 465 on southern Hess Rise can be interpreted from the 476-meter cored interval. The site is in 2161 meters of water just north of Mellish Bank, near the center of a small, apparently fault-bounded basin. Plans were to sample a calcareous section that had been above the CCD for its entire history, and to sample the underlying igneous basement.

Basement Rocks and Physical Properties

Deeply weathered trachyte and calcite-cemented trachyte breccia underlie the sediment sequence at Site 465. Trachyte breccia makes up the upper 17 meters, and the remaining 47 meters are trachyte flows. Based on vesicle and grain-size changes, the sequence was divided into 30 layers, which subsequently were placed in five groups (Seifert et al, this volume). Many of the layers represent individual flows, but in no place was a complete flow unit recovered; apparently, the fine-grained and clay-rich flow boundaries were washed out during coring. No glassy flow margins occur in the recovered sequence. Vesicles are abundant and range from submicroscopic to more than 5 mm in diameter. Many are filled with calcite and smectite. Although most specimens are gray, the slight red coloration of some pieces indicates a low degree of oxidation. Pyrite is a common vein mineral, and barite was observed in one vein. The fragments increase in angularity with depth and the amount of fracturing decreases. The cause of brecciation is unknown, but it probably occurred *in situ*, and may have been caused by the explosive release of trapped gas. The trachyte breccia is cemented together mostly by calcite.

Petrographic studies reveal mostly trachytic textures. Pervasive alteration has affected the original mineralogy, so that only a few of the primary minerals remain. The original minerals were plagioclase, possible pyroxene, and iron-ore microphenocrysts, set in a groundmass of glass, iron-ore minerals, and feldspar microlites. The present minerals include plagioclase as phenocrysts, laths, and microlites; mafic-mineral pseudomorphs; and iron-ore minerals; set in a groundmass of smectite and calcite.

The igneous rocks are altered trachyte with nearly 60% SiO_2 and high percentages of Na_2O and K_2O. We believe that these rocks are differentiated products of alkali basalt magma and probably are the result of oceanic-island or seamount volcanism. The large vesicles and the lack of glassy flow margins suggest that the eruptions occurred either subaerially or in very shallow water. Rounded volcanic clasts and the presence of several ash or volcanic sandstone beds in immediately overlying sediments indicate that a volcanic source was nearby after sedimentation began, implying that the site also may have been above sea level at some time in its history. Undoubtedly, parts of Hess Rise were above sea level during the early stages of its growth, which further suggests that it may have been a landmass of significant size, or at least a large archipelago before late Albian sediment deposition began.

Variations in magnetic intensity, susceptibility, and Curie temperature indicate that trachyte Units 1 and 2 are highly oxidized and have been completely remagnetized. In addition, it is possible that low-titanium titanomagnetites and(or) large magnetic-grain sizes may characterize the center of Unit 3. Paleolatitude estimates indicate that the site was near the Equator during formation of the trachytes. The measured velocities of sediment and rock samples agree well with those calculated from the seismic-reflection profiles. Unit 1, nannofossil ooze and chert, has a mean velocity of about 1.58 km/s. Unit 2, the olive laminated limestone, has a mean value of about 2.89 km/s. The trachyte of Unit 3 has a low velocity compared to that of oceanic basalts, averaging about 3.60 km/s. The low velocity for the trachyte is caused in part by its intense alteration. Heat-flow measurements were attempted at four depths in Holes 465 and 465A. A value of 1.36 HFU was calculated for Hess Rise, which is similar to North Pacific averaged data for crust 100 m.y. old, indicating that Hess Rise is thermally extinct.

Hiatuses

Evidence from the igneous rocks, which were extruded in shallow water or even subaerially, and from the shallow-water fossils in the immediately overlying sediments, indicates that the deposits recovered at Site 465 are from a depositional environment which has been deepening from close to the sea surface in late Albian time to more than 2 km water depth today. However, the continuously cored sediments (Fig. 21) have major hiatuses which represent approximately 75% of the time elapsed between the deposition of the oldest limestone and the thin veneer of Plio–Pleistocene deposits close to the sea floor at Site 465. The sediments which document the remaining 25 to 30 m.y. therefore offer relatively short and discontinuous records of the depositional regime at this site. The major hiatuses span the time from early Cenomanian to Santonian, from Santonian to late Campanian (exact time span unknown), and from late Paleocene to early Pliocene. It is also unknown whether the oldest sediments overlie nearly penecontemporaneous volcanic rocks, or if the volcanic rocks are much older. If older, how many years elapsed between the eruptions of the volcanic rocks and the initiation of sedimentation? The highly altered state of the volcanic rocks suggests that they have been exposed to weathering for a considerable time.

Naturally, it is impossible to known how much and what kind of sediments were deposited during the intervals now represented by hiatuses; however, the differences in lithology and the degree of lithification and diagenesis between Lithologic Units II and I (separated by the early Cenomanian to Santonian hiatus) suggest that a thick sedimentary sequence once was laid down at Site 465 and subsequently was eroded.

Biostratigraphy

Nannofossils and planktonic foraminifers occur throughout the entire sedimentary column at Site 465, whereas benthic foraminifers seem to be lacking in the deepest sediment cores, of Albian age. Rare radiolarians are restricted to Cretaceous and Pleistocene deposits; diatoms were not found. The youngest sediment interval above the late Paleocene to early Pliocene hiatus

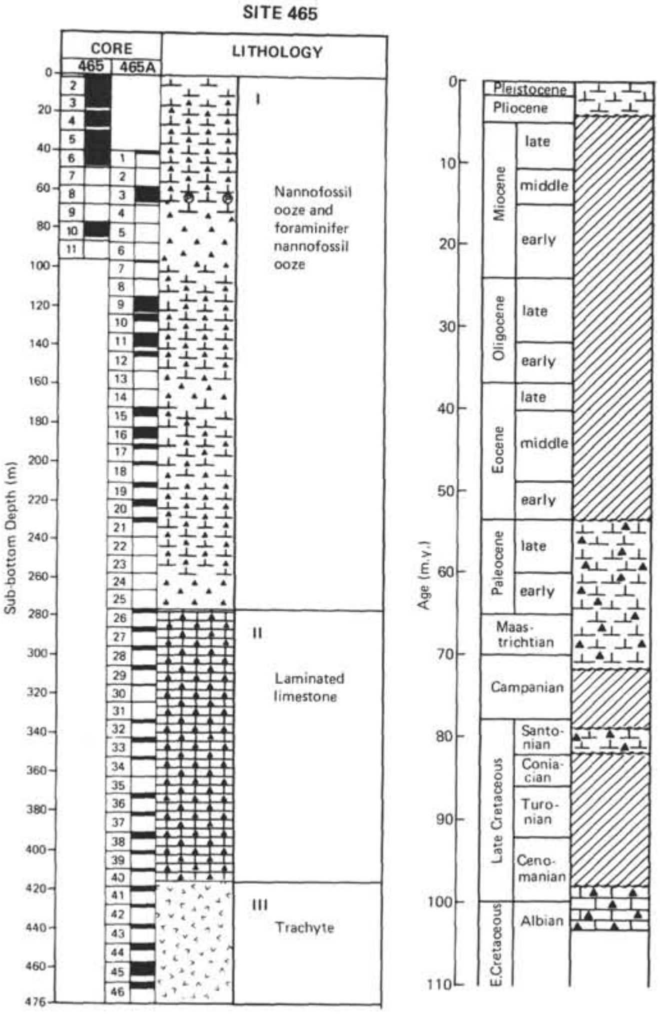

Figure 21. Stratigraphic column and major lacunas, Site 465.

comprises Pliocene and lower Pleistocene nannofossil oozes (upper Pleistocene deposits were not recovered at Site 465), which are mixed with Eocene and Paleocene sediments.

The late Albian to late Paleocene part of the column at Site 465 comprises two of the hiatuses discussed above, but it also encompasses some uniquely well-preserved parts of the stratigraphic column which only rarely have been sampled in the history of DSDP. An outstanding accomplishment at Site 465 is the apparently complete recovery of sediments documenting the transition from Cretaceous to Tertiary. A part of Core 465A-3 more than 100 cm thick, nannofossil ooze with uniquely well-preserved fossil faunas and floras, belongs to the basal Tertiary *G. eugubina* Zone (Boersma, this volume).

Although several horizons of extensive dissolution were observed, and although recrystallization and etching of calcareous fossils increase down-core, nannofossils from the Lower to Upper Cretaceous sediments are usually moderately well preserved, allowing a very detailed biostratigraphic zonation. Radiolarians were observed only in discrete horizons in Upper Cretaceous deposits, and most may be redeposited.

It is not possible to construct a reversal stratigraphy for Hole 465A, because magnetic inclinations in both the limestones and the trachytes are very low.

Lithostratigraphy

The biostratigraphic framework for Site 465 allows us to date the deposition of the major lithologic units (Fig. 20). A site-summary chart (Fig. 22) gives physical and chemical data. The sedimentary section was deposited during four relatively short intervals spread over more than 100 m.y.; only 25% of this time is actually represented in the sedimentary column. It is somewhat surprising, therefore, that the deposits are so remarkably uniform. Because of their uniformity, the sediments were grouped into only two lithologic units.

The older Unit II overlies altered trachyte of the volcanic basement (Unit III) and consists of olive-gray laminated limestone of late Albian to early Cenomanian age. The limestone consists dominantly of pelagic components mixed with a small proportion of clay. Most calcareous fossils are recrystallized and(or) etched, whereas radiolarians have been almost entirely replaced by $CaCO_3$; their silica probably migrated into the chert. Outstanding features of these limestones (> 130 m thick) are the relatively high organic-carbon content and the laminations. Gray, fine-grained limestones occur in beds throughout this unit, their lower sharp and upper gradational boundaries with the olive-gray limestones suggest that they contain displaced material. Clear indications of current activity, such as truncated ripple laminations, were observed at several places throughout this unit, but horizons with graded bedding were observed only in the top and bottom parts. The difference in composition, degree of compaction, and diagenesis between Unit II and the overlying Unit I is so striking that it is assumed that a thick sediment pile, later eroded, was deposited during early Cenomanian to Santonian time.

The thick Santonian to Pleistocene soupy to stiff nannofossil and foraminifer nannofossil oozes of Unit I are very homogeneous, but usually moderately to highly disturbed because chert was a common component in all cores except the most topmost one. The only macrofossils in the oozes are large *Inoceramus* fragments in the upper Campanian to lower Maastrichtian.

Depositional History

The planktonic faunas and floras in Site 465 sediments have changed in a very specific manner as the site moved northward from a probable location just south of the equator under tropical surface-water masses during mid-Cretaceous time to its present location under temperate to subtropical, oligotrophic central North Pacific surface waters. The Cretaceous and Paleocene planktonic foraminifers are therefore typical of tropical surface-water masses, whereas the faunas of the Pleistocene sediments resemble those of Site 310, farther to the north, except that the Site 465 faunas contain fewer *G. pachyderma*.

Besides their tropical planktonic-foraminifer faunas, the olive-gray Albian to Santonian laminated limestones

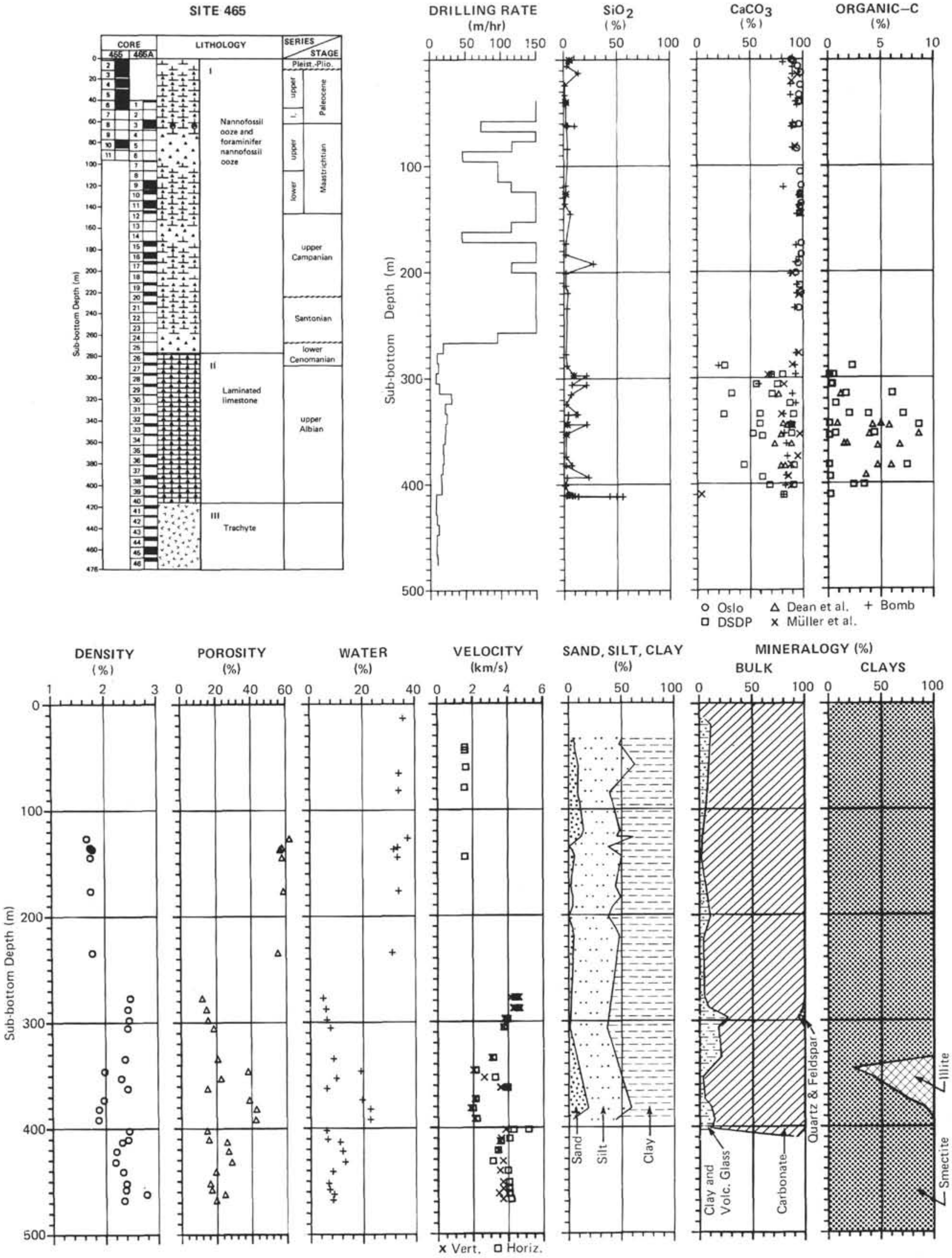

Figure 22. Site-summary chart, Site 465, southern Hess Rise. The data for the summary are compiled from the following sources: % $CaCO_3$ and % organic carbon from Dean (this volume); density, % porosity, water content (% water), and sound velocity from Appendix D (this chapter) and Fujii (this volume); % sand, silt, and clay from Appendix E (this chapter); and clay mineralogy from Appendix C (this chapter) and Nagel and Schumann (this volume).

of Unit II display many features characteristic of sediment deposited in relatively shallow water (a few hundreds of meters), beneath the fertile equatorial-current regime. Although many of the features can be attributed to distal turbidite sedimentation, the coincidence of laminated sediments, high organic-carbon contents (possibly in part terrigenous), an oxygen-poor depositional environment as indicated by the benthic foraminifers, high concentrations of radiolarians, and high bulk sedimentation rates seem to indicate very fertile surface-water masses of the equatorial-current regime. It is interesting to note that the time of the Equator crossing (applying the model of Lancelot and Larson, 1975) coincides with the Cenomanian to Coniacian hiatus, when southern Hess Rise was a fairly shallow and possibly large feature, which might have caused significant disturbances of the equatorial-current regime.

Important chemical and physical changes of the surface water during the global crises at the end of the Mesozoic are indicated by the very small lowermost Paleocene planktonic-foraminifer faunas and anomalous nannofossil floras. The apparently complete recovery of the Upper Cretaceous and lower Tertiary interval allows a detailed assessment of changes in the surface waters and bottom waters (Boersma and Shackleton, this volume).

Changes in the depositional environment under the influence of the bottom-water masses are much more difficult to assess, because it is obvious that the depth of deposition has changed from a few hundreds of meters during mid-Cretaceous time to more than 2 km in modern times. It is therefore difficult to tell whether changes were caused only by subsidence, or if they were caused by small changes of the bottom-water hydrography. We have no indications that the water depth at this site was ever greater than it is today, but it probably was always shallower. The subsidence of the site can be interpreted through geophysical data and evidence from the Site 465 samples. The trachytic rocks underlying the older sediments were extruded either subaerially or in shallow water. Mollusk fragments and the oldest benthic foraminifers in sediments which overlie cross-laminated ash beds on top of the trachyte indicate a deposition depth of a few hundreds of meters during Albian time, then rapid subsidence to lower bathyal depth.

The composition of the benthic-foraminifer faunas and the laminated nature of Unit II point to oxygen-poor (mid-water oxygen minimum) conditions close to the sediment/water interface. However, despite this fact, Unit II, which was deposited in a few hundreds of meters of water, also displays sedimentary structures indicating at least some bottom-current activity (graded beds, ripple marks, clastic limestones with basalt pebbles, reworked material, size sorting of radiolarians, etc.).

At present, it is not clear what hydrographic events were responsible for the presence of the three important hiatuses, and for the discontinuous occurrence of reworked sediment components (particularly in the upper Maastrichtian, upper Campanian, and upper Albian to lower Cenomanian). On the other hand, an apparently complete sedimentary sequence across the Cretaceous/Tertiary boundary was recovered.

The site apparently has remained well above the CCD since mid-Cretaceous time, and the sediment sequence represents a record of normal pelagic carbonate deposition. However, despite the relatively shallow water, horizons of intense dissolution occur at irregular intervals. We do not understand what hydrographic or chemical changes near the benthic boundary layer are able to drastically change the dissolution rate of calcareous particles. Although similar observations have been made at Site 463, and at other DSDP sites, it is unknown whether these dissolution events are local phenomena, or if they can be correlated across the entire ocean.

REFERENCES

Chase, T. E., Menard, H. W., and Mammerickx, J., 1971. *Topography of the North Pacific:* La Jolla (Univ. Calif.).

Lancelot, Y., 1978. Relations entre evolution sedimentaire et tectonique de la Plaque Pacifique depuis la Cretace Inferieur. *Mem. Soc. Geol. France*, 134.

Lancelot, Y., and Larson, R. L., 1975. Sedimentary and tectonic evolution of the northwestern Pacific. *In* Larson, R. L., Moberly, R., et al., *Init. Repts. DSDP*, 32: Washington (U.S. Govt. Printing Office), 925–939.

Larson, R. L., Lancelot, Y., Gardner, J. V., et al., 1975. Magnetic, bathymetric, seismic reflection, and positioning data collected underway on *Glomar Challenger*, Leg 32. *In* Larson, R. L., Moberly, R., et al., *Init. Repts. DSDP*, 32: Washington (U.S. Govt. Printing Office), 393–427.

Larson, R. L., Moberly, R., et al., 1975. Site 310: Hess Rise. *In* Larson, R. L., Moberly, R., et al., *Init. Repts. DSDP*, 32: Washington (U.S. Govt. Printing Office), 233–293.

Thierstein, H., 1973. Lower Cretaceous calcareous nannoplankton biostratigraphy. *Abh. Geol. Bundesanst. Wien*, 64:1–52.

Uyeda, S., and Horai, K., in press. Heat flow measurements, DSDP Leg 60. *In* Hussong, D., Uyeda, S., et al., *Init. Repts. DSDP*, 60: Washington (U.S. Govt. Printing Office).

Vincent, E., 1975. Neogene planktonic foraminifers from the central North Pacific, Leg 32, DSDP. *In* Larson, R. L., Moberly, R., et al., *Init. Repts. DSDP*, 32: Washington (U.S. Govt. Printing Office), 765–801.

Yokota, T. H., Kinoshita, H., and Uyeda, S., 1980. New DSDP downhole temperature probe utilizing digital off-line recording system with IC RAM elements. *Bull. Earthquake Res. Inst.*, 55:75–88.

APPENDIX A
Smear-Slide Summary, Site 465

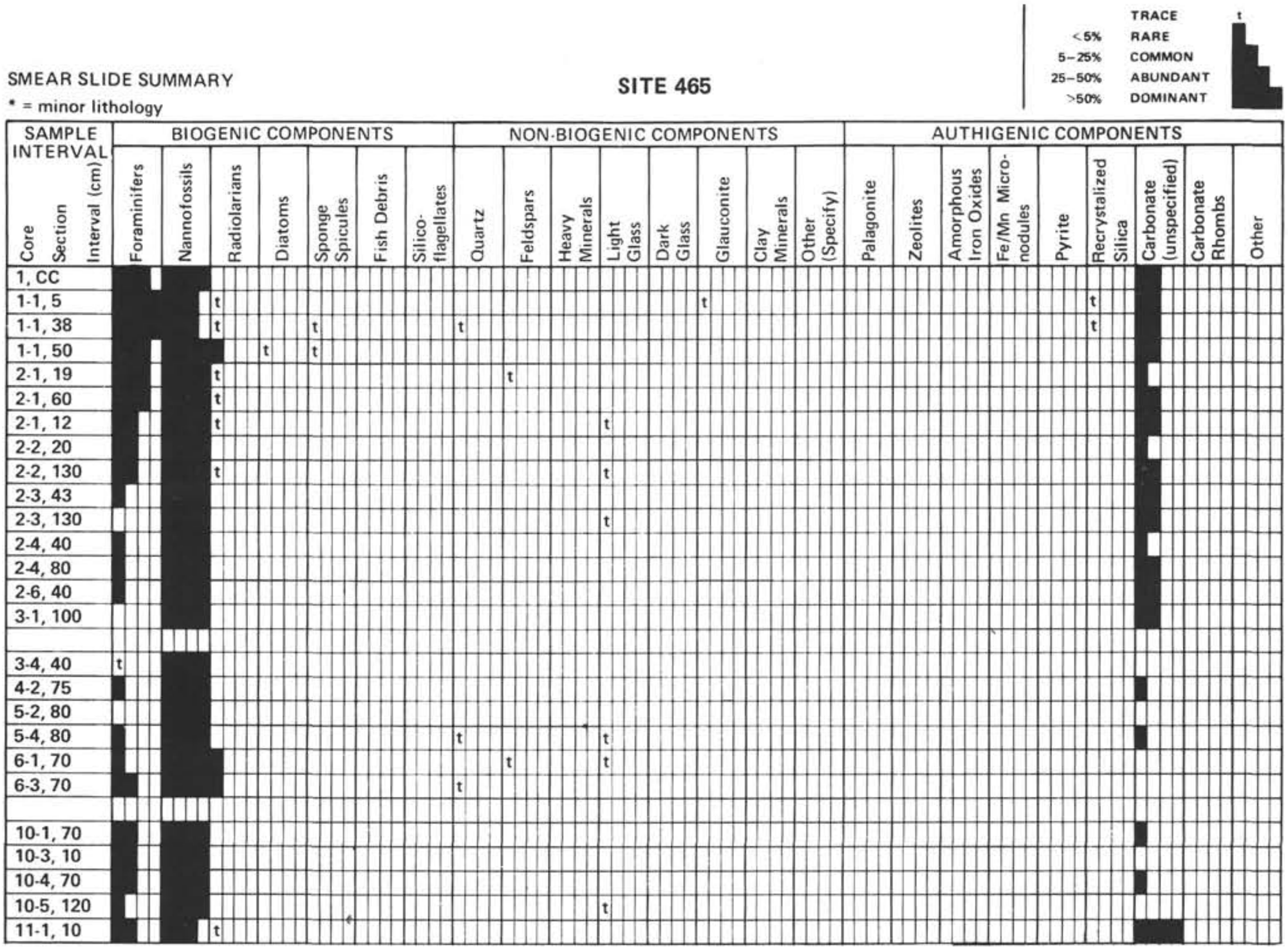

Appendix A. (Continued).

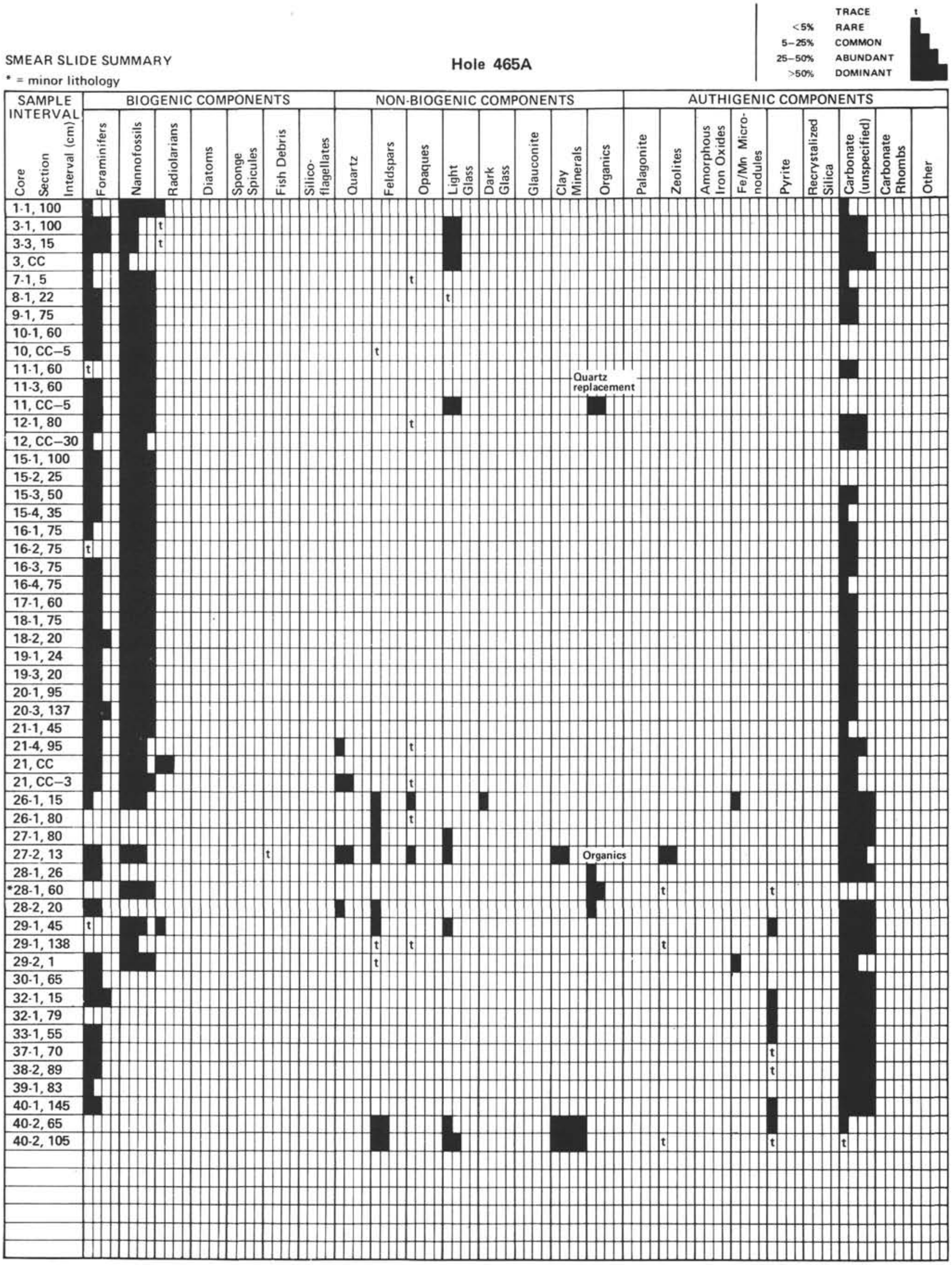

Appendix A. (Continued).

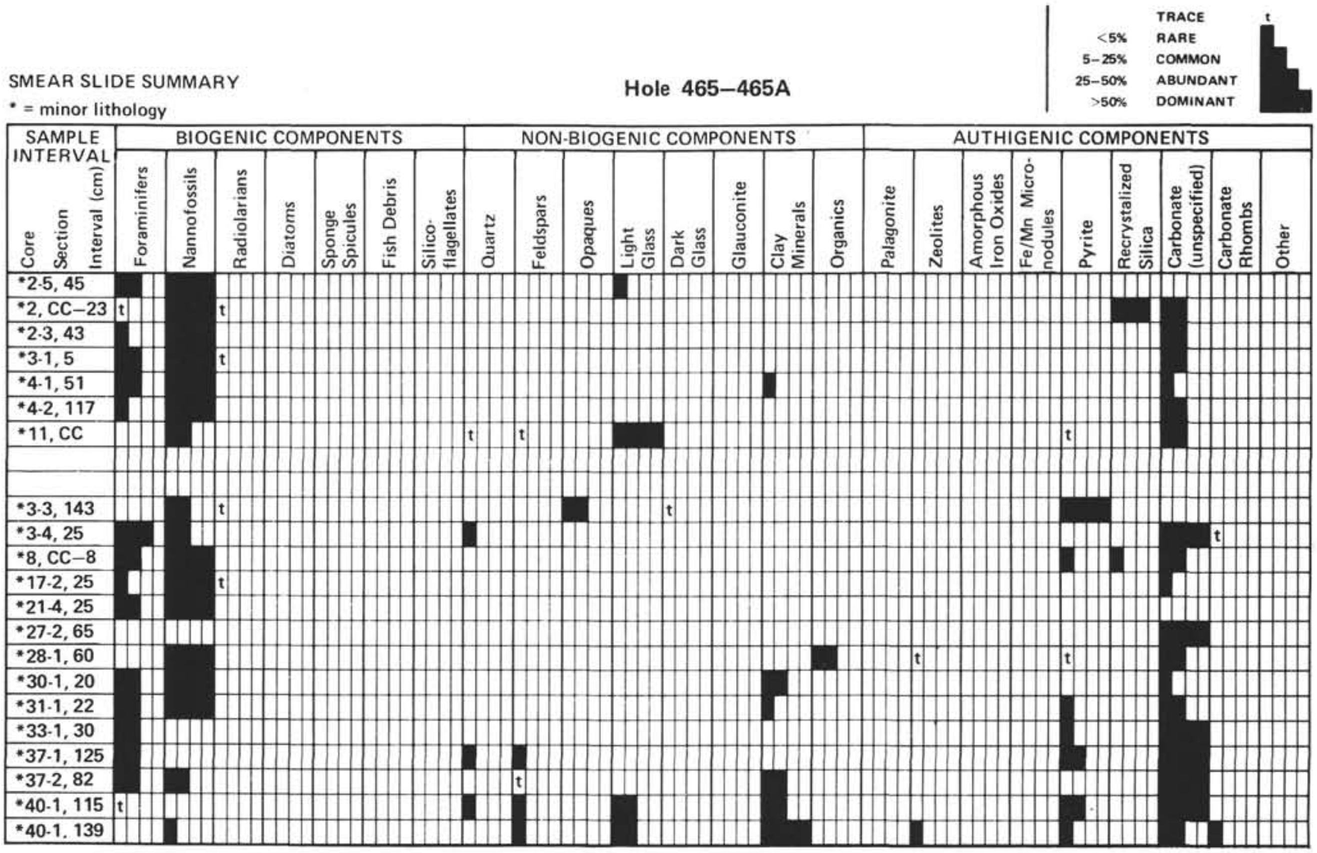

APPENDIX B
Bulk Mineralogy and Clay Mineralogy, Site 465

				Sub-bottom		Bulk Mineralogy (%)							Clay Mineralogy (%)				
Core	Section	Interval (cm)	Sample	Depth (m)	Clay Minerals + Volcanic Glass	Quartz	Feldspar	Carbonates	Opal-CT	Pyrite	Clinoptil-olite	Others	Smectite	Illite	Chlorite	Kaolinite	Others
Hole 465																	
3	3	108–110	1	14.59	5.1	—	—	94.9		—	Tr.		100	—			CPT
4	1	49–50	2	20.49	10.9	—	—	89.1		—	—		—	—			—
10	4	20–22	3	81.71	7.7	—	—	92.3		—	Tr.		—	—			CPT
Hole 465A																	
10	3	34–36	1	127.85	2.6	—	—	97.4		—	Tr.		—	—			CPT
12	2	5–7	2	145.06	1.9	—	—	98.1		—	Tr.		—	—			CPT
18	2	4–6	3	202.05	10.3	—	—	89.7		—	—		100	—			—
20	2	104–106	4	222.05	3.9	—	—	96.1		—	Tr.		—	—			CPT
26	1	18–19	5	276.68	4.5	—	—	95.5		—	—		100	—			—
27	2	24–25	6	287.74	8.7	—	~1.5	89.7		—	—		100	—			—
28	2	7–8	7	297.07	27.0	—	6.4	66.6		1.0	—		100	—			—
29	1	136–137	8	306.36	18.0	—	—	82.0		—	—		—	—			—
32	1	84–84	9	334.36	20.5	—	—	79.5		—	—		100	—			—
33	2	63–64	10	345.13	10.3	—	—	89.7		—	—		23.7	76.3			—
34	1	80–81	11	353.30	3.2	—	—	96.8		—	—		42.5	57.5			—
36	2	112–113	12	374.12	5.1	—	—	94.9		—	—		76.0	24			—
37	1	29–30	13	381.90	11.5	—	—	88.5		—	—		92.0	8.0			—
38	2	84–85	14	392.84	14.1	—	—	85.9		—	—		100	—			—
39	2	36–37	15	401.86	11.5	—	—	88.5		—	—		—	—			—
40	1	42–43	16	409.92	8818	1.6	3.0	3.8		3.8	—		100	—			—

APPENDIX C
Physical-Property Measurements, Site 465 (Fujii, this volume)

Core	Section	Interval (cm)	Sub-bottom Depth (m)	Velocity (km/s)		Grape			Gravimetric			Mean Wet-Bulk Density (g/cm³)	Impedance 10^5 g/cm³/s	Heat Cond. (R.T.) $\left(\frac{\text{mcal}}{\text{cm·s·°C}}\right)$	Remarks
				Vert.	Horiz.	Density (g/cm³)	Porosity (%)	W.C. (%)	Porosity (%)	Density (g/cm³)	G.D. (g/cm³)				
Hole 465															
1	1	50–60	0–1			1.66	62.3								
	1	55				1.66	62.3							2.82	Nannofossil ooze and foraminifer nannofossil ooze
2	1	60–80	1.0–10.5			1.54	69.3								
	2	60–90				1.50	71.9								
	3	20–40				1.47	73.2								
	4	50–70				1.51	70.6								
	4	111				1.55	68.7							3.62	
	5	60–80				1.53	70.0								
3	1	90–110	10.5–20.0			1.51	71.2								
	2	60–90				1.50	71.9	36.8	(144–150)						
	3	50–100				1.54	69.3								
	3	111				1.55	68.7							3.54	
	4	30–50				1.56	68.1								
4	1	60–100	20.0–29.5			1.54	69.3								
	2	74												3.80	
	3	50–100				1.57	67.4								
5	1	60–90	29.5–39.0			1.52	70.6								
	3	110												3.55	
	5	60–90				1.56	68.1								
6	2	60–90	39.0–48.5			1.57	67.4								
	2	75–78			1.56	1.57	67.4						2.45		
	2	83				1.57	67.4							3.35	
	4	60–90				1.58	66.8								
	4	79–81			1.58	1.58	66.8						2.50		
10	2	60–90	77.0–86.5			1.54	69.3								
	2	62–65			1.55	1.54	69.3						2.39		
	2	78				1.54	69.3							3.40	
	3	146–150					35.0								
	4	60–90				1.52	70.6								
	5	50–80				1.54	69.3								
Hole 465A															
3	2	60–90	58.0–67.5			1.44	75.1								
	2	63–65			1.63	1.44	75.1						2.35		Nannofossil ooze and foraminifer nannofossil ooze
	2	89				1.44	75.1							3.12	
	4	60–90				1.57	67.4								
	5	144–150						35.0							
10	2	40–60	124.5–134.0			1.55	62.7								
	2	56–58				1.56	68.1	38.5	62.8	1.67	2.76				
	2	105				1.54	69.3							4.29	
	3	30–40				1.51	71.2								
11	1	125–127	134.0–143.5					34.5	58.4	1.74	2.73				
11	2	40–80				1.61	64.9								
	2	144–150				1.60	65.5	33.0	57.2	1.78	2.78				
	3	40–70				1.61	64.9								
	4	60–70				1.58	66.8								
	4	53				1.58	66.8							3.65	
	4	71				1.58	66.8							3.47	
12	1	60–90	143.5–153.0			1.61	64.9								
	1	110–112				1.59	66.2	34.5	58.5	1.74	2.74				
	1	112				1.59	66.2							3.57	
	1	102–104			1.56	1.59	66.2						2.48		
15	1	60–90	172.0–181.5			1.61	64.9								
	2	40–60				1.61	64.9								
	3	144–150						34.8	59.1	1.74	2.77				
16	1	60–90	181.5–191.0			1.58	66.8								
	2	60–90				1.59	66.2								
	3	60–90				1.62	64.2								
	3	85				1.62	64.2							3.60	
	4	40–70				1.60	65.5								
17	1	60–90	191.0–200.5			1.58	66.8								
	1	40				1.56	68.1							3.49	
18	1	60–90	200.5–210.0			1.62	64.6								
19	3	40–50	210–219.5			1.58	66.8								
20	1	60–90	219.5–229.0			1.57	67.4								
21	4	30–70	229.0–238.5			1.59	66.2								
	4	88–96				1.65	63.0	32.4	55.9	1.77	2.72				
26	1	68–70	276.5–286.0	4.40	4.48	2.52	10.7	5.02	12.2	2.48	2.68	2.50	11.00		Limestone (olive-gray)
27	2	07	286.0–295.5											5.17	Limestone (olive-gray)
		11–13		4.32	4.60	2.57	8.1	6.2	14.7	2.44	2.68	2.51	10.84		Limestone (olive-gray)
28	2	65	295.5–305.0											4.77	Limestone (gray, hard)
		64–66		3.82	3.95	2.54	9.8	6.5	15.5	2.46	2.73	2.50	9.55		Limestone (gray, hard)
29	1	32	305.0–314.5											5.05	Limestone (gray, hard)
		33–35		3.73	3.77	2.48	13.0	7.9	18.8	2.43	2.76	2.46	9.18		
32	1	73	333.5–343.0											4.23	Limestone (gray, soft)
		74–76		3.05	3.28	2.31	23.6	9.1	21.0	2.37	2.73	2.34	7.14		
33	1	49–61	343.0–352.5			2.29	24.2 (W)								
		93–100				2.27	25.9 (W)								
	2	133–150				1.95	44.7 (W)							3.67	Limestone (olive-gray, soft)
		140–142		2.03	2.15	2.04	39.3	19.9	38.5	1.99	2.59	2.02	4.10		Limestone (olive-gray, soft)
34	1	1–3	352.5–362.0	2.64	3.27	2.32	22.6	10.2	22.9	2.31	2.68	2.32	6.12		Limestone (olive-gray, soft)
		39–41				2.19	30.6 (W)								
		104–110				2.05	38.7 (W)								
	2	41–52				1.80	53.9 (W)								
35	1	6–12	362.0–371.5			2.32	22.8 (W)								
		5–7		3.57	3.96	2.49	12.6	6.4	15.1	2.43	2.68	2.46	8.78		

Appendix C. (Continued).

				Velocity (km/s)		Grape			Gravimetric						
Core	Section	Interval (cm)	Sub-bottom Depth (m)	Vert.	Horiz.	Density (g/cm^3)	Porosity (%)	W.C. (%)	Porosity (%)	Density (g/cm^3)	G.D. (g/cm^3)	Mean Wet-Bulk Density (g/cm^3)	Impedance 10^5 g/cm^3/s	Heat Cond. (R.T.) $\left(\frac{\text{mcal}}{\text{cm} \cdot \text{s} \cdot {}^\circ\text{C}}\right)$	Remarks
Hole 465A (Cont.)															
35	1	31-33												5.40	
		38-46				2.47	14.0 (W)								
36	1	52-67	371.5-381.0			1.91	47.0 (W)								
		90-101				1.83	51.9 (W)								
36	1	132-134	375.5-810.0	2.11	2.15	1.96	43.9	20.5	39.4	1.97	2.59	1.97	4.16		Limestone (olive-gray)
		135												3.71	
	2	0-22				1.81	53.1 (W)								
		76-95				1.81	53.0 (W)								
37	1	30-37	381.0-390.5			1.84	51.2 (W)								
		52-54		(1.88)	(1.99)	1.94	45.7	23.7	43.4	1.88	2.53	1.91	3.59		Limestone (olive-gray)
		70-80				2.41	17.4 (W)								Limestone (olive gray)
		126-134				2.35	20.8 (W)								Limestone (gray)
	2	0-7				2.36	20.6 (W)								
		16-36				1.77	55.6 (W)								
		64-70				2.26	26.2 (W)								
38	1	100-120	390.5-400.0			1.85	51.0 (W)							3.32	
		105-107		2.09	2.20	1.88	48.8	23.5	42.8	1.87	2.49	1.88	3.93		Limestone (olive-gray)
		44-58				1.82	52.3 (W)								
	2	0-7				1.87	49.7 (W)								
		141-150				2.41	17.6 (W)								
39	1	53-60	400.0-409.5			2.39	18.3 (W)								
	1	118-124				1.91	47.2 (W)								
	2	24-27			5.15										Chert (black)
		45-53				2.42	16.7 (W)							4.02	Limestone (light olive-gray)
		45-47		3.85	4.29	2.53	10.3	6.1	14.7	2.45	2.69	2.49	9.59		Limestone (light olive-gray)
		72-77				2.17	31.6 (W)								Limestone (light olive-gray)
40	1	80-87	409.5-419.0			2.38	18.9 (W)								Limestone (olive gray)
		-85		3.59	4.06	2.54	9.3	6.6	15.7	2.43	2.69	2.49	8.94		Limestone (olive gray)
40	1	100	409.5-419.0											4.76	Limestone (olive-gray) black lamination
40	2	15-21				1.98	43.1(W)*								(Volcanic breccia)
		23-35				2.24	27.6(W)*								
	3	35												4.09	
		35-37		3.51	3.58	(2.31	23.2)*	11.7	26.3	2.31	2.77	2.31	8.11		
						2.30	29.9								
41	1	91-99	419.0-428.5			2.27	32.0(W)								Trachyte
	2	103-109				2.18	36.7(W)							3.18	Trachyte
		108-110		3.43	3.41	2.22	34.7	12.6	27.2	2.20	2.64	2.21	7.58		Trachyte
42	3	24	428.5-438.0											3.43	
		24-26		3.70	3.12	2.19	36.0	13.6	29.1	2.18	2.66	2.19	8.10		Trachyte
43	2	134-136	438.0-447.5	3.53	3.98	2.29	30.5	8.7	19.7	2.34	2.66	2.32	8.19		Trachyte
44	3	124	447.5-457.0											3.37	Trachyte
		120-122		3.70	4.09	2.31	29.8	7.1	16.5	2.40	2.67	2.36	8.73		
45	1	81	457.0-466.5											3.12	Trachyte
		83-85		3.73	4.06	2.33	28.5	7.5	17.4	2.39	2.67	2.36	8.80		Trachyte
	4	80												3.24	Trachyte
		77-79		3.47	4.07	2.20	35.5	9.3	21.1	2.33	2.68	2.27	7.88		Trachyte
46	1	120	466.5-476.0											3.21	Trachyte
		117-119		3.69	4.16	2.35	27.5	8.7	19.9	2.35	2.68	2.35	8.67		

Note: (W) whole core 2 minutes GRAPE; *) Grain density ϱ_g = 2.70 g/cc is assumed, other basalt: ϱ_g = 2.85.

APPENDIX D
Coarse-Fraction (> 62 μm) Components, Site 465

		Planktonic Foraminifers		Coarse-Fraction Components																		P: present R: rare < 5% R-C: rare to common 5–25% C: common C-A: common to abundant 25–50% A: abundant > 50% VA: very abundant > 90% P: poor M: moderate G: good
Sample	Foraminifer Preservation	Whole	Fragments	Benthic Foraminifers	Radiolarians	Sponge Spicules	Ostracodes	Mollusk Fragments	Echinoderm Fragments	*Inoceramus* Fragments	Plant Debris	Ash Shards	Volcanic Glass	Quartz Grains	Mica	Pyrite	Carbonate Rhombs	Glauconite	Chalk Aggregates	Limestone Chips	Chert Fragments	Comments
465-1,CC	P	C	C	R	R				P													
2,CC	G	VA	R-C	R				P	P												R	
3,CC	G	VA	R	R																		
4,CC	G	VA	R	R			P									R			P			
5,CC	G	VA	R-C	R																	C	
6,CC	G	VA	R-C	R			P									P			R		R	
7,CC	G	VA	R-C	R			P									P			R			
8,CC	G	VA	R	R							P?											?wood fiber (possible contaminant)
9,CC	P	P		C			P		R*							R			C		C	*silicified
10,CC	G	VA	R	R																	C	
465A-1,CC	G	VA	R	R																	R	
2,CC	G	VA	R	R			P									P			R-C		P	large benthic forams
3,CC	P	R		R															R-C		A	
6,CC	M	A	R													P					C	
8,CC	M	VA	R	R		P	P		P													
9,CC	M	VA	R	R					P													
10,CC	M	VA	R	R															R			
11,CC	M	VA	R	R																		
12,CC	P	A	R	R					R*							P			C		R	small amount of coarse fraction
15,CC	M	VA	R	R					P										R		P	
16,CC	M	VA	R	R															C			
17,CC	M	A	R	R															C		C	
18,CC	M	VA	R	R			P		P										R-C			
19,CC	M	VA	R	R															R		R-C	
20,CC	M	VA	R	R					P										R		C	
21,CC	M	C	R	R	A											R			R		R	
22,CC																						
23,CC	M	VA	R	R			P		P										R		R	
24,CC	P	A	C											P			P	R			C	
25,CC	P	A	R	R						P				P			P	R	R		C	
27-2, 150	P	C									R**			R						A		**wood fiber (possible contaminant?) and amber flakes some with striate surface (uncertain origin)
28-1 (liner scraping)	P	A									R *			R						C	P	
31-1, 19	P	C									R**			R						A	R	
32-1, 60	P	R												A						C		
33,CC	P	R												R						A		
34-1, 142	P	A												R						C		
35,CC	P	A												R				P		C	C	
35-1, 61	P	A												R-C								
36-2, 38	P	VR																		VA		
37-1, 37	P	A												C								
40-1, 2	P	A												C		R				R	R	
40-1, 115														C		C		R		C		
40-1, 126												C		A		R		R		C		
40-2, 65														A				R				

APPENDIX E
Grain-Size Analysis, Site 465

Hole	Core	Section	Interval (cm)	Sub-bottom Depth (m)	Sand (%)	Silt (%)	Clay (%)	Classification
465	1	1	22.0	0.22	19.2	43.5	37.2	Clayey silt
465	2	1	52.0	1.52	18.3	36.7	45.0	Silty clay
465	2	4	52.0	6.02	3.4	65.4	31.2	Clayey silt
465	3	2	77.0	12.77	1.4	62.3	36.3	Clayey silt
465	4	3	106.0	24.06	5.9	52.7	41.3	Clayey silt
465	5	3	75.0	33.25	4.0	46.4	49.6	Silty clay
465	6	1	110.0	40.10	5.1	44.3	50.6	Silty clay
465	10	5	110.0	84.10	9.0	29.9	61.2	Silty clay
465A	1	1	30.0	39.30	6.0	41.6	52.4	Silty clay
465A	3	1	50.0	58.50	9.0	53.6	37.3	Clayey silt
465A	9	4	46.0	119.96	14.2	34.2	51.6	Silty clay
465A	10	1	120.0	125.70	12.1	33.5	54.4	Silty clay
465A	10	2	62.0	126.62	11.2	50.1	38.7	Clayey silt
465A	11	2	30.0	135.80	0.3	37.1	62.6	Silty clay
465A	11	4	30.0	138.80	3.4	38.7	57.9	Silty clay
465A	12	1	100.0	144.50	5.7	44.5	49.8	Silty clay
465A	15	1	90.0	172.90	1.7	42.4	55.9	Silty clay
465A	16	2	37.0	183.37	3.8	45.3	50.9	Silty clay
465A	17	1	120.0	192.20	3.7	37.6	58.7	Silty clay
465A	18	1	111.0	201.61	0.2	37.3	62.5	Silty clay
465A	19	2	103.0	212.53	3.7	40.9	55.4	Silty clay
465A	20	1	22.0	219.72	4.9	43.2	51.9	Silty clay
465A	29	1	137.0	306.37	1.2	35.1	63.7	Silty clay
465A	37	1	104.0	382.04	18.7	40.6	40.8	Silty clay
465A	38	2	83.0	392.83	3.7	40.6	55.7	Silty clay

SITE 465 HOLE CORE 1 CORED INTERVAL 0.0 to 1.0 m

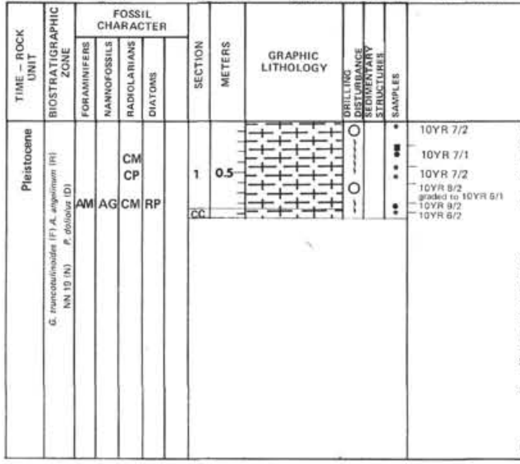

LITHOLOGIC DESCRIPTION

NANNOFOSSIL FORAMINIFER OOZE, highly disturbed to soupy. Nannofossil foraminifer ooze light gray (10YR 7/1 and 7/2) and white (10YR 8/2) in color. A layer of gray (10YR 6/1) is between 60 and 75 cm. The Core-Catcher is light brownish gray (10YR 6/2).

SMEAR SLIDE SUMMARY %

	1-5	1-38	1-50	CC
Quartz	—	Tr	—	—
Feldspar	—	—	—	—
Carbonate unsp.	10	5	5	6
Recrystallized SiO_2	Tr	Tr	—	—
Foraminifers	60	45	34	35
Nannofossils	30	50	60	59
Radiolaria	Tr	Tr	1	—
Sponge spicules	—	Tr	Tr	—

Silica and Iron Content: 1-26
SiO_2 = 6.0%
Fe = 0.57%

Carbonate Content: * 1-30 = 89%

SITE 465 HOLE CORE 2 CORED INTERVAL 1.0 to 10.5 m

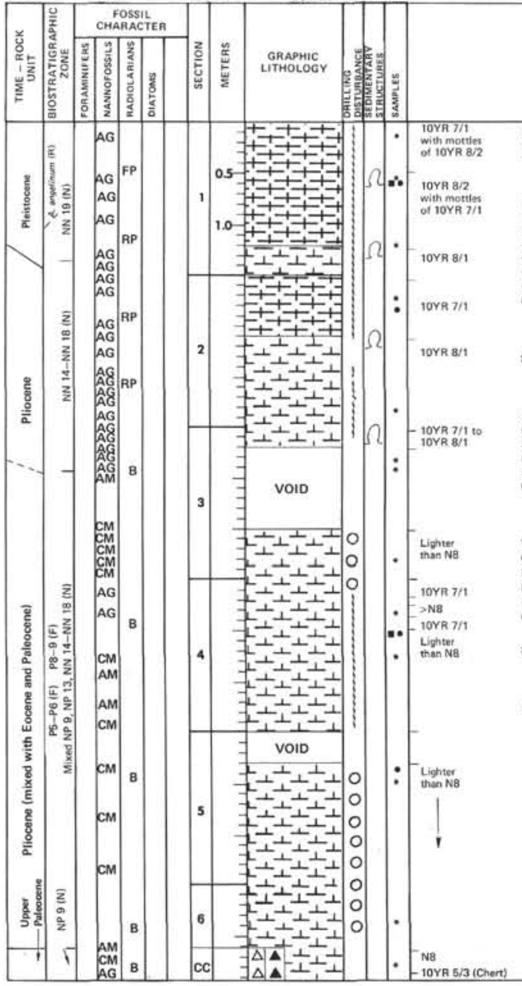

LITHOLOGIC DESCRIPTION

NANNOFOSSIL OOZE AND NANNOFOSSIL FORAMINIFER OOZE, highly disturbed to soupy, mostly white (10YR 8/1, 10YR 8/2, and lighter than N8).

0-120 cm	Nannofossil foraminifer ooze
120-150 cm	Nannofossil ooze
150-210 cm	Foraminifer nannofossil ooze (light gray, 10R 7/1)
210-320 cm	Nannofossil ooze
320-400 cm	Void
400-600 cm	Nannofossil ooze
600-635 cm	Void
635-810 cm	Nannofossil ooze
Core-Catcher	Nannofossil ooze (N8) with white (N8) porcellanite and brown (10YR 5/3) chert.

SMEAR SLIDE SUMMARY %

	2-1-19	1-60	1-120	2-20	2-130	3-30	3-43
Volcanic glass	—	Tr	Tr	—	Tr	Tr	—
Carbonate unsp.	5	—	20	5	15	10	15
Foraminifers	40	32	5	15	5	2	5
Nannofossils	55	68	75	80	80	88	80
Radiolaria	Tr	Tr	Tr	—	Tr	—	—
Chert	—	—	—	—	—	—	—

	3-130	4-40	4-80	5-45	6-40	CC
Volcanic glass	Tr	—	—	3	—	Tr
Carbonate unsp.	15	4	10	—	10	10
Foraminifers	—	5	2	15	5	Tr
Nannofossils	85	91	88	82	85	60
Radiolaria	—	—	—	—	—	Tr
Chert	—	—	—	—	—	30

Silica and Iron Content: 1-60, 4-60
SiO_2 = 6.0%, 3.0%
Fe = 0.51%, 0.09%

Carbonate Content:
* 1-57 = 91%
2-33 = 81%
*4-57 = 95%
5-33 = 90%

SITE 465 HOLE CORE 3 CORED INTERVAL 10.5 to 20.0

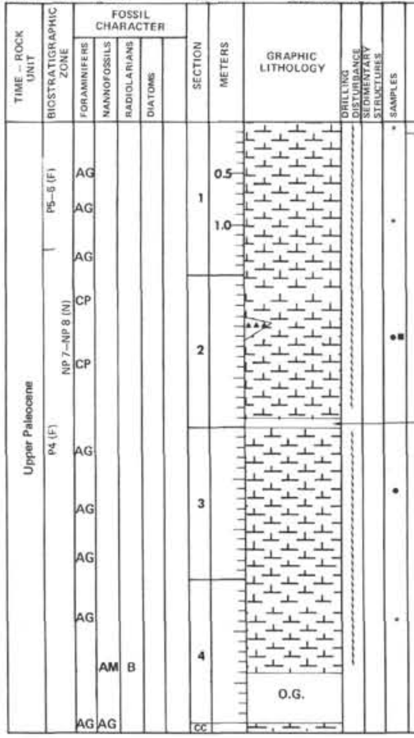

10YR 7/2	
Lighter than N8	
I.W.	

LITHOLOGIC DESCRIPTION

NANNOFOSSIL OOZE, highly disturbed, mostly stark white (lighter than N8). Light gray (10YR 7/2) at top (probable downhole contamination); light gray (N7) chert chips at 195 and 210 cm.

SMEAR SLIDE SUMMARY

	1-5	1-100	4-40
Carbonate unsp.	20	10	—
Foraminifers	8	—	Tr
Nannofossils	72	90	100
Radiolaria	Tr	—	—

Silica and Iron Content: 2-60
SiO_2 = 15%
Fe = 0.04%

Carbonate Content: 3-66 = 90%
*2-65 = 98%

SITE 465 HOLE CORE 4 CORED INTERVAL 20.0 to 29.5 m

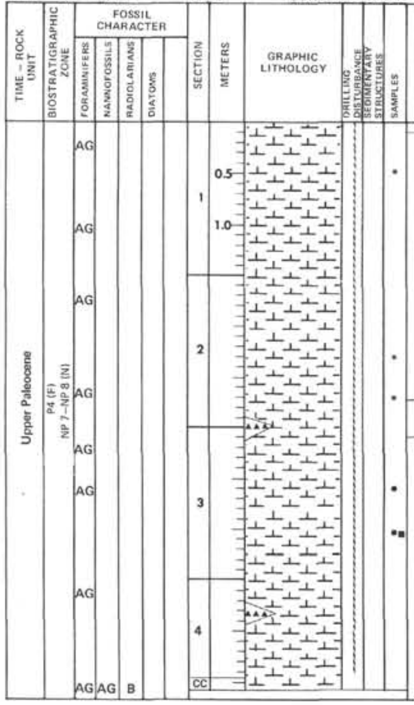

2.5Y 6/4	
Lighter than N8	
5B 8/1	
Lighter than N8	

LITHOLOGIC DESCRIPTION

NANNOFOSSIL OOZE, highly disturbed, mostly stark white (lighter than N8). Light yellowish brown (2.5Y 6/4) at the top (probable down-hole contamination). Light bluish white ooze (5B 8/1) at 260-300 cm. Gray (N6) chips of chert at 300 cm and 480 cm.

SMEAR SLIDE SUMMARY

	1-51	2-117	2-75
Clay	3	—	—
Pyrite	2	—	—
Carbonate unsp.	1	15	5
Foraminifers	6	5	5
Nannofossils	88	80	90

Silica and Iron Content: 3-100
SiO_2 = 1.0%
Fe = 0.16%

Carbonate Content: 3-59 = 88%
*3-103 = 97%

SITE 465 HOLE CORE 5 CORED INTERVAL 29.5 to 39.0 m

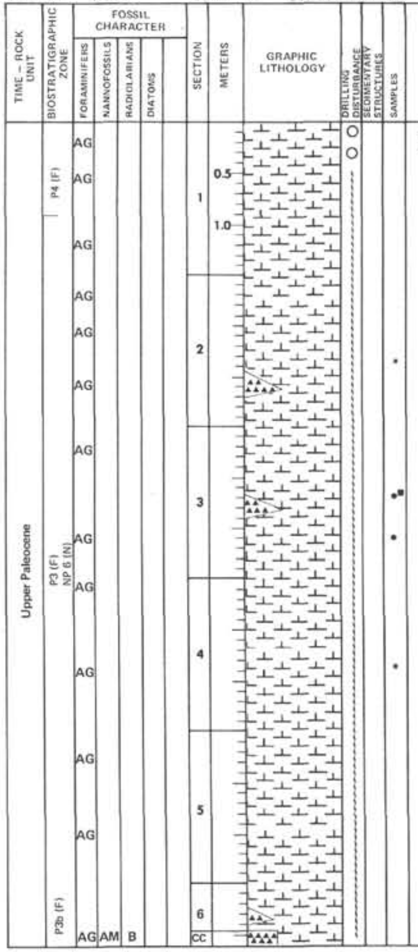

LITHOLOGIC DESCRIPTION

Lighter than N8

NANNOFOSSIL OOZE, highly disturbed, mostly stark white (lighter than N8) ooze. Dark gray (N3) chert fragments are at 255-265 cm and 380 cm and 775-790 cm and Core-Catcher.

SMEAR SLIDE SUMMARY %

	2-80	4-80
Quartz	—	Tr
Volcanic glass	—	Tr
Carbonate unsp.	—	1
Foraminifers	—	2
Nannofossils	100	97

Silica and Iron Content: 3-66
SiO_2 = 1.0%
Fe = 0.04%

Carbonate Content: *3-70 = 96%
3-109 = 88%

SITE 465 HOLE CORE 6 CORED INTERVAL 39.0 to 48.5 m

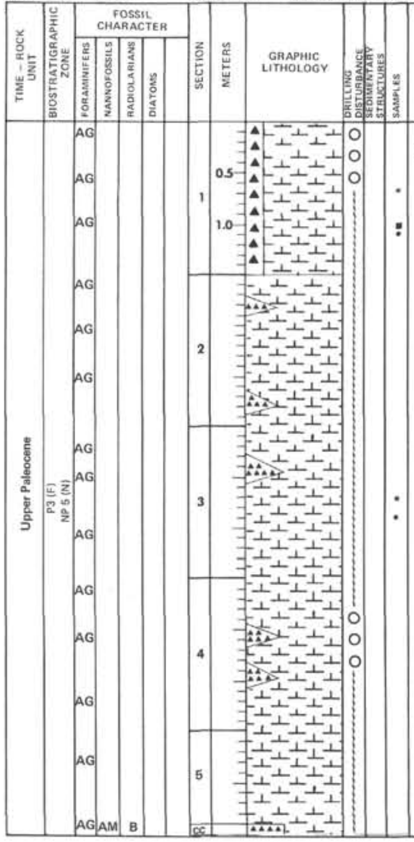

LITHOLOGIC DESCRIPTION

Lighter than N8

NANNOFOSSIL OOZE, highly disturbed, mostly stark white (lighter than N8); small (2-3 cm), angular fragments of gray (N6) to dark gray (N4) chert scattered from 0-150 cm, and larger fragments of the same color chert at 180 cm, 275 cm, 340 cm, 500-520 cm, 545 cm, and Core-Catcher.

SMEAR SLIDE SUMMARY %

	1-70	3-70
Quartz	Tr	Tr
Volcanic glass	Tr	—
Carbonate unsp.	Tr	—
Foraminifers	5	7
Nannofossils	95	93
Radiolaria	Tr	Tr

Silica and Iron Content: 1-100
SiO_2 = 2.0%
Fe = 0.07%

Carbonate Content: *1-105 = 96%
3-99 = 84%

SITE 465 HOLE CORE 7 CORED INTERVAL 48.5 to 58.0 m

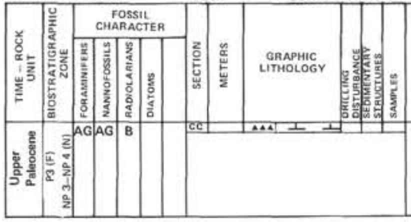

LITHOLOGIC DESCRIPTION

NANNOFOSSIL OOZE AND CHERT, stark white (lighter than N8) nannofossil ooze with fragments of gray (10YR 5/1) and dark gray (10YR 4/1) chert.

SITE 465 HOLE CORE 8 CORED INTERVAL 58.0 to 67.5 m

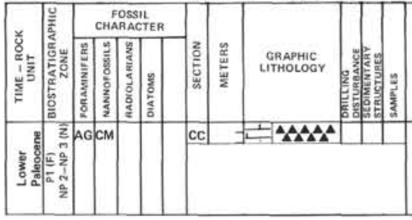

LITHOLOGIC DESCRIPTION

CHERT, chips and pieces of dark gray (10YR 4/1) and gray (10YR 5/1) chert. One piece of chert has a coating of stark white (lighter than N8) **NANNOFOSSIL CHALK.**

SITE 465 HOLE CORE 9 CORED INTERVAL 67.5 to 77.0 m

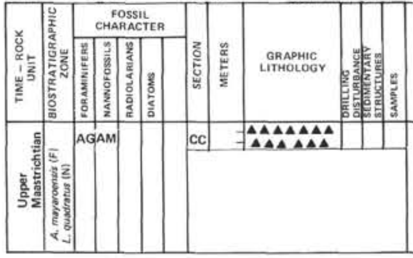

LITHOLOGIC DESCRIPTION

CHERT, several fragments of gray (N6) to light gray (N7) chert.

SITE 465 HOLE CORE 10 CORED INTERVAL 77.0 to 86.5 m

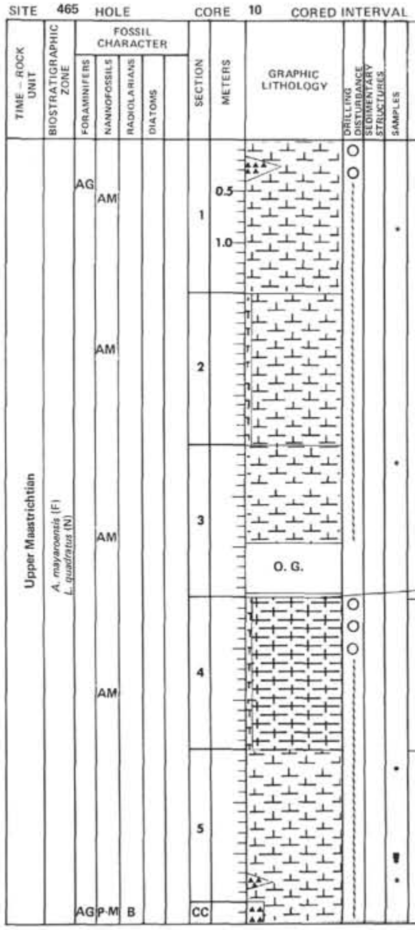

LITHOLOGIC DESCRIPTION

Lighter than N8

NANNOFOSSIL OOZE AND FORAMINIFERA NANNOFOSSIL OOZE, soupy, mostly stark white (lighter than N8); gray (N5) cherts are at 25-28 cm, 260 cm. Chert fragments are scattered throughout the intervals from 150-300 cm, 450-600 cm, and 720-735 cm.

0-395 cm	Nannofossil Ooze
450-600 cm	Foraminifera Nannofossil Ooze
600-750 cm	Nannofossil Ooze

SMEAR SLIDE SUMMARY %

	1-70	3-10	4-70	5-120
Volcanic glass	—	—	—	Tr
Carbonate unsp.	1	—	3	—
Foraminifers	6	6	15	4
Nannofossils	93	94	82	96

Silica and Iron Content: 5-100
SiO_2 = 4.0%
Fe = 0.03%

Carbonate Content: 5-16 = 90%
*5-106 = 94%

I.W.

Lighter than N8

Lighter than N8

SITE 465 HOLE CORE 11 CORED INTERVAL 86.5 to 96.0 m

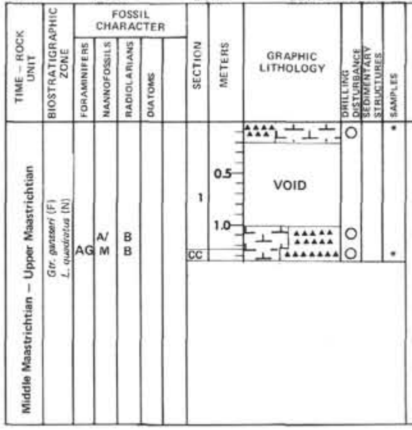

LITHOLOGIC DESCRIPTION

N8

NANNOFOSSIL OOZE AND CHERT, soupy, white (N8) ooze. Numerous small (2-3 cm) fragments of very dark gray (N3), dark gray (N4), gray (N5 and N6), and white (N8) chert scattered throughout. The Core-Catcher contains numerous chert fragments ranging in size from 1 mm to 3 cm. Colors are mostly black (N2) and very dark gray (N3). Fragments are in a soupy matrix of white (N8) nannofossil ooze.

SMEAR SLIDE SUMMARY %

	1-10	CC-20
Feldspar	—	Tr
Quartz	—	Tr
Volcanic glass	—	60
Carbonate unsp.	65	25
Pyrite	—	Tr
Foraminifers	10	—
Nannofossils	20	25
Radiolaria	Tr	—

SITE 465 HOLE A CORE 1 CORED INTERVAL 39.0 to 48.5 m

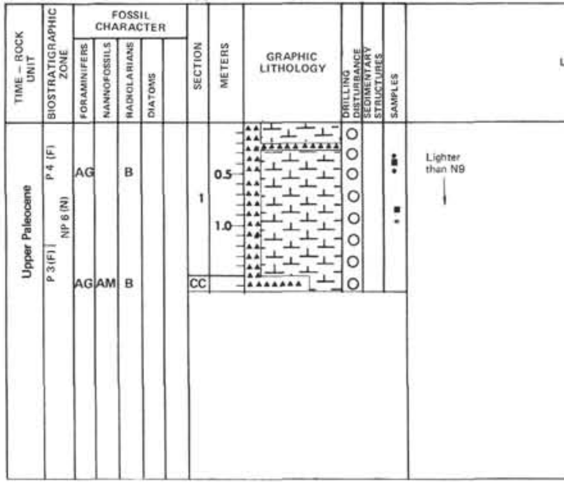

LITHOLOGIC DESCRIPTION

NANNOFOSSIL OOZE
Soupy, white (lighter than N9) ooze. A few small (1–2 mm) **CHERT** fragments are scattered throughout; several larger (>1 cm) fragments are at 145–150 cm. A large piece is at 20–25 cm. Colors of the chert are shades of medium to light gray (N4–N7), with most medium dark gray (N4).

The Core-Catcher has fragments of N4 chert in a matrix of soupy nannofossil ooze.

SMEAR SLIDE SUMMARY: %

	1-100
Carbonate unspec.	2
Foraminifers	2
Nannofossils	95
Radiolarians	1

Silica and Iron Content:	1-37	1-88
SiO_2 =	2.0%	4.0%
Fe =	0.04%	0.37%

Carbonate Content: *1-34 = 97%
1-55 = 93%

SITE 465 HOLE A CORE 2 CORED INTERVAL 48.5 to 58.0 m

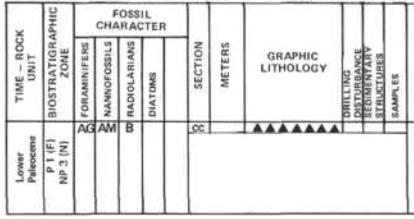

LITHOLOGIC DESCRIPTION

CHERT
The Core-Catcher consists of 4 pieces of chert up to 2 cm long; medium dark gray (N4) with coatings of white (N8) porcellanite(?).

SITE 465 HOLE A CORE 3 CORED INTERVAL 58.0 to 67.5 m

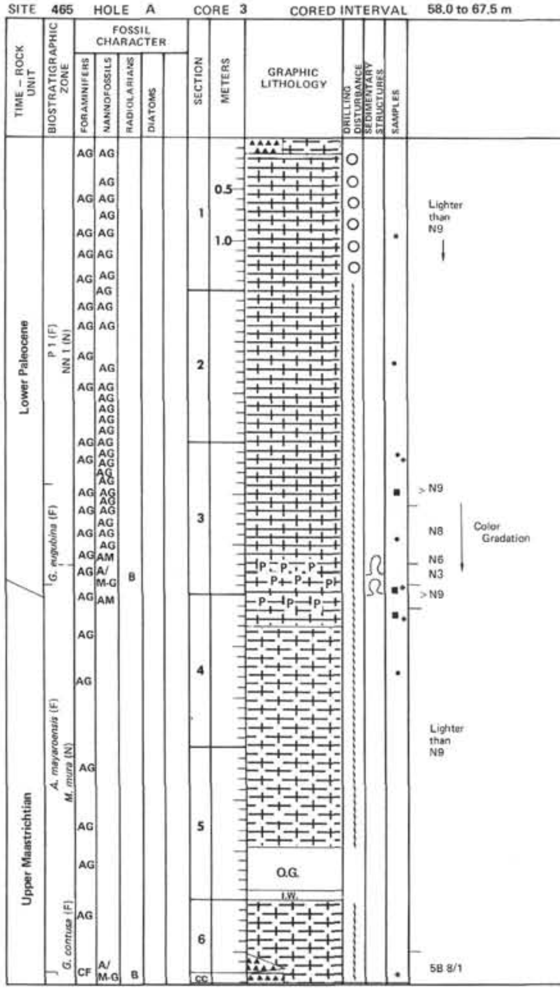

LITHOLOGIC DESCRIPTION

NANNOFOSSIL FORAMINIFERA OOZE with CHERT and PYRITE
Soupy, white (lighter than N9) ooze with medium dark gray (N4) fragments of CHERT, up to 2 cm long at 0–12 cm. Two pieces of very dark gray (N3) chert are at 808–815 cm. Blebs consisting mainly of pyrite (SS 3-143) are at 420–442 cm and are very dark gray (N3). Smearing of the dark color with the overlying white ooze causes a color gradation from 365 cm (white, N8) to 420 cm (medium light gray, N6); mottles of dark gray (N3) and light gray (N7) also occur at 455–480 cm.

The Core-Catcher is a bluish white (5B 8/1) ooze with chert.

SMEAR SLIDE SUMMARY %

	1-100	3-15	3-143 (M)	4-25	CC
Quartz	—	—	—	1	—
Opaque	—	—	20	—	—
Volcanic glass	20	20	Tr	Tr	15
Pyrite	—	—	55	—	—
Carbonate unspec.	30	40	20	59	75
Carbonate rhombs	—	—	—	Tr	—
Foraminifers	40	30	—	30	5
Nannofossils	10	10	5	10	5
Radiolarians	Tr	Tr	Tr	—	—

Silica and Iron Content:	3-11	3-137	4-14
SiO_2 =	2.0%	11%	3.0%
Fe =	0.05%	1.6%	0.07%

Carbonate Content: 2-70 = 90%
*3-14 = 96%
*3-90 = 91%
4-70 = 89%

SITE 465 HOLE A CORE 4 CORED INTERVAL 67.5 to 77.0 m

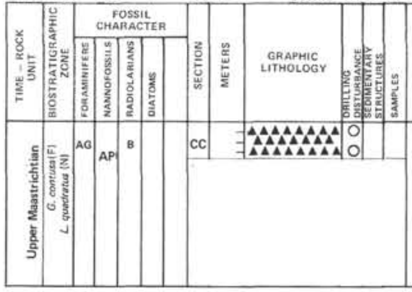

LITHOLOGIC DESCRIPTION

CHERT
A drilling breccia of dark gray (N3) to medium light gray (N6) chert chips ranging from several mm to 7 cm (7 pieces >2 cm); several pieces contain a white (N9) rind of porcellanite.

Site 465A, Core 5, 77.0–86.5 m: No sediment recovered.

SITE 465 HOLE A CORE 6 CORED INTERVAL 86.5 to 96.0 m

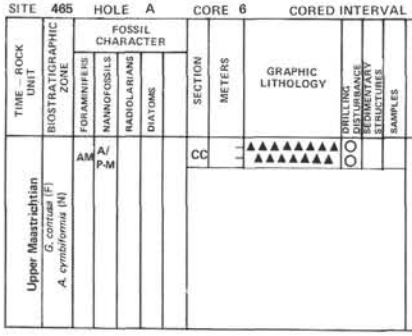

LITHOLOGIC DESCRIPTION

CHERT
A drilling breccia of medium gray (N5) to light gray (N7) translucent chert chips with white (N9) porcellanite rims; chips range in size from several mm to 5 cm (7 pieces >2 cm).

SITE 465 HOLE A CORE 7 CORED INTERVAL 96.0 to 105.5 m

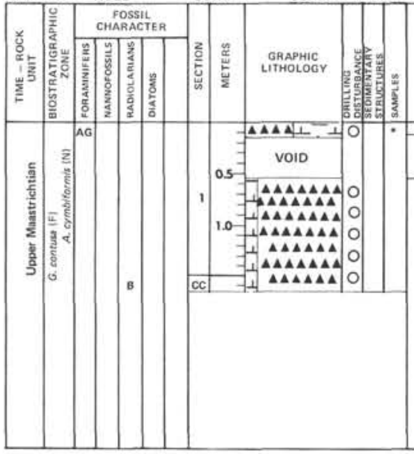

LITHOLOGIC DESCRIPTION

Lighter than N9

NANNOFOSSIL OOZE
0–10 cm: A drilling breccia containing soupy white (lighter than N9) ooze with chert fragments ranging in size from <1 mm to 4 mm.

CHERT
55–165 cm: A drilling breccia containing angular, chert fragments ranging in size from <1 mm to 8 cm; their color ranges from very dark gray (N3) to light gray (N7), with some pinkish gray (7.5YR 7/2). Some chert fragments contain rinds of white (N9) porcellanite. Some fragments contain remnants of white NANNOFOSSIL OOZE (as above).

SMEAR SLIDE SUMMARY %

	1-5
Opaques	Tr
Carbonate unspec.	5
Foraminifers	5
Nannofossils	90

SITE 465 HOLE A CORE 8 CORED INTERVAL 105.5 to 115.0 m

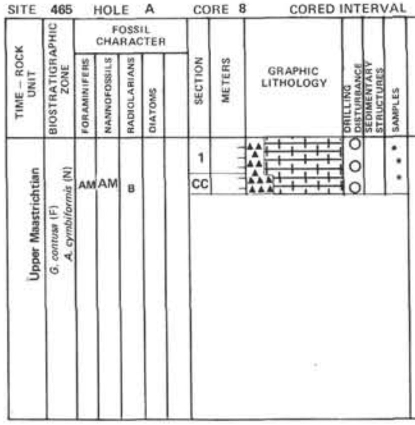

LITHOLOGIC DESCRIPTION

> N9

FORAMINIFER NANNOFOSSIL OOZE
A highly disturbed soupy white (lighter than N9) ooze. Fragments of gray CHERT are scattered throughout. The largest (about 5 cm) is at 35 cm and is dark gray (N4). A dark bleb at about 50 cm contains pyrite and chert chips.

SMEAR SLIDE SUMMARY %

	1-22	CC-8
Chert	—	2
Volcanic glass	Tr	—
Carbonate unspec.	20	10
Foraminifers	20	15
Nannofossils	60	71
Pyrite	—	2

Carbonate Content: *1-14 = 97%

SITE 465 HOLE A CORE 9 CORED INTERVAL 115.0 to 124.5 m

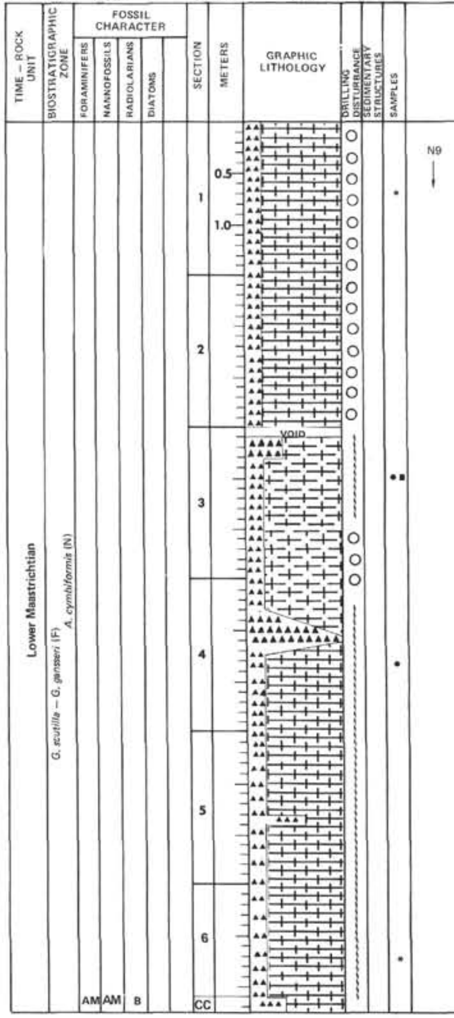

LITHOLOGIC DESCRIPTION

FORAMINIFER NANNOFOSSIL OOZE
A highly disturbed soupy white (N9) ooze. A few small fragments (most several mm) of chert occur throughout mixed in with ooze; most are light to medium gray (N7–N4). Concentrations of chert fragments occur at 310–330 cm and 480–520 cm. Inoceramus fragments, about 1 cm thick and up to 3.5 cm in diameter occur at about 290 cm, 320 cm, and 480 cm.

SMEAR SLIDE SUMMARY %

	1-75	6-75
Quartz	—	1
Opaques	—	Tr
Carbonate unspec.	10	15
Foraminifers	20	15
Nannofossils	70	69
Radiolarians	—	Tr

Silica and Iron Content: 3-48
SiO_2 = 2.0%
Fe = 0.03%

Carbonate Content: *3-51 = 98%
4-82 = 81%

SITE 465 HOLE A CORE 10 CORED INTERVAL 124.5 to 134.0 m

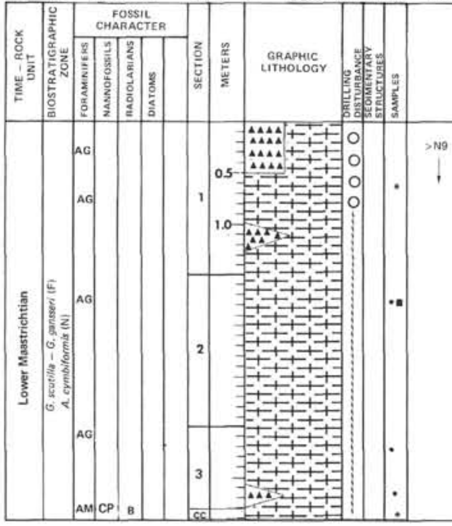

LITHOLOGIC DESCRIPTION

FORAMINIFER NANNOFOSSIL OOZE
A highly disturbed soupy white (lighter than N9) ooze. Chert fragments are at approximately 0–47 cm, 105–115 cm, 360–370 cm, and are gray (N6) to light gray (N7) in color.

SMEAR SLIDE SUMMARY %

	1-60	CC-5
Feldspar	—	Tr
Foraminifers	25	15
Nannofossils	75	85

Silica and Iron Content: 2-30
SiO_2 = 2.0%
Fe = 0.02%

Carbonate Content: *2-29 = 97%
*3-29 = 97%
3-64 = 96%

SITE 465 HOLE A CORE 11 CORED INTERVAL 134.0 to 143.5 m

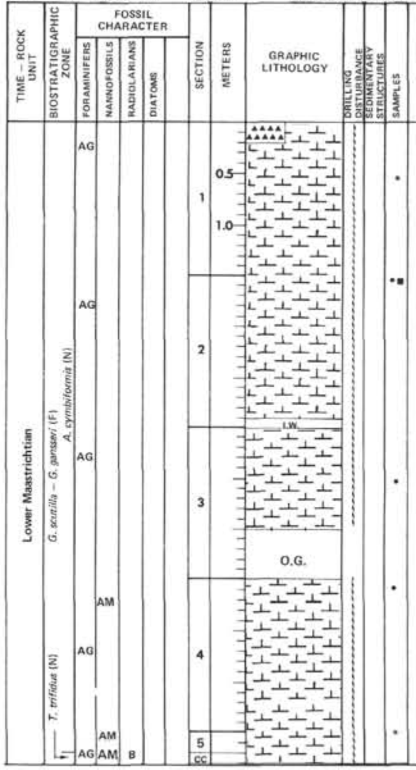

LITHOLOGIC DESCRIPTION

>N9

NANNOFOSSIL OOZE
A highly disturbed white (lighter than N9) ooze.
Chert fragments are at 0–20 cm (dark gray, N4).

SMEAR SLIDE SUMMARY %

	1-60	3-60	CC-5
Feldspar	—	—	Tr
Volcanic glass	—	—	5
Rexl. SiO_2	—	—	5
Carbonate unspec.	15	—	—
Foraminifers	Tr	9	25
Nannofossils	85	91	65

Silica and Iron Content: 2-12
SiO_2 = 1.0%
Fe = 0.03%

Carbonate Content: *2-10 = 98%
3-60 = 96%
*4-10 = 97%

SITE 465 HOLE A CORE 12 CORED INTERVAL 143.5 to 153.0 m

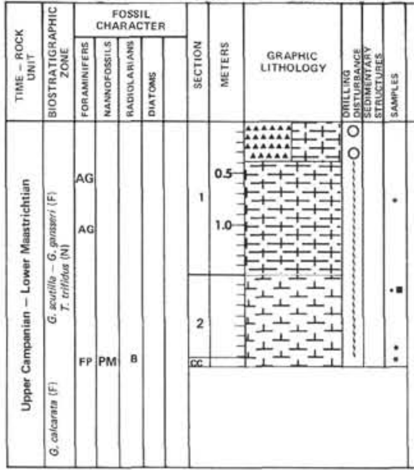

LITHOLOGIC DESCRIPTION

N9

FORAMINIFER NANNOFOSSIL OOZE and NANNOFOSSIL OOZE
A highly disturbed white (N9) ooze.
0–40 cm: Drilling breccia of ooze and chert fragments, 2 mm to 4 cm, very dark gray (N3) to light gray (N7).
An odor of H_2S was apparent when the core was opened.

SMEAR SLIDE SUMMARY %

	1-80	CC-10
Opaques	Tr	—
Carbonate unspec.	40	50
Foraminifers	10	1
Nannofossils	50	49

Silica and Iron Content: 2-13
SiO_2 = 6.8%
Fe = 0.03%

Carbonate Content: *2-10 = 97%
2-72 = 94%

SITE 465 HOLE A CORE 13 CORED INTERVAL 153.0 to 162.5 m

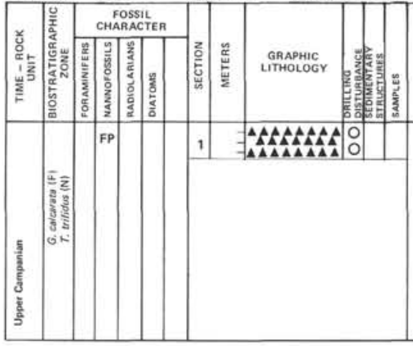

LITHOLOGIC DESCRIPTION

CHERT
Fragments of chert (drilling breccia).
The dominant color is medium dark gray (N4) with some medium gray (N5) and light gray (N7); several pieces have a white (N9) rind of porcellanite.

An inoceramus fragment, 3 cm long and 9 mm thick is at 28–31 cm.

SITE 465 HOLE A CORE 14 CORED INTERVAL 162.5 to 172.0 m

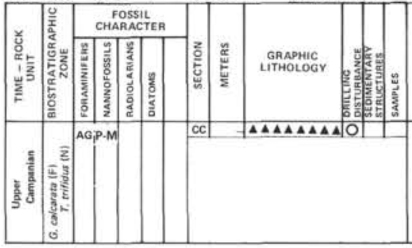

LITHOLOGIC DESCRIPTION

CHERT
Drilling breccia of small (several mm) chert fragments, mostly in shades of light gray (N6 + N7). Several fragments of inoceramus several mm long.

SITE 465 HOLE A CORE 15 CORED INTERVAL 172.0 to 181.5 m

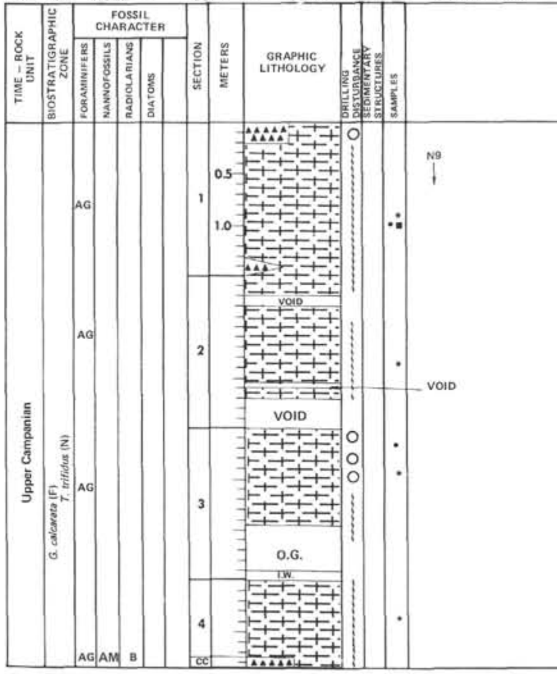

LITHOLOGIC DESCRIPTION

FORAMINIFER NANNOFOSSIL OOZE
A highly disturbed white (N9) ooze, stiff, but not firm enough to be called chalk.

Chert is found at 0–22 cm and in the Core-Catcher. There are numerous fragments, most several mm in size and in various shades of medium to light gray (N4–N7).

SMEAR SLIDE SUMMARY %

	1-100	2-85	3-50	4-35
Carbonate unspec.	—	—	10	5
Foraminifers	15	10	10	10
Nannofossils	85	90	80	85

Silica and Iron Content: 1-100
SiO_2 = 2.0%
Fe = 0.06%

Carbonate Content: *1-106 = 98%
3-20 = 93%

SITE 465 HOLE A CORE 16 CORED INTERVAL 181.5 to 191.0 m

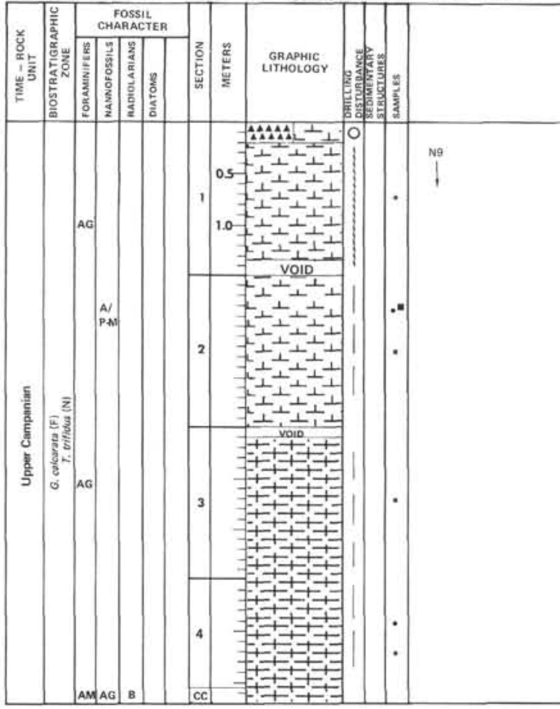

LITHOLOGIC DESCRIPTION

NANNOFOSSIL OOZE and FORAMINIFER NANNOFOSSIL OOZE
Highly to moderately disturbed white (N9) ooze, stiff, but not firm enough to call chalk. Chert occurs as fragments with ooze (0–20 cm is drilling breccia); and are various shades of medium to light gray (N4–N7).

SMEAR SLIDE SUMMARY %

	1-75	2-75	3-75	4-75
Carbonate unspec.	15	10	10	5
Foraminifers	5	Tr	10	12
Nannofossils	85	90	80	83

Silica and Iron Content: 2-30
SiO_2 = 2.0%
Fe = 0.02%

Carbonate Content: *2-33 = 98%
4-37 = 96%

SITE 465 HOLE A CORE 17 CORED INTERVAL 191.0 to 200.5 m

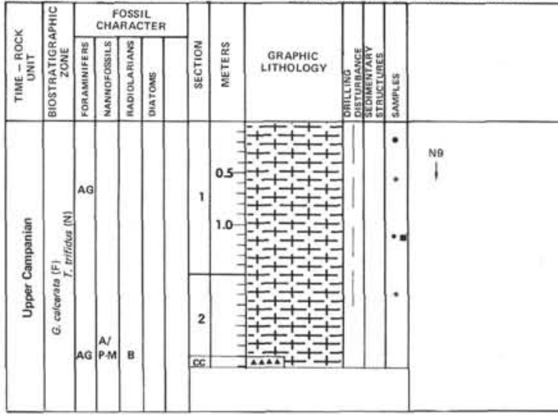

LITHOLOGIC DESCRIPTION

FORAMINIFER NANNOFOSSIL OOZE
A moderately disturbed white (N9) ooze.
A drilling breccia of gray chert chips and ooze, is at 0–4 cm and in the Core-Catcher.

SMEAR SLIDE SUMMARY %

	1-60	2-25
Carbonate unspec.	8	5
Foraminifers	20	5
Nannofossils	72	90
Radiolarians	—	Tr

Silica and Iron Content: 1-110
SiO_2 = 30%
Fe = 0.03%

Carbonate Content: 1-20 = 93%
*1-114 = 95%

SITE 465 HOLE A CORE 18 CORED INTERVAL 200.5 to 210.0 m

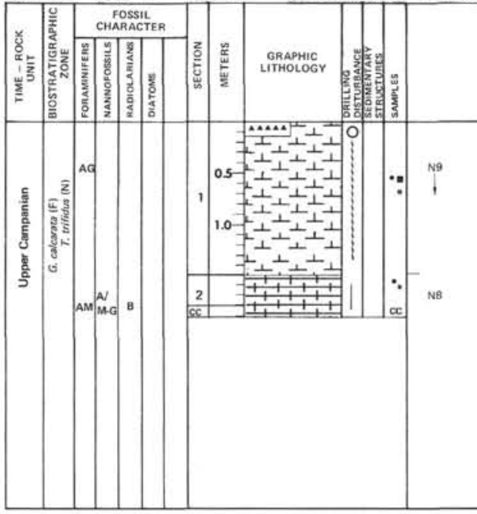

LITHOLOGIC DESCRIPTION

NANNOFOSSIL OOZE and FORAMINIFER NANNOFOSSIL CHALK

0–12 cm: Drilling breccia containing fragments of gray chert in ooze
12–150 cm: Intensely deformed, white (N9) nannofossil ooze; stiff
150–190 cm: Moderately deformed foraminifer nannofossil chalk; very light gray (N8)

SMEAR SLIDE SUMMARY %

	1-75	2-20
Carbonate unspec.	15	8
Foraminifers	8	35
Nannofossils	77	57

Silica and Iron Content: 1-50
SiO_2 = 2.0%
Fe = 0.01%

Carbonate Content: *1-55 = 93%
2-4 = 88%

Carbon-Carbonate: CC-6
% Carbonate 83.3
% Organic Carbon 0.1

SITE 465 HOLE A CORE 19 CORED INTERVAL 210.0 to 219.5 m

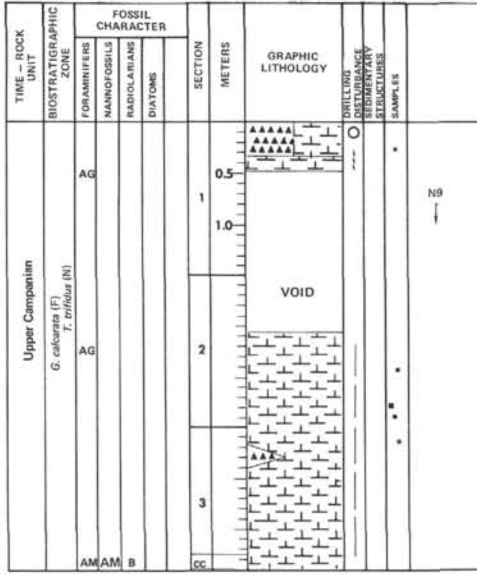

LITHOLOGIC DESCRIPTION

NANNOFOSSIL OOZE

A moderately to highly disturbed white (N9) ooze. From 0–32 cm is a drilling breccia of gray chert chips and ooze.

SMEAR SLIDE SUMMARY %

	1-24	3-20
Carbonate unspec.	15	5
Foraminifers	9	8
Nannofossils	76	87

Silica and Iron Content: 2-127
SiO_2 = 2.0%
Fe = 0.02%

Carbonate Content: 2-92 = 94%
*2-131 = 97%

SITE 465 HOLE A CORE 20 CORED INTERVAL 219.5 to 229.0 m

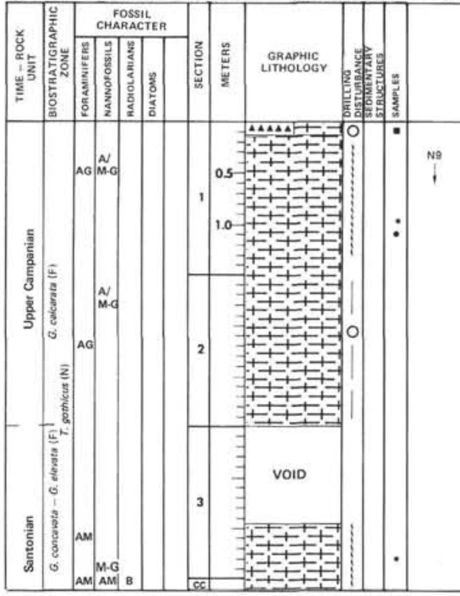

LITHOLOGIC DESCRIPTION

FORAMINIFER NANNOFOSSIL OOZE

Moderately to highly disturbed white (N9) ooze. From 0–10 cm is a drilling breccia of gray chert chips and ooze.

SMEAR SLIDE SUMMARY %

	1-95	3-137
Carbonate unspec.	10	15
Foraminifers	25	30
Nannofossils	65	55

Silica and Iron Content: 1-14
SiO_2 = 4.0%
Fe = 0.04%

Carbonate Content: *1-18 = 98%
1-110 = 94%

SITE 465 HOLE A CORE 21 CORED INTERVAL 229.0 to 238.5 m

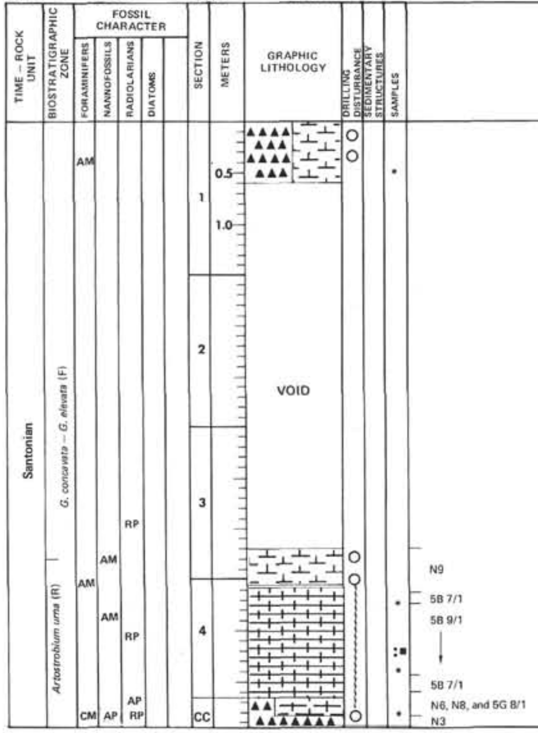

LITHOLOGIC DESCRIPTION

NANNOFOSSIL OOZE, FORAMINIFER NANNOFOSSIL CHALK AND CHERT

0–60 cm: Drilling breccia of gray chert chips in ooze (N9)

420–455 cm: Moderately to highly disturbed white (N9) ooze

455–565 cm: Moderately to highly disturbed chalk. Most is bluish white (5B 9/1), with one thin bed and several streaks of light bluish gray (5B 7/1).

465–494 cm: A drilling breccia of chert fragments and soupy ooze; several large fragments of chert at the base.

SMEAR SLIDE SUMMARY %

	1-45	4-25	4-95	CC
Carbonate unspec.	5	—	40	20
Foraminifers	10	15	10	23
Nannofossils	85	85	50	42
Quartz	—	—	2	5
Opaques	—	—	Tr	—
Radiolarians	—	—	—	10

Silica and Iron Content: 4-67

SiO_2 = 3.0%

Fe = 0.09%

Carbonate Content: *4-71 = 96%

4-75 = 92%

SITE 465 HOLE A CORE 22 CORED INTERVAL 238.5 to 248.0 m

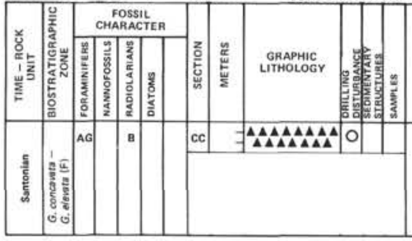

LITHOLOGIC DESCRIPTION

CHERT

Three larger pieces of chert (up to 6 cm long) with smaller chips (several mm). All are medium to dark gray (N3 and N4).

SITE 465 HOLE A CORE 23 CORED INTERVAL 248.0 to 257.5 m

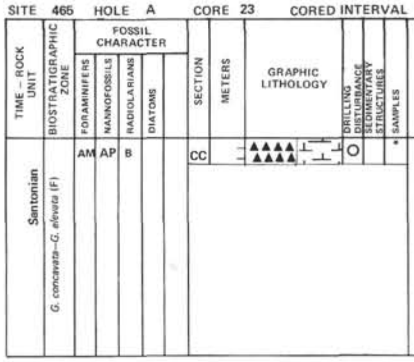

LITHOLOGIC DESCRIPTION

CHERT and NANNOFOSSIL OOZE

0–2 cm: A dark gray (N3) chert.

2–6 cm: White (N9) nannofossil ooze.

6–23 cm: Dark gray to light gray (N3–N6) chips and pieces of chert.

SMEAR SLIDE SUMMARY %

	CC-3
Quartz	10
Opaques	Tr
Carbonate unspec.	20
Foraminifers	9
Nannofossils	61

SITE 465 HOLE A CORE 24 CORED INTERVAL 257.5 to 267.0 m

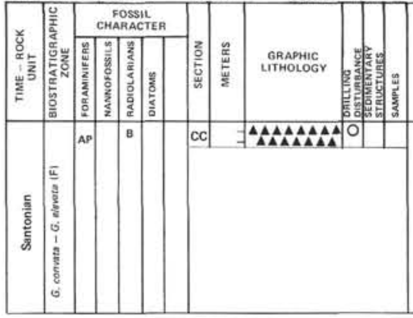

LITHOLOGIC DESCRIPTION

CHERT

One piece (2.5x6.5 cm) of medium dark gray (N4) chert with a light bluish gray (5B 7/1) coating of porcellanite; the rest of the Core-Catcher being drilled breccia of chert chips, 2–4 mm, of various shades of gray (N5, N6, and N7).

SITE 465 HOLE A CORE 25 CORED INTERVAL 267.0 to 276.5 m

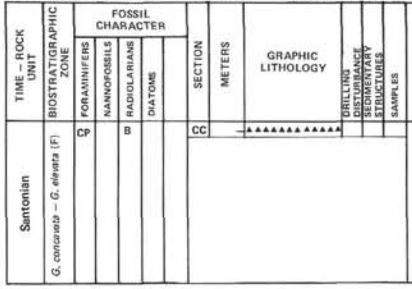

LITHOLOGIC DESCRIPTION

CHERT

One piece of dark gray (N3) chert.

SITE 465 HOLE A CORE 26 CORED INTERVAL 276.5 to 286.0 m

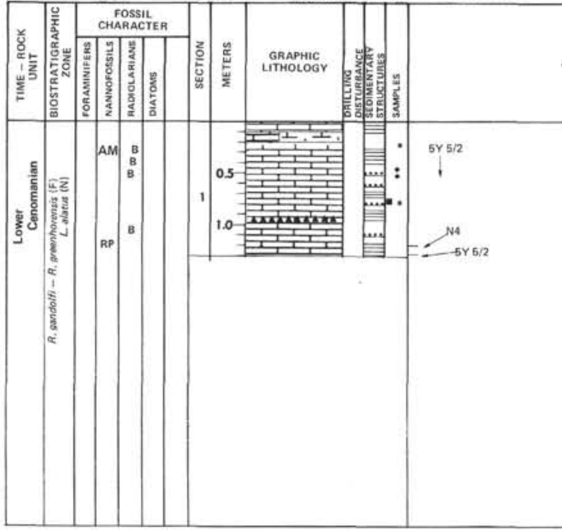

LITHOLOGIC DESCRIPTION

LIMESTONE and NANNOFOSSIL OOZE
Minor amounts of nannofossil ooze, olive gray (5Y 5/2) at 10 cm and 14–16 cm. Black (N2) chert is at 91–96 cm. Limestone, the dominant lithology is olive gray (5Y 5/2) with laminations of slightly lighter and slightly darker colors; turbidites are common as indicated in sedimentary structures column; one bed of dark gray (N4) limestone at 119–125 cm.

SMEAR SLIDE SUMMARY %

	1-15	1-80
Feldspar	1	1
Opaques	—	Tr
Volcanic glass	1	—
Fe/Mn Nodules	3	—
Carbonate unspec.	51	99
Formainifers	3	–
Nannofossils	40	—

Silica and Iron Content: 1-75
SiO_2 = 2.0%
Fe = 0.08%

Carbonate Content: 1-44 = 93%
1-49 = 94%

SITE 465 HOLE A CORE 27 CORED INTERVAL 286.0 to 295.5 m

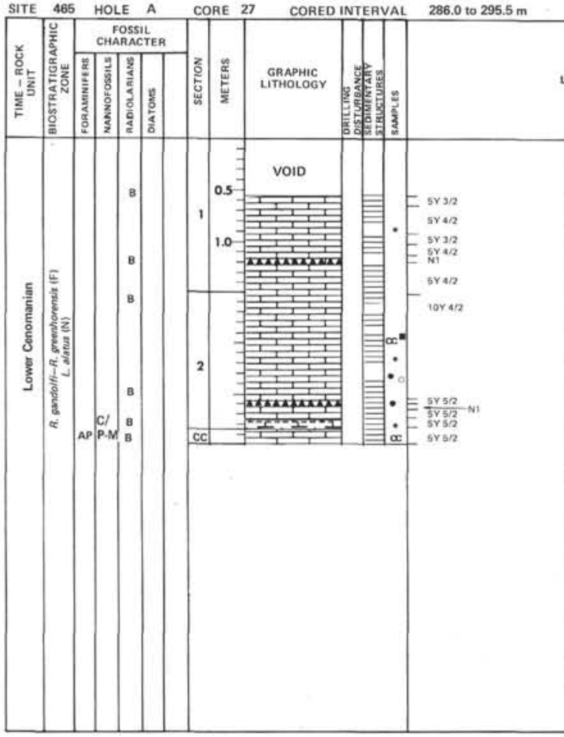

LITHOLOGIC DESCRIPTION

LIMESTONE
Olive gray (5Y 4/2), dark olive gray (5Y 3/2), light olive gray (5Y 5/2), and grayish olive (10Y 4/2) limestone. Most is finely laminated with slightly darker and slightly lighter colors; laminae are mostly very fine with subtle color variations and horizontal streaks (0.5–1 mm) of white specks parallel to stratification. Thin beds of black (N1) chert at 114–119 cm and 259–266 cm. Nannofossil ooze is at 277–283 cm; light olive gray (5Y 5/2) in color. Vertical calcite veins are present from 175–183 cm and 203–230 cm.

SMEAR SLIDE SUMMARY %

	1-80	2-65	2-133
Quartz	—	—	10
Feldspar	2	—	1
Clay	—	—	5
Opaques	—	—	3
Volcanic ash	1	—	3
Zeolites	—	—	5
Carbonate unspec.	97	100	36
Foraminifers	—	—	8
Nannofossils	—	—	30
Radiolarians	—	—	—
Fish remains	—	—	Tr

Silica and Iron Content: 2-48
SiO_2 = 3.0%
Fe = 0.16%

Carbonate Content: 2-89 = 92%
2-110 = 20%

Organic Carbon: 2-89 = 0.50%

Carbon-Carbonate:	2-47	CC-16
% Carbonate	90.0	25.8
% Organic Carbon	0.5	2.3

SITE 465 HOLE A CORE 28 CORED INTERVAL 295.5 to 305.0 m

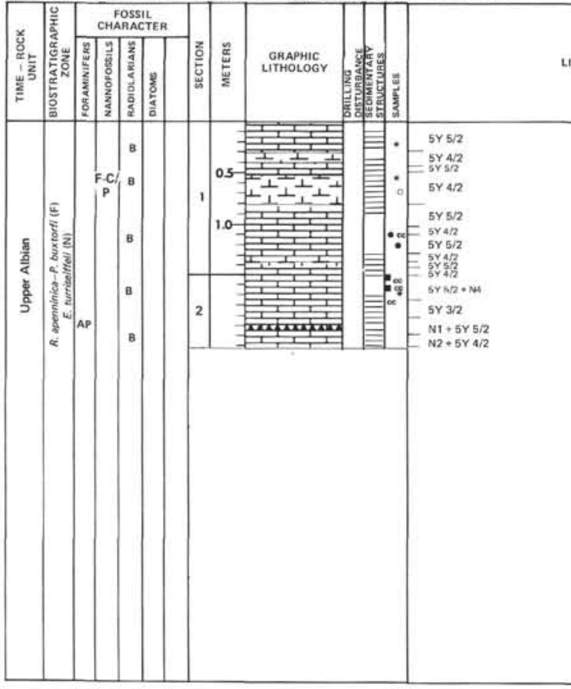

LITHOLOGIC DESCRIPTION

LIMESTONE AND NANNOFOSSIL OOZE
The dominant colors of limestone are olive gray (5Y 4/2 and 5Y 5/2) with beds of black (N2) fine-grained limestone at 124 cm and 145 cm; 150 to 176 cm consists of alternating layers of olive gray (5Y 4/2 and 5Y 5/2) and dark gray (N4) very fine-grained limestones; most olive gray limestones are finely laminated. The laminae are subtle color differences and streaks of white material parallel to stratification. Intervals of olive gray (5Y 4/2) nannofossil ooze at 30–39, 52–80, and 130–136 cm. A bed of black (N2) chert with thinner beds of laminated limestone (5Y 4/2) "sandwiched" within it at 202–208 cm.

SMEAR SLIDE SUMMARY %

	1-20	1-60	2-20
Quartz and Feldspar	—	—	2
Organic	Tr	5	—
Pyrite	—	Tr	—
Zeolite	—	Tr	—
Carbonate unspec.	90	15	91
Nannofossils	—	80	—
Foraminifers	10	—	7

Silica and Iron Content:	2-10	2-19
SiO_2 =	10%	23%
Fe =	3.1%	1.1%

Carbonate Content: 1-111 = 93%
1-123 = 70%

Organic Carbon: 1-65 = 4.6%

Carbon-Carbonate:	1-107	2-9	2-15	2-20
% Carbonate	10.8	80.8	70.0	55.8
% Organic Carbon	1.9	0.5	0.1	0.1

SITE 465 HOLE A CORE 29 CORED INTERVAL 305.0 to 314.5 m

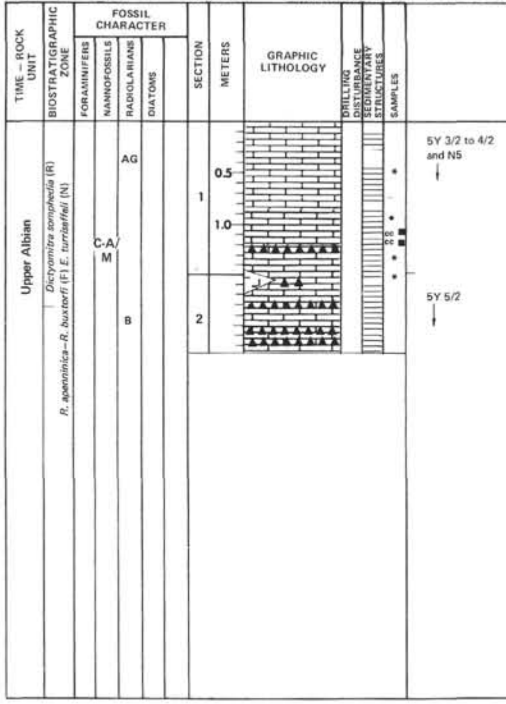

LITHOLOGIC DESCRIPTION

LIMESTONE

Alternating beds of gray (N5) and olive gray (5Y 5/2) to dark olive gray (5Y 3/2) limestone; olive-colored beds usually finely laminated; most beds are on the order of 2–5 cm. Nannofossil ooze is at 150–154 cm; olive gray (5Y 5/2) in color. Beds and nodules of dark gray (5Y 3/1) and black (N2.5) chert at 124–128, 154, 174, 207–208, and 215–218 cm.

SMEAR SLIDE SUMMARY %

	1-45	1-138	2-1
Feldspar	1	Tr	Tr
Opaques	—	Tr	—
Volcanic glass	2	—	—
Pyrite	1	—	—
Fe/Mn Nodules	—	—	2
Zeolites	—	Tr	—
Carbonate unspec.	60	85	25
Foraminifers	Tr	—	20
Nannofossils	35	15	53
Radiolarians	1	—	—

Silica and Iron Content:	1-109[a]	1-117[b]
SiO_2 =	8.0%	23%
Fe =	1.6%	1.3%

Carbonate Content: 1-93 = 58%

Organic Carbon: 1-93 = 0.04%

Carbon-Carbonate:	1-110	1-118
% Carbonate	75.8	55.8
% Organic Carbon	0.3	0.4

a = from olive gray laminated beds

b = from gray massive beds

SITE 465 HOLE A CORE 30 CORED INTERVAL 314.5 to 324.0 m

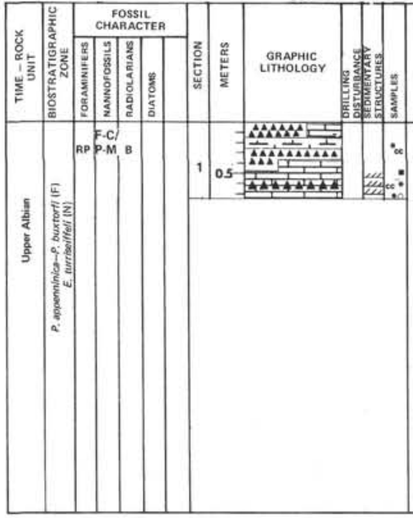

LITHOLOGIC DESCRIPTION

LIMESTONE, CHERT, and NANNOFOSSIL OOZE

An olive gray (5Y 5/2), finely laminated and cross-laminated limestone at 47–49 cm, 54–56 cm, and 60–63 cm. Olive gray (5Y 5/2) nannofossil ooze is at 18–25 cm. Black (N2.5) chert is at 0–3 cm, 8–16 cm, 26–45 cm, and 59–61 cm.

SMEAR SLIDE SUMMARY %

	1-20	1-65
Clay	10	—
Carbonate unspec.	2	90
Foraminifers	10	10
Nannofossils	78	—

Silica and Iron Content:	1-59
SiO_2 =	7.2%
Fe =	0.6%

Carbonate Content: 1-71 = 90%

Organic Carbon: 1-71 = 0.30%

Carbon-Carbonate:	1-23	1-58
% Carbonate	32.5	70.8
% Organic Carbon	6.1	1.7

SITE 465 HOLE A CORE 31 CORED INTERVAL 324.0 to 333.5 m

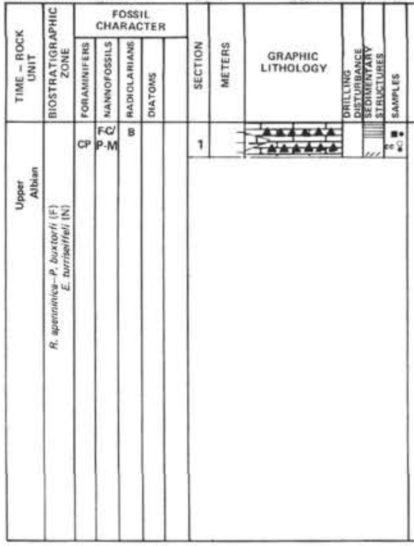

LITHOLOGIC DESCRIPTION

LIMESTONE, CHERT, and NANNOFOSSIL OOZE

Olive gray limestone (5Y 5/2) finely laminated at 0–8 cm; medium dark gray (N4) at 28–34 cm with faint laminae and cross-stratification. Black (N2.5) chert at 7–12 cm and 25–27 cm. Olive gray (5Y 5/2) nannofossil ooze at 16–23 cm.

SMEAR SLIDE SUMMARY %

	1-22
Clay	2
Pyrite	3
Carbonate unspec.	25
Foraminifers	5
Nannofossils	65

Silica and Iron Content:	1-13
SiO_2 =	2.0%
Fe =	0.07%

Carbonate Content: 1-15 = 93%

Organic Carbon: 1-15 = 0.36%

Carbon-Carbonate:	1-14
% Carbonate	87.5
% Organic Carbon	0.7

SITE 465 HOLE A CORE 32 CORED INTERVAL 333.5 to 343.0 m

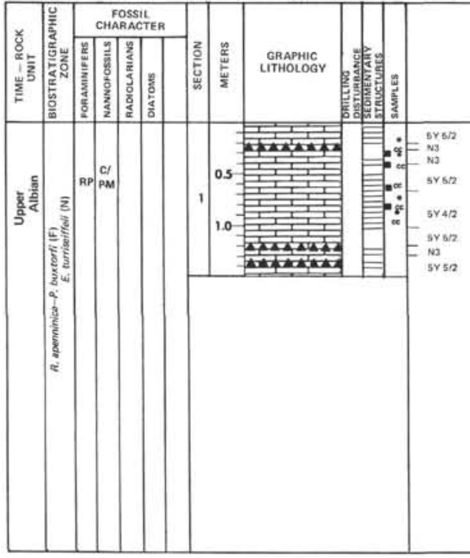

LITHOLOGIC DESCRIPTION

LIMESTONE AND CHERT

Olive gray (5Y 5/2 and 4/2), finely laminated (< 1 mm) limestone alternating with beds of very dark gray (N3) finely crystalline limestone, massive to faintly laminated. Black (N3) chert at 23–27 cm, 119–120 cm and 137–140 cm.

SMEAR SLIDE SUMMARY %

	1-15	1-35	1-79
Quartz and Feldspar	—	5	—
Clay	—	85	—
Pyrite	Tr	10	8
Carbonate unspec.	70	—	92
Foraminifers**	30	—	—

** clots of finely crystalline carbonate, some of which exhibit relict structure of foraminifers

Silica and Iron Content:	1-32	1-39	1-64	1-85
SiO_2 =	14%	12%	4%	4%
Fe =	0.76%	0.17%	0.24%	0.29%

Carbonate Content: 1-94 = 81%

Carbon-Carbonate:	1-32	1-38	1-63	1-84	1-96
% Carbonate	76.6	59.1	90.8	25.0	90.8
% Organic Carbon	0.2	2.0	0.1	7.1	3.8

SITE 465 HOLE A CORE 33 CORED INTERVAL 343.0 to 352.5 m

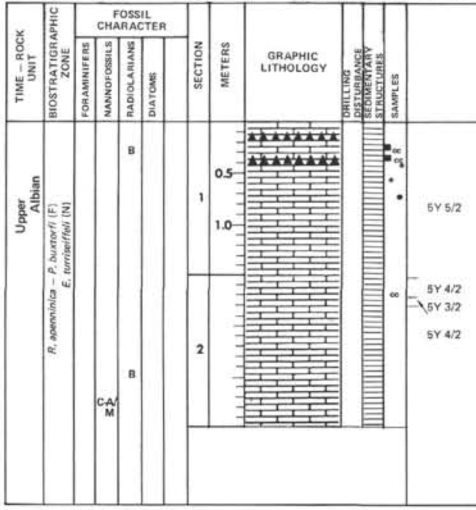

LITHOLOGIC DESCRIPTION

LIMESTONE and CHERT

Olive gray (5Y 5/2 and 4/2) and dark olive gray (5Y 3/2), finely laminated (<1 mm) limestone with layers of gray (N4) finely crystalline, massive-appearing limestone at 29–32, 76 and 118 cm. Black (N2) chert chips at 13–15 cm and 37–38 cm.

SMEAR SLIDE SUMMARY %

	1-30	1-55
Pyrite	3	33
Carbonate unspec.	92	1
Foraminifers **	5	55

** Brown clots, up to 0.1 mm, of finely crystalline calcite; some exhibit structures of foraminifers.

Silica and Iron Content:	1-21	1-29 (gray, N4)
SiO_2 =	3.0%	23%
Fe =	0.14%	1.3%

Carbonate Content: 1-65 = 88%

Carbon-Carbonate:	1-22	1-30	2-20
% Carbonate	88.3	59.1	89.1
% Organic Carbon	0.7	0.1	8.6

SITE 465 HOLE A CORE 34 CORED INTERVAL 352.5 to 362.0 m

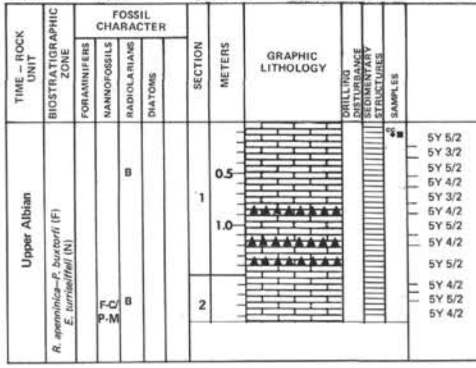

LITHOLOGIC DESCRIPTION

LIMESTONE and CHERT

Olive gray (5Y 5/2 and 4/2), and dark olive gray (5Y 3/2), finely laminated (<1 mm) limestone. Black (N2) chert at 83, 113–117, and 138–140 cm.

Silica and Iron Content:	1-10
SiO_2 =	2.0%
Fe =	0.07%

Carbonate Content: 1-15 = 82%

Carbon-Carbonate:	1-9
% Carbonate	89.1
% Organic Carbon	0.7

SITE 465 HOLE A CORE 35 CORED INTERVAL 362.0 to 371.5 m

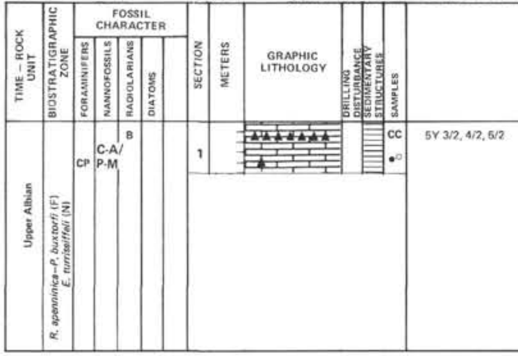

LITHOLOGIC DESCRIPTION

LIMESTONE

Olive gray (5Y 5/2 and 4/2) and dark olive gray (5Y 3/2) finely laminated (<1 mm) limestone. Chert (black, N2) is at 17–19 cm and 40 cm.

Carbonate Content: 1-37 = 84%

Organic Carbon: 1-37 = 1.89%

Carbon-Carbonate:	1-10
% Carbonate	52.5
% Organic Carbon	4.4

SITE 465 HOLE A CORE 36 CORED INTERVAL 371.5 to 381.0 m

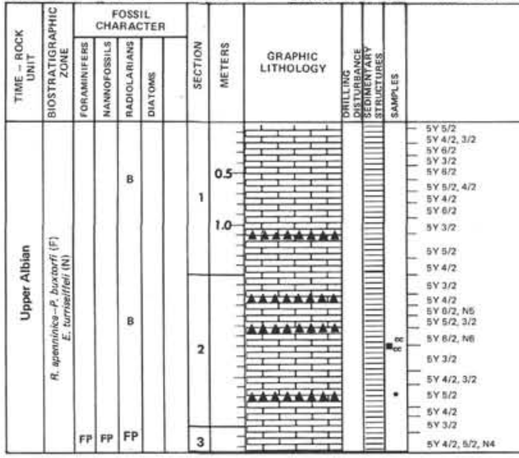

LITHOLOGIC DESCRIPTION

LIMESTONE and CHERT

Olive gray (5Y 5/2 and 4/2), light olive gray (5Y 6/2), and dark olive gray (5Y 3/2) limestone, with thin beds of massive-appearing, dark gray (N4 and N5) limestone at 183–185, 206–207, 212–215, and 320–323 cm. Black (N2) chert is at 115–118, 178–180, 208–209, and 273–277 cm.

Silica and Iron Content:	2-62
SiO_2 =	2.0%
Fe =	0.15%

Carbonate Content: 2-120 = 85%

Carbon-Carbonate:	2-61	2-64
% Carbonate	84.1	61.6
% Organic Carbon	0.5	0.5

SITE 465 HOLE A CORE 37 CORED INTERVAL 381.0 to 390.5 m

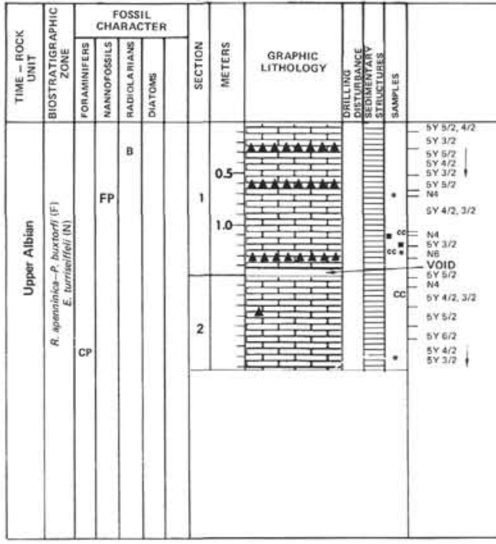

LITHOLOGIC DESCRIPTION

LIMESTONE

Olive gray (5Y 5/2 and 4/2), dark olive gray (5Y 3/2), and light olive gray (5Y 6/2) finely laminated (<1 mm) limestone. Beds of gray (N4, N5, and N6) massive-appearing to faintly laminated limestone at 75–77, 83, 89, 110–113, 139–142, and 157–161 cm. Black (N2) chert is at 21–23, 65–66, and 132–136 cm.

SMEAR SLIDE SUMMARY %

	1-70	1-125	2-82
Quartz and Feldspar	—	2	Tr
Clay	—	—	10
Pyrite	Tr	8	—
Carbonate unspec.	95	85	60
Foraminifers**	5	5	20
Nannofossils	—	—	10

** Brown clots of carbonate, probably are recrystallized foraminifers.

Silica and Iron Content:		1-104	1-111
SiO_2	=	8.2%	2.0%
Fe	=	0.50%	1.0%

Carbon-Carbonate:	1-103	1-112	2-20
% Carbonate	55.0	44.2	91.6
% Organic Carbon	3.5	0.1	7.5

SITE 465 HOLE A CORE 38 CORED INTERVAL 390.5 to 400.0 m

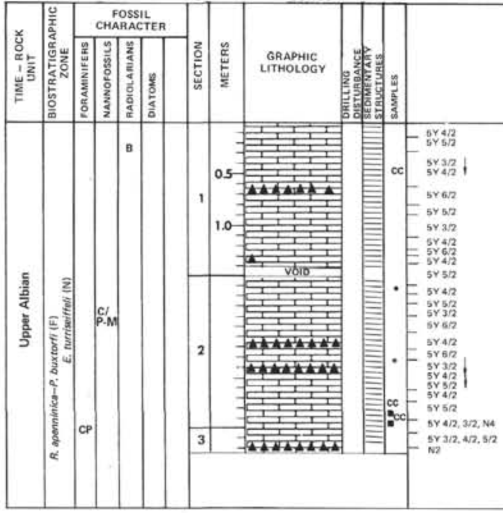

LITHOLOGIC DESCRIPTION

LIMESTONE

Olive gray (5Y 5/2 and 4/2), dark olive gray (5Y 3/2), and light olive gray (5Y 6/2) finely laminated (<1 mm) limestone. CHERT: Black (N2) chert at 70–71, 133, 216–218, 230–232 and 322–327 cm.

SMEAR SLIDE SUMMARY %

	2-89
Pyrite	Tr
Carbonate unspec.	80
Foraminifers**	20

** Light brown clots of finely crystalline carbonate up to 0.06 mm probably replaced foraminifers.

Silica and Iron Content:		2-129	2-137
SiO_2	=	25%	3.0%
Fe	=	1.3%	0.09%

Carbonate Content: 2-15 = 84%

Carbon-Carbonate:	1-47	2-128	2-136
% Carbonate	90.8	90.8	61.6
% Organic Carbon	4.3	0.4	0.2

SITE 465 HOLE A CORE 39 CORED INTERVAL 400.0 to 409.5 m

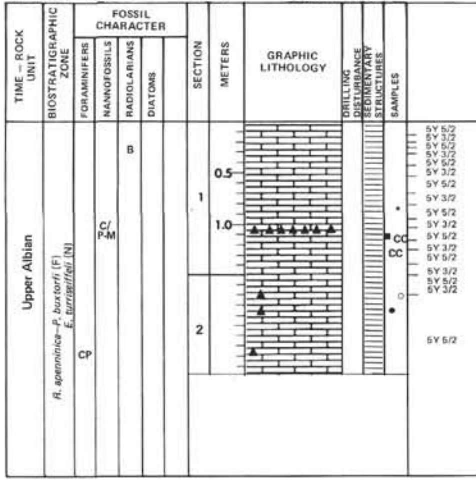

LITHOLOGIC DESCRIPTION

LIMESTONE

Olive gray (5Y 5/2 and 3/2): finely laminated limestone (<1 mm) with two thin beds of very dark gray (N3) limestone at 35–36 cm and 64–65 cm. CHERT: Black (N2) chert at 102–105, 174–176, 186 and 221 cm.

SMEAR SLIDE SUMMARY %

	1-83
Carbonate unspec.	97
Foraminifers	3

Silica and Iron Content:		1-111
SiO_2	=	1.0%
Fe	=	0.05%

Carbonate Content: 2-34 = 83%

Organic Carbon: 2-25 = 0.83%

Carbon-Carbonate:	1-111	1-121
% Carbonate	68.3	90.8
% Organic Carbon	2.4	3.4

SITE 465 HOLE A CORE 40 CORED INTERVAL 409.5 to 419.0 m

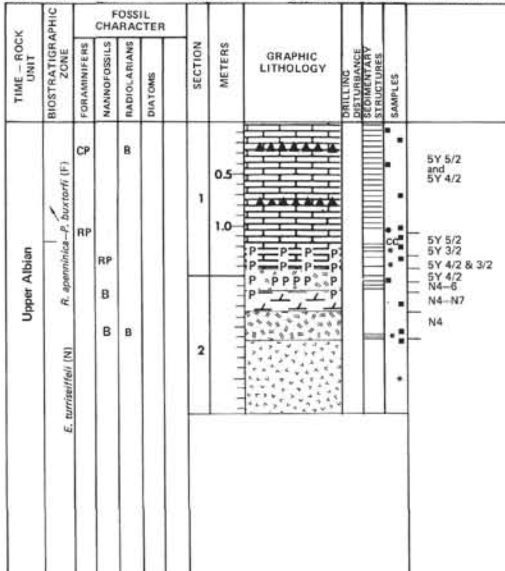

LITHOLOGIC DESCRIPTION

LIMESTONE, VOLCANIC ASH, and TRACHYTE

0–107 cm: Olive gray (5Y 4/2 and 5/2) limestone finely laminated (<1 mm); CHERT: black (N2) at 24–27 and 71–72 cm.

107–141 cm: Limestone whose dominant colors are olive gray (5Y 5/2 and 4/2) and dark olive gray (5Y 3/2) and black (N2); massive to laminated; abundant pyrite, organic-rich layers, and calcite veins.

143–215 cm: Gray (N4 to N7) massive to laminated volcanic ash; abundant pyrite; a bed of clastic dolomite with veins of dolomite is at 166–184 cm (white, N8; gray, N4–N7; very dark olive, 5Y 3/2; and reddish yellow, 7.5YR 8/4); organic-rich layers and dolomite, 143–148 cm.

215–285 cm: Trachyte.

SMEAR SLIDE SUMMARY %

	1-111	1-129	1-138	2-64	2-105
Quartz	2	—	—	—	—
Feldspar		4	—	20	5
Heavy minerals	—	Tr	—	—	—
Clay	10	64	—	74	87
Volcanic glass	15	10	—	2	8
Zeolites	—	1	—	—	Tr
Carbonate rhombs	—	2	—	—	—
Carbonate unspec.	68	15	93	1	Tr
Foraminifers	Tr	—	5	—	—
Nannofossils	—	3	—	—	—
Pyrite	5	1	2	3	Tr

Silica and Iron Content:		1-01	1-29	1-44	1-73	1-104	1-111
SiO_2	=	5.0%	5.5%	3.0%	7.8%	11%	2.0%
Fe	=	0.31%	0.27%	0.35%	0.48%	0.53%	0.72%
		1-113	1-139	2-1	2-32	2-56	2-65
SiO_2	=	8.8%	46%	53%	14%	59%	59%
Fe	=	0.55%	1.2%	4.4%	17%	2.0%	1.4%

Carbonate Content: 1-108 = 81%

Carbon-Carbonate:	1-111
% Carbonate	81.6
% Organic Carbon	0.2

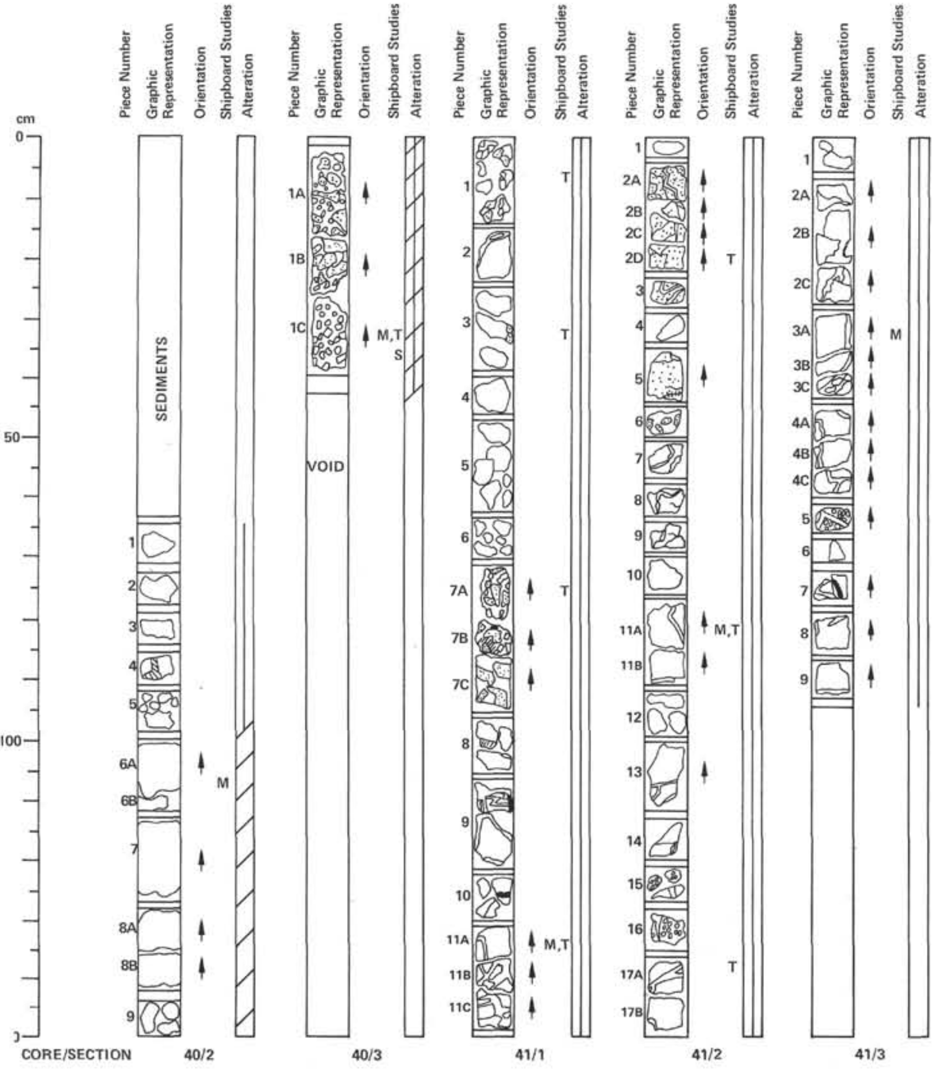

62-465A-40 **Depth: 409.5 to 419.0 m**

SECTION 2: VOLCANIC (TRACHYTE) BRECCIA, medium bluish gray (5B 5/1)

Pieces 1–5 are fine-grained with visible plagioclase laths under the binocular microscope. Highly altered; possible to mark with the fingernail. Pyrite and calcite coatings on boundries. In Piece 4 a vein is dark red to white and may contain barite in addition to calcite and pyritu.

Pieces 6–9 are larger and obviously brecciated. The volcanic rock is generally slightly coarser grained than in Pieces 1–5 and contains plagioclase microphenocrysts. This volcanic rock is not so badly altered. The veins are filled with calcite and a green mineral. The volcanic rock contains fairly abundant pyrite in places. The volcanic rock pieces are angular to subrounded.

SECTION 3: VOLCANIC (TRACHYTE) BRECCIA

Clasts of volcanic rock cemented by veins of calcite. The texture of the individual clasts varies from very fine-grained to medium-grained. The coarser grained clasts contain plagioclase laths that are visible under the binocular microscope. The clasts range in color from gray (N5) to medium bluish gray (5B 5/1). Many of the clasts contain veins of pyrite; often pyrite occurs at the clast-carbonate interface. Flow layering, exemplified by alignment of feldspar crystals, is present in some clasts. A few clasts contain microphenocrysts of plagioclase. No holohyaline clasts were seen; some highly altered clasts were found, however, that may represent altered glass.

TS (40-3, 31 cm): Hyalopilitic to pilotaxitic trachyte from the flow interior containing less than 1% euhedral olivine phenocrysts, 0.1–0.2 mm in size, and 8% plagioclase phenocrysts, 0.25–0.75 mm in size. The groundmass contains 15.4% plagioclase, dominantly microlites, 3.0% magnetite and ilmenite and 73.4% glass which is replaced by clay. Alteration of the original trachyte to clays is extensive.

62-465A-41 **Depth: 419.0 to 428.5 m**

SECTION 1: TRACHYTE/VOLCANIC BRECCIA

Piece 1: Rubble of volcanic breccia. Clasts of varying grain sizes in a calcite matrix. A smear slide of a light colored (light bluish gray, 5B 7/1) clast contained devitrified glass and feldspar crystals. The clast is presumed to be an altered glass fragment; no crystals are large enough to be seen even with the binocular microscope.

Pieces 2–5: Very fine-grained trachyte containing rare plagioclase microphenocrysts; patches of altered glass are common. Thin coatings of pyrite, with or without calcite, occur on several pieces. Color is a fairly uniform light bluish gray (5B 7/1).

Piece 6: Consists of a rubble of small pieces of trachyte, some brecciated and containing calcite and pyrite veins.

Pieces 7A–C: Breccia containing highly angular trachyte fragments in a matrix of calcite. The trachyte is badly altered. Plagioclase crystals, some apparently flow aligned, may be seen with the binocular microscope. Dessimated pyrite occurs in many clasts. Color varies from gray (N5) to medium bluish gray (5B 5/1), except one clast which is about pinkish gray (5YR 8/1) and banded. Several pieces show layering, probably flowage induced.

Pieces 8–11: Similar to above except that brecciation appears to have occurred *in situ*. Pieces are very angular and appear to fit together across the calcite veins. Piece 9 shows flow layering that has been folded. A green alteration mineral is abundant; it is either an alteration product of glass, or a vesicle filling.

TS (41-1, 30 cm): Hyalopilitic trachyte containing 8.0% plagioclase phenocrysts, 0.05–0.2 mm in size. The larger crystals are zoned. The groundmass contains 12.3% plagioclase microlites and 1.2% magnetite.

Glass altered to clays makes up about 76.5%. Rare carbonate veins (0.2%) are present. Irregularly shaped vesicles filled with clay cover about 1.8% of the surface.

TS (41-1, 75 cm): Hyalopilitic trachyte from a breccia clast containing 6.2% phenocrysts of plagioclase laths 0.1–1.0 mm in size, some of which are zoned. The groundmass contains 26.8% plagioclase microlites, 1.2% magnetite, and 65.7% glass which has been altered to clay. A small amount of carbonate (0.1%) is present.

SECTION 2: TRACHYTE

Altered trachyte , gray (N5–N7), that has been highly fractured; fractures now filled with calcite occasionally with a bright green, unidentified mineral. In contrast to the upper part of Section 1, transportation of brecciated clasts does not appear to have occurred, with the possible exception of Piece 6 in which calcite accounts for about one-half of the specimen. Brecciation is most intense in the upper 30 cm of the section.

Texturally, Piece 2 is fine- to medium-grained with visible plagioclase laths and phenocrysts of plagioclase and pseudomophed olivine (?). Grain size appears to decrease downward to at least Piece 14. Piece 15 is highly vesicular; Pieces 16 and 17 are also vesicular, but contain fewer vesicles than Piece 15.

Alteration is pervasive and the rock can easily be scratched with a spatula. A green material is ubiquitous, occuring as patches throughout the trachyte. It is probably a replacement product of either glass, or is a vesicle filling.

Layering is present in Pieces 12 and 13 and possibly in Piece 2. The layering is presumed due to flowage. Layering in Piece 12 is folded.

Pyrite occurs sparsely disseminated throughout the trachyte.

TS (41-2, 19 cm): A trachyte from a flow interior with microphenocrysts of plagioclase. Magnetite and ilmenite are present in greater that 1% abundance. Calcite is present in veins and glass has been altered to clays.

TS (41-2, 82 and 137 cm): A hyalopititic trachyte from next to a glassy margin. It contains both phenocrysts and microphenocrysts of plagioclase with some partly fresh plagioclase in the groundmass. Magnetite and ilmenite are present in greater than 1% abundance. Clays are abundant dominantly as altered glass.

SECTION 3: TRACHYTE, gray (N6)

Piece 1: Vesicular trachyte; number of vesicles appears to continue trend noted at bottom of Section 2. Grain size is small.

Piece 2: Top of Piece 2C vesicular. Pieces 2B and 2C non-vesicular. Number of open vesicles decreases from Piece 1 downward and grain size increases to Piece 2C.

Grain size approximately constant from Piece 2C through 3B, then decreases to Piece 4C. Piece 5 is fine-grained and vesicular. Grain size increases from Piece 5 downward to bottom of core.

Degree of fracturing is reduced from top of core (see Sections 1 and 2), but some fracturing is still present. Calcite fills virtually all of the fractures. Fracturing is most intense in Piece 3C.

Pyrite is very sparse in this section. A dark green material is abundant throughout the trachyte. It appears to be either replacing glass or filling vesicles.

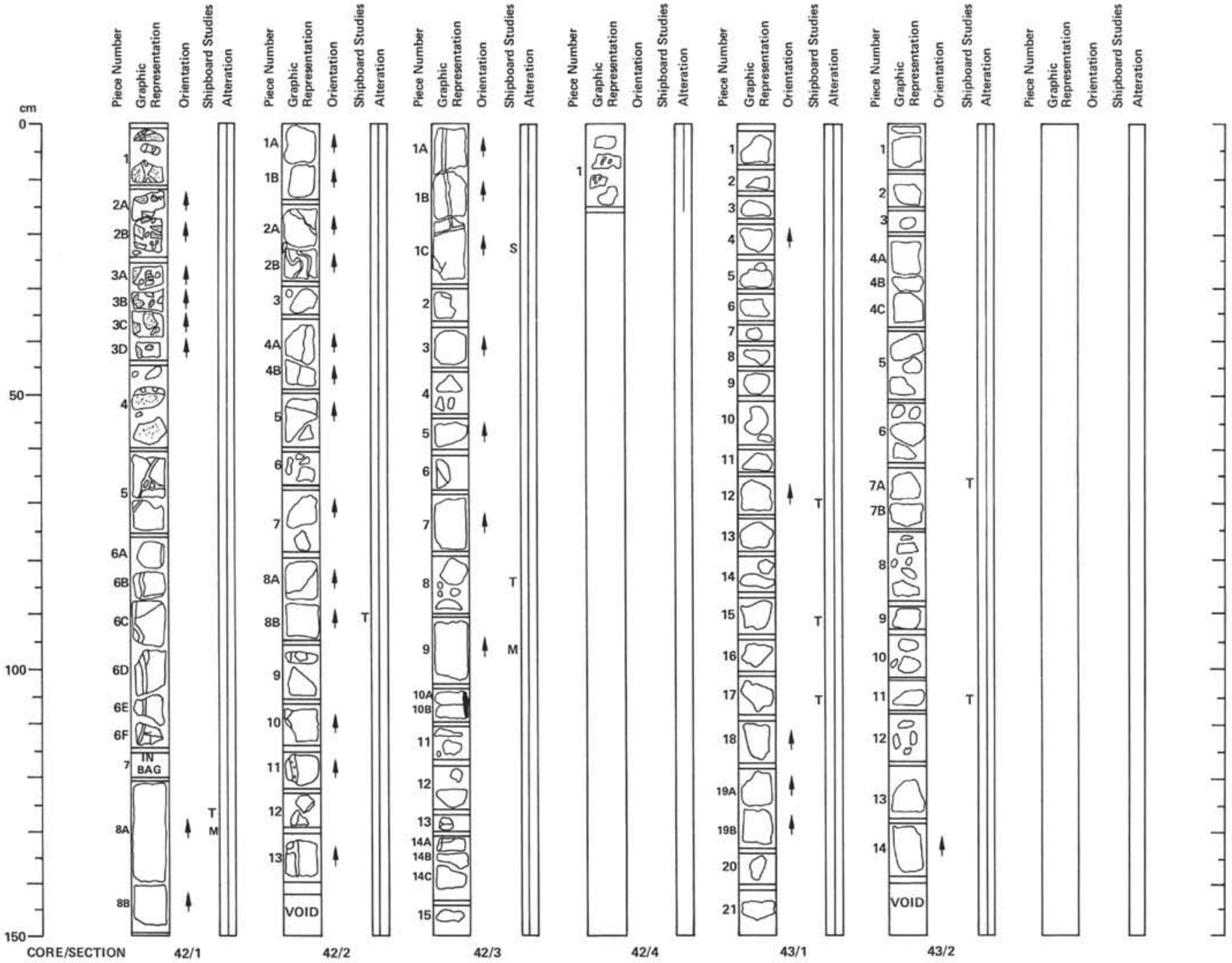
cm
0
50
100
150
Piece Number
Graphic Representation
Orientation
Shipboard Studies
Alteration
CORE/SECTION
42/1
42/2
42/3
42/4
43/1
43/2
1
2A
2B
3A
3B
3C
3D
4
5
6A
6B
6C
6D
6E
6F
7
IN BAG
8A
8B
T
M
1A
1B
2A
2B
3
4A
4B
5
6
7
8A
8B
9
10
11
12
13
VOID
T
1A
1B
1C
2
3
4
5
6
7
8
9
10A
10B
11
12
13
14A
14B
14C
15
S
T
M
1
1
2
3
4
5
6
7
8
9
10
11
12
13
14
15
16
17
18
19A
19B
20
21
T
T
T
1
2
3
4A
4B
4C
5
6
7A
7B
8
9
10
11
12
13
14
VOID
T
T

62-465A-42 Depth 428.5 to 438.0 m

SECTION 1: TRACHYTE/BRECCIA

Pieces 1–3: Breccia containing very angular fragments of trachyte that range in texture from fine-grained vesicular trachyte and altered glass to medium-grained trachyte containing oriented feldspars. The matrix is mostly calcite; an unidentified light-green mineral, commonly occurring as crystals, is observed in the open vugs between clasts. Several clasts are surrounded by pyrite. One clast in Piece 3C is very different in appearance from the other trachyte (olive gray, 5Y 4/1) and may represent a differentiate.
Piece 4 consists of several small, vesicular pieces. One of these exhibits an interface of breccia with vesicular trachyte. The vesicular trachyte is aphyric aphanitic.
Pieces 5–8: Aphyric aphanitic vesicular trachyte, gray (N6). Veins of calcite occur in Pieces 5A, 5B, 6A–6F, and rubble in bag (No. 7). Sparse pyrite dessimated throughout this interval.

TS (42-1, 127 cm): A hyalopilitic vesicular trachyte with 3.8% plagioclase phenocrysts 0.06–0.4 mm in size. The groundmass contains 0.7% magnetite and 27.5% plagioclase. Glass altered to clay is dominant, 57.4%. Vesicles cover 8.6% of the surface and some are filled with calcite, 2.4%.

SECTION 2: TRACHYTE, light gray (N7)

Very fine-grained aphyric trachyte with many vesicules. Veins are filled with calcite, Vesicule size is generally >1 mm but range up to 1 cm and range from unaligned to fairly well aligned. Dessiminated sulfides occur throughout. Vesicle fillings are generally a rim of smectite? and a central filling of calcite.
Piece 5: Slightly larger plagioclase microphenocrysts.
Pieces 11 and 13: Slightly larger plagioclase microphenocrysts.

TS (42-2, 90 cm): A flow-aligned trachyte from next to a glassy margin which contains phenocrysts and microphenocrysts of plagioclase. The groundmass contains plagioclase which in part appears fresh, rare magnetite and ilmenite, and glass which has been altered to clay.

SECTION 3: VESICULAR TRACHYTE, light gray (N7)

Very fine-grained aphyric vesicular trachyte, badly altered. Most vesicles are >1 mm, but some are a few mm in size.
Veins are filled with calcite.
Vesicules are sometimes oriented, ranging from equidemensional poorly aligned to flattened elliptical, and well aligned.
Sulfides are dessiminated throughout the trachyte, but occurs in larger amounts in Pieces 1A and 1B.
In Pieces 9–11 the vesilces are filled; lined with smectite? and the center filled with other material.
Flow unit, Pieces 6–9.
Flow unit, Pieces 9–15.

TS (42-3, 84 cm): A flow-aligned trachyte from next to a glassy margin which contains microphenocrysts of plagioclase. The groundmass contains plagioclase which in part appears fresh, rare magnetie and ilmenite, and glass which has been altered to clay.

SECTION 4: TRACHYTE, gray (N5)
Altered trachyte, very fine-grained. Two pieces contain a few small vesicles.

62-465A-43 Depth 438.0 to 447.5 m

SECTION 1: VESICULAR TRACHYTE, light gray (N7)

Fine-grained highly altered vesicular trachyte. Small parallel to subparallel plagioclase microphenocrysts throughout. Finely disseminated pyrite in small amounts, concentrations in veins.
Flow unit, Pieces 1–5; with Pieces 2, 3, and 4 slightly coarser grained and 1 and 5 finer grained and more vesicular.
Flow unit, Pieces 6–9.
Flow unit, Pieces 9–13.
Flow unit, Pieces 13–16.
Flow unit, Pieces 16–19.
Flow unit, Pieces 19–21.
Flow units based on vesicle and microphenocryst size variations.
Vesicle size ranges up to about one-half cm, but is generally about 1 mm.

TS (43-2, 69 cm): A trachyte which contains microphenocrysts of plagioclase. The groundmass contains flow-aligned plagioclase which is mostly fresh, rare magnetite and ilmenite, and glass which has been alter to clay.

TS (43-1, 91 cm): A hyalopilitic trachyte from next to a glassy margin which contains phenocrysts and microphenocrysts of plagioclase. The groundmass contains partly fresh plagioclase, over 2% magnetite and ilmenite, and glass which has been altered to clay.

TS (43-1, 105 cm): A hyalopilitic trachyte from next to a glassy margin containing phenocrysts and microphenocrysts of plagioclase. Partly fresh plagioclase is in the groundmass as well as rare magnetite and ilmenite, and glass altered to clay.

SECTION 2: VESICULAR TRACHYTE, light gray (N7)

Very fine-grained highly altered vesicular trachyte. Vesicle size ranges up to one-half cm but is generally near 1 mm or less.
Flow unit, Pieces 1–4C.
Pieces 5–7 all very vesicular and fine-grained with only small plagioclase microphenocrysts.
Flow unit, Pieces 7–10.
Flow unit, Pieces 10–14.
Disseminated pyrite in small amounts throughout. Less in Core 43 than in Core 42.
Filled vesicles with smectite? linings and central calcite fillings in Pieces 1, 2, 8, and 9.

TS (43-2, 65 cm): A hyalopilitic trachyte with microphenocrysts of plagioclase. The groundmass contains partly fresh plagioclase, rare magnetite and ilmenite and glass altered to clay.

TS (43-2, 107 cm): A vesicular hyalopilitic–pilotaxitic trachyte contains 4.1% plagioclase laths, 0.08–0.5 mm size. The groundmass contains plagioclase microlites 31.1%, magnetite, 1.0%, and glass altered to clay, 61.1%. Vesicles cover 2.5% of the surface.

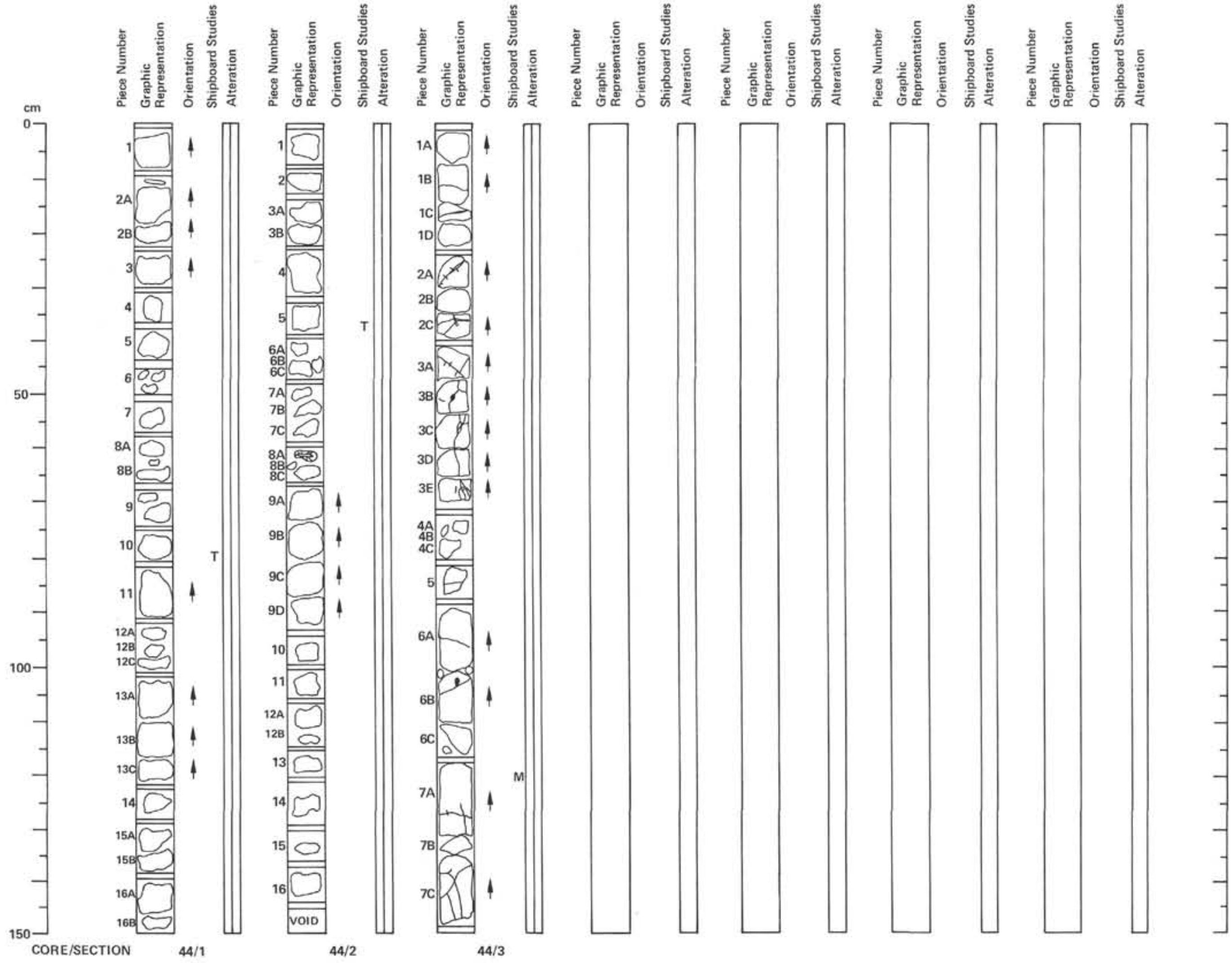

62-465A-44 **Depth 447.5 to 457.5 m**

SECTION 1: VESICULAR TRACHYTE, light gray (N7)

Fine-grained highly altered trachyte with plagioclase microphenocrysts. Vesicular throughout with vesicles ranging from ≥1 mm in general to one-half cm.

Some very finely disseminated pyrite.

Flow unit, Pieces 1–8B

Flow unit, Piece 8B–13B.

Flow unit, Pieces 13B–16B.

TS (44-1, 78 cm): Trachyte with both phenocrysts and microphenocrysts of plagioclase. The groundmass contains rather fresh plagioclase, rare magnetite and ilmenite, and glass altered to clay.

SECTION 2: VESICULAR TRACHYTE, light gray (N7)

Fine-grained highly altered trachyte with plagioclase microphenocrysts. Vesicles range from generaly ≥1 mm to one-half cm in size.

Finely disseminated pyrite in very small amounts.

Flow unit, Piece 1–3A.

Flow unit, Piece 3B–7C.

Flow unit, Piece 7C—9B?

Fine-grained and vesicular from 9A on through the remainder of core – Piece 16.

TS (44-2, 37 cm): A hyalopilitic trachyte with microphenocrysts of plagioclase. The groundmass contains partly fresh plagioclase, rare magnetite and ilmenite and glass altered to clay.

SECTION 3: VESICULAR TRACHYTE, gray (N6)

Altered aphyric vesicular trachyte. Veins filled with calcite are common, alteration of trachte present around veins Some vesicles are flattened perpendicular to axial direction of core. Finely disseminated pyrite occurs throughout section.

Pieces 6A and 6B show a very faint reddish color.

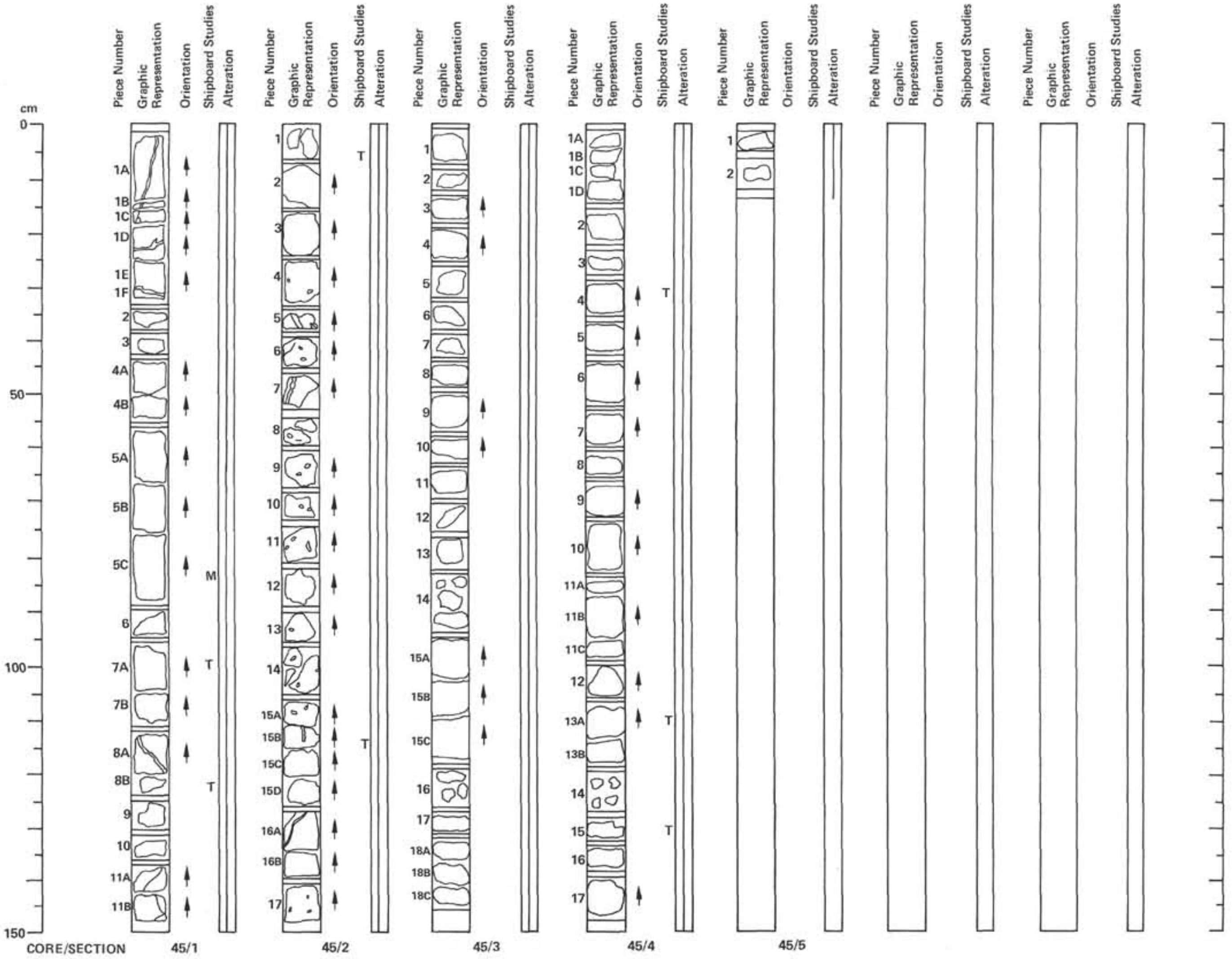

62-465A-45 Depth 457.0 to 466.5 m

SECTION 1: VESICULAR TRACHYTE, gray (N6)

Altered aphyric aphanitic vesicular trachyte. Degree of vesiculation variable; Pieces 4A–B contain fewer vesicles than Pieces above or below, and Pieces 8A–B also contain fewer than surrounding pieces. Several pieces contain fractures filled with calcite; alteration is common around the veins. Calcite also occurs in patches scattered throughout the trachyte. Pieces 6, 7A–B, 9, 10, 11, and 12A have a faint reddish tint, especially surrounding some of the larger veicles.

TS (45-1, 99 cm): A hyalopilitic trachyte with microphenocrysts of plagioclase. The groundmass contains partly fresh plagioclase, rare magnetite and ilmenite, and glass altered to clay. Some carbonate formed from plagioclase is present.

TS (45-1, 123 cm): A pilotaxitic trachyte with phenocrysts and microphenocrysts of plagioclase. The groundmass contains mostly fresh plagioclase, greater than 2% magnetite and ilmenite, and glass altered to clay.

SECTION 2: VESICULAR TRACHYTE,,gray (N6)

Altered aphyric aphanitic trachyte. Vesicles commonly flattened perpendicular to axis of core. Calcite veins common. Number and size of vesicles decreases in bottom of Piece 3. Pieces 4–7 contain more than bottom of 3, but less than 1, 2 and top of 3. Vesicle size then increases from Piece 8 to bottom of section, Piece 17. Pieces 3, 9, 10, 11, 14A–D, and 15A–B have a faint reddish tint.

TS (45-2, 6 cm): A hyalopilitic trachyte with microphenocrysts of plagioclase. The groundmass contains partly fresh plagioclase, over 2% magnetite and ilmenite, and glass altered to clay. Some large crystals of carbonate are present as an alteration product.

TS (45-2, 114 cm): A hyalopilitic trachyte with phenocrysts and microphenocrysts of plagioclase. The groundmass contains mostly fresh plagioclase, rare magnetite and ilmenite, and glass altered to clays.

SECTION 3: VESICULAR TRACHYTE, light gray (N7)

Fine-grained highly altered vesicular trachyte with relic olivine and fresh plagioclase microphenocrysts. The olivine has been pseudomorphed by a bright green soft mineral, but has maintained good euhedral outlines. Portions of the cut surface have a reddish cast. Small amounts of pyrite are scattered throughout.

Flow unit, Pieces 8–18C continued.

Pieces 1–7 all fine-grained and highly vesicular.

SECTION 4: VESICULAR TRACHYTE, light gray (N7)

Fine- to medium-grained highly altered trachyte with varying amounts of vesicles. Vesicle size normally is ≥ 1 mm, but ranges to one-half cm. Abundant plagioclase microphenocrysts and a few euhedral, bright green, olivine (?) pseudomorphs are observed. Pyrite veins are disseminated throughout the core.

Flow unit, continued Piece 1–4.

Flow unit, Pieces 5–11C.

Flow unit, Pieces 11C–16.

TS (45-4, 31 cm): A pilotaxitic trachyte with phenocrysts and microphenocrysts of plagioclase. The groundmass contains partly fresh plagioclase, over 2% magnetite and ilmenite, and glass altered to clays. Veins containing calcite are present.

SECTION 5: VESICULAR TRACHYTE, light gray (N7)

Fine-grained highly altered vesicular trachyte with plagioclase microphenocrysts.

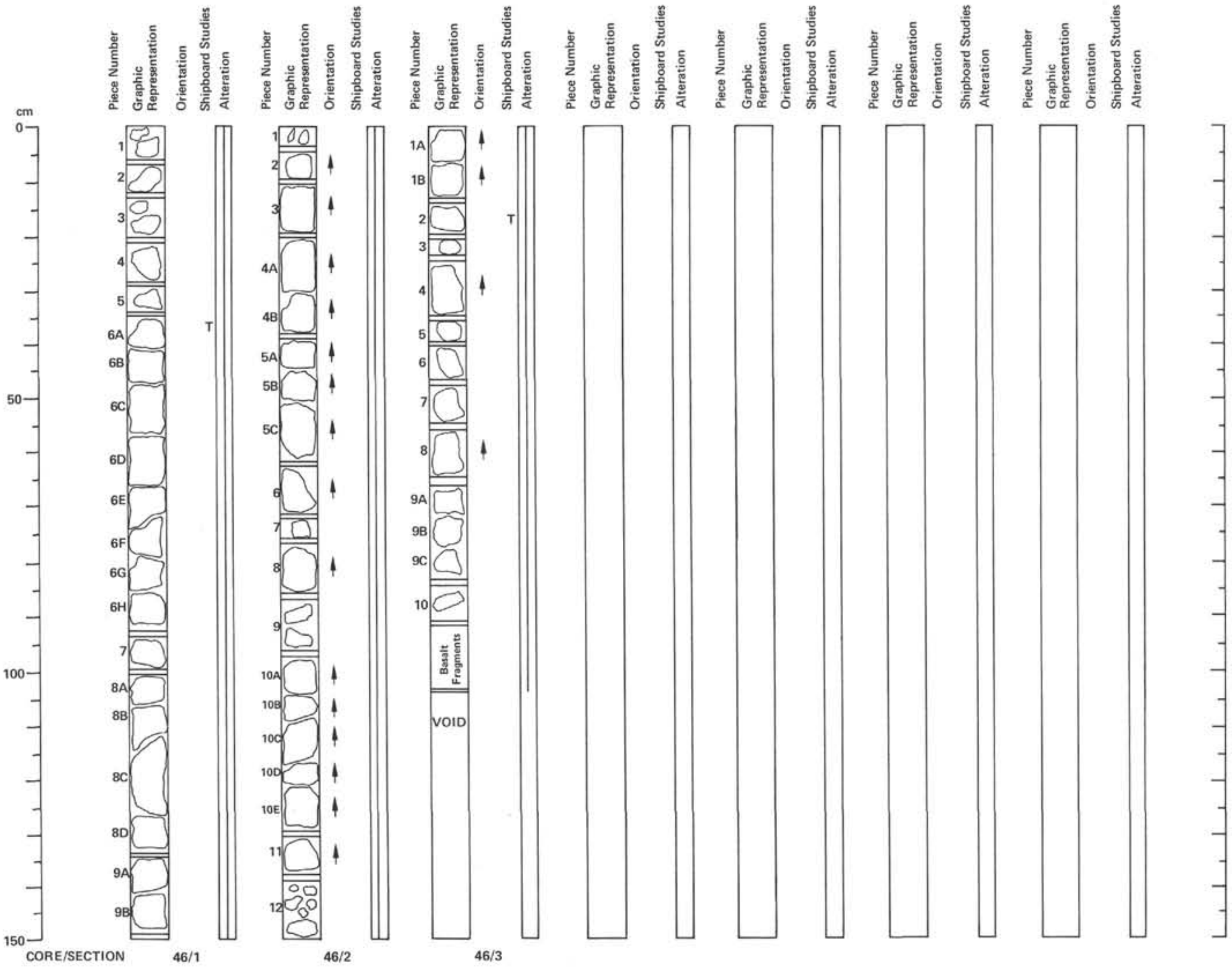

62-465A-46 Depth 466.5 to 476.0 m

SECTION 1: VESICULAR TRACHYTE, light gray (N7)

Fine-grained highly vesicular trachyte that is badly altered to smectite. Fine plagioclase microphenocrysts throughout and occasional bright green olivine (?) pseudomorphs. Pieces 6E, 6F, and 6G have abundant bright green patches, perhaps olivine pseudomorphs in part. In Piece 9B similar green patches are partly olivine pseudomorphs and partly vesicle fillings.

Finely disseminated pyrite occurs throughout.

Vesicle size generally is >1 mm but ranges up to one-half cm as in previous cores.

TS (46-1, 37 cm): A trachyte with flow-aligned phenocrysts and microphenocrysts of plagioclase. The groundmass contains partly fresh plagioclase, rare magnetite and ilmenite and glass altered to clays.

SECTION 2: TRACHYTE, light gray (N7)

Fine-grained badly altered trachyte with plagioclase microphenocrysts and occasional olivine pseudomorphs. Finely disseminated pyrite occurs in small amounts.

Pieces 1–4 have the vesicles mostly filled with green or white material.

Flow unit, Pieces 4B–7.

Pieces 9–12 medium grained and vesicular.

Pieces 4C–12 are unfilled vesicles.

SECTION 3: VESICULAR TRACHYTE, light gray (N7)

Medium-grained vesicular trachyte with plagioclase microphenocrysts. Highly altered throughout.

Vesicles are filled in Pieces 6, 8, 9A, and 10.

Vesicle size still the same, generally >1 mm but up to one-half cm.

Piece 7 is fine-grained.

TS (46-3, 16 cm): A hyalopilitic trachyte with phenocrysts and microphenocrysts of plagioclase. The groundmass contains partly fresh plagioclase, rare magnetite and ilmenite, and glass altered to clay.

465-1

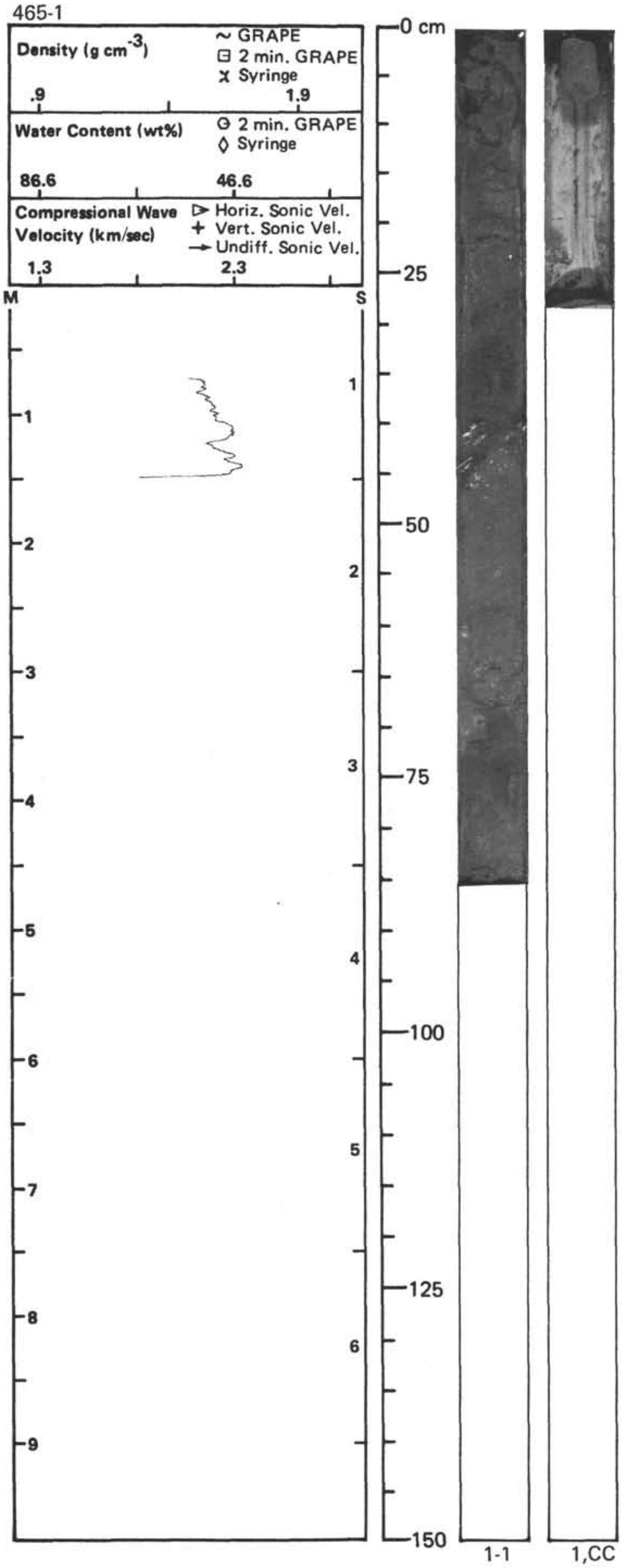
Density (g cm-3)
~ GRAPE
⊟ 2 min. GRAPE
x Syringe
.9
1.9
Water Content (wt%)
⊖ 2 min. GRAPE
◊ Syringe
86.6
46.6
Compressional Wave Velocity (km/sec)
▷ Horiz. Sonic Vel.
+ Vert. Sonic Vel.
→ Undiff. Sonic Vel.
1.3
2.3
M
S
1
2
3
4
5
6
7
8
9
0 cm
25
50
75
100
125
150
1-1
1,CC

465-2

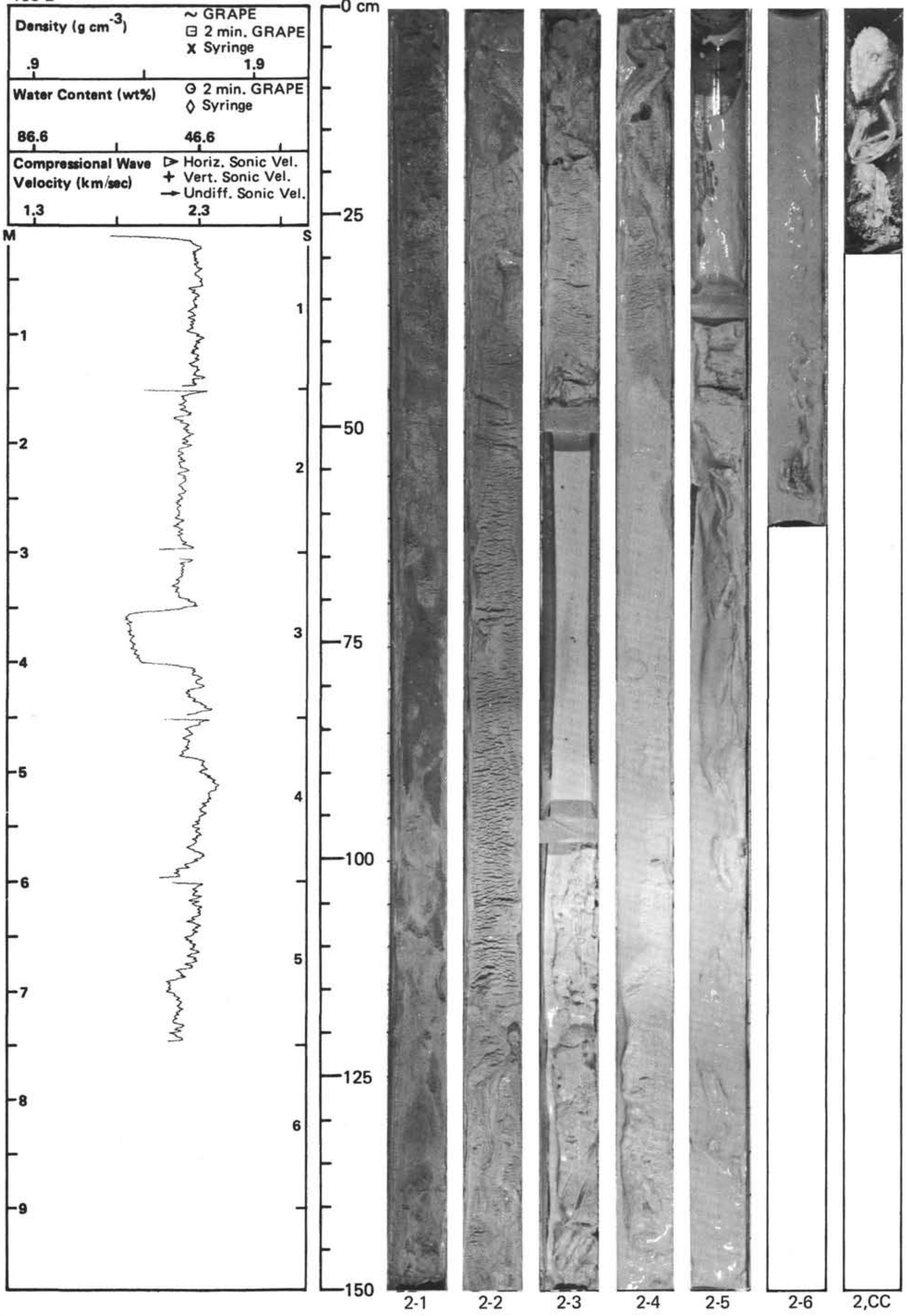
Density (g cm^{-3})
~ GRAPE
⊟ 2 min. GRAPE
X Syringe
.9
1.9
Water Content (wt%)
ʘ 2 min. GRAPE
◊ Syringe
86.6
46.6
Compressional Wave Velocity (km/sec)
▷ Horiz. Sonic Vel.
+ Vert. Sonic Vel.
→ Undiff. Sonic Vel.
1.3
2.3
M
S
1
2
3
4
5
6
7
8
9
0 cm
25
50
75
100
125
150
2-1
2-2
2-3
2-4
2-5
2-6
2,CC

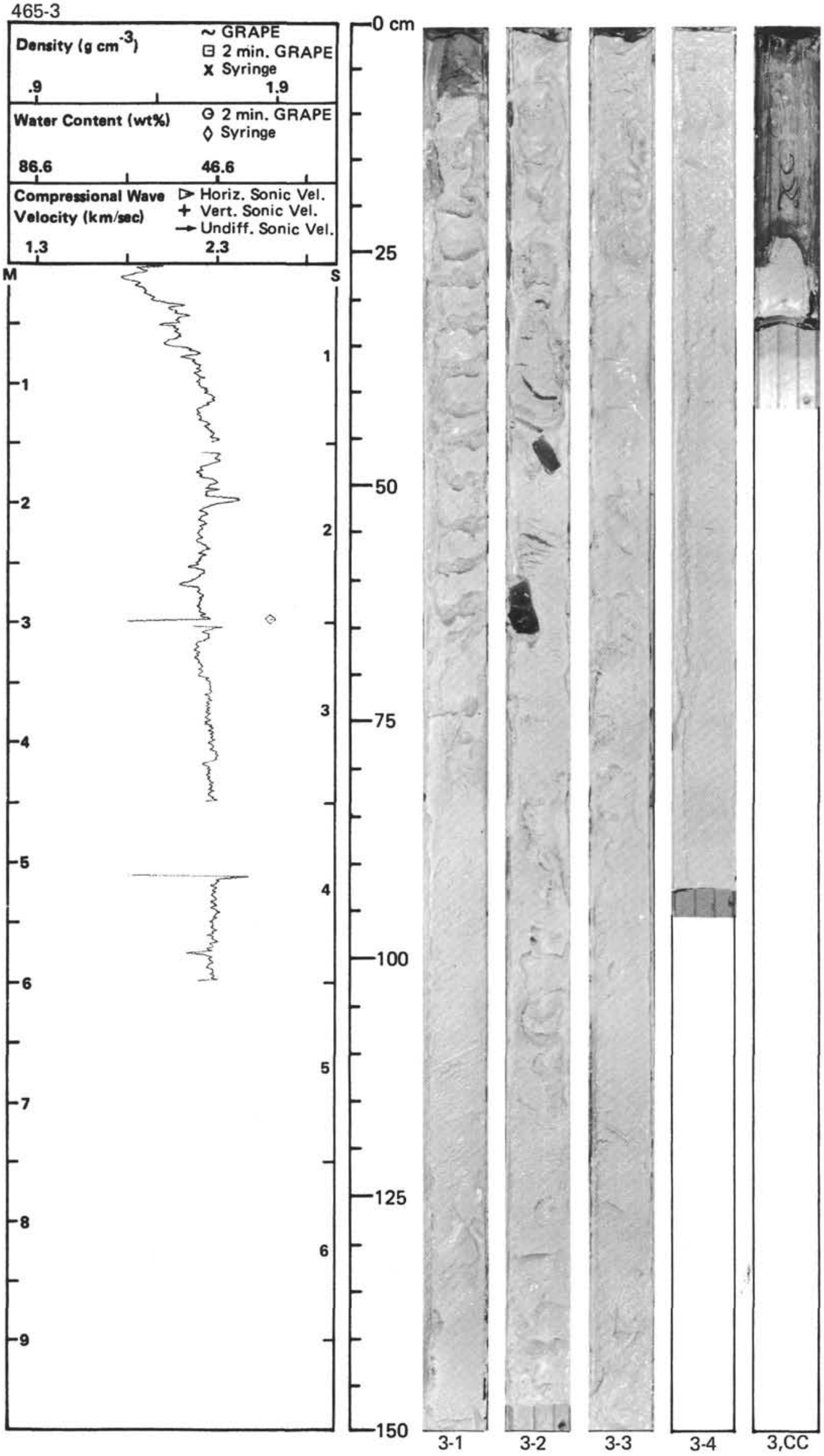
465-3
Density (g cm^{-3})
~ GRAPE
⊟ 2 min. GRAPE
X Syringe
.9
1.9
Water Content (wt%)
ʘ 2 min. GRAPE
◊ Syringe
86.6
46.6
Compressional Wave Velocity (km/sec)
▷ Horiz. Sonic Vel.
+ Vert. Sonic Vel.
→ Undiff. Sonic Vel.
1.3
2.3
M
S
1
2
3
4
5
6
7
8
9
0 cm
25
50
75
100
125
150
3-1
3-2
3-3
3-4
3,CC

465-4

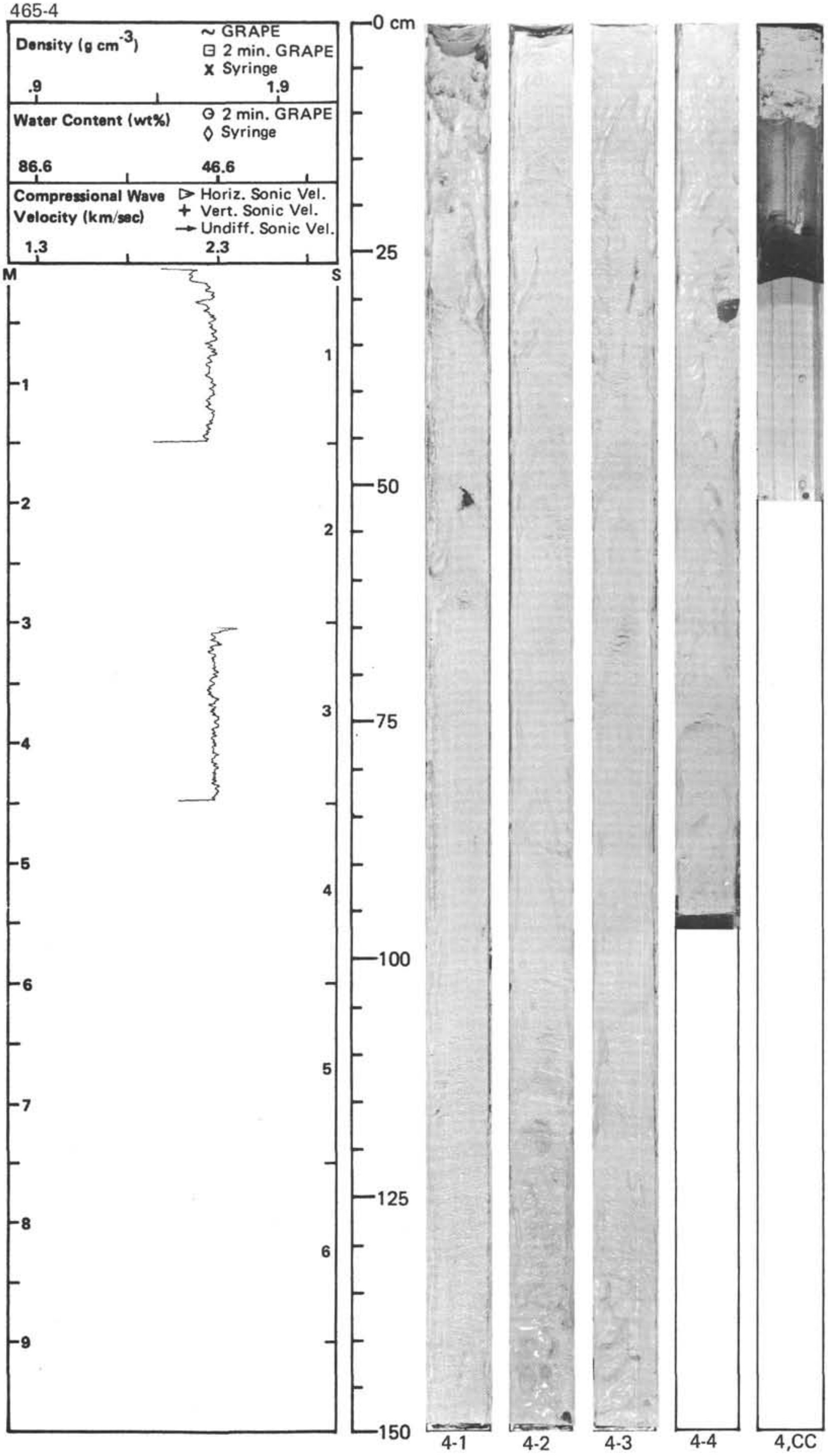
Density (g cm^{-3})
~ GRAPE
⊟ 2 min. GRAPE
X Syringe
.9
1.9
Water Content (wt%)
ʘ 2 min. GRAPE
◊ Syringe
86.6
46.6
Compressional Wave Velocity (km/sec)
▷ Horiz. Sonic Vel.
+ Vert. Sonic Vel.
→ Undiff. Sonic Vel.
1.3
2.3
M
S
1
2
3
4
5
6
7
8
9
1
2
3
4
5
6
0 cm
25
50
75
100
125
150
4-1
4-2
4-3
4-4
4,CC

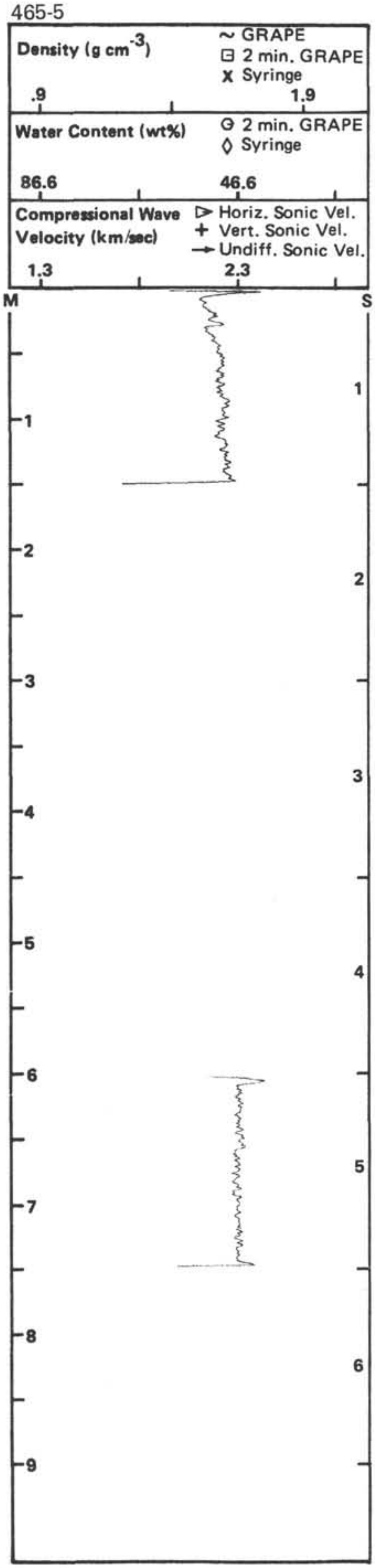
465-5
Density (g cm^{-3})
~ GRAPE
⊟ 2 min. GRAPE
X Syringe
.9
1.9
Water Content (wt%)
ϴ 2 min. GRAPE
◊ Syringe
86.6
46.6
Compressional Wave Velocity (km/sec)
▷ Horiz. Sonic Vel.
+ Vert. Sonic Vel.
→ Undiff. Sonic Vel.
1.3
2.3
M
S
1
2
3
4
5
6
7
8
9

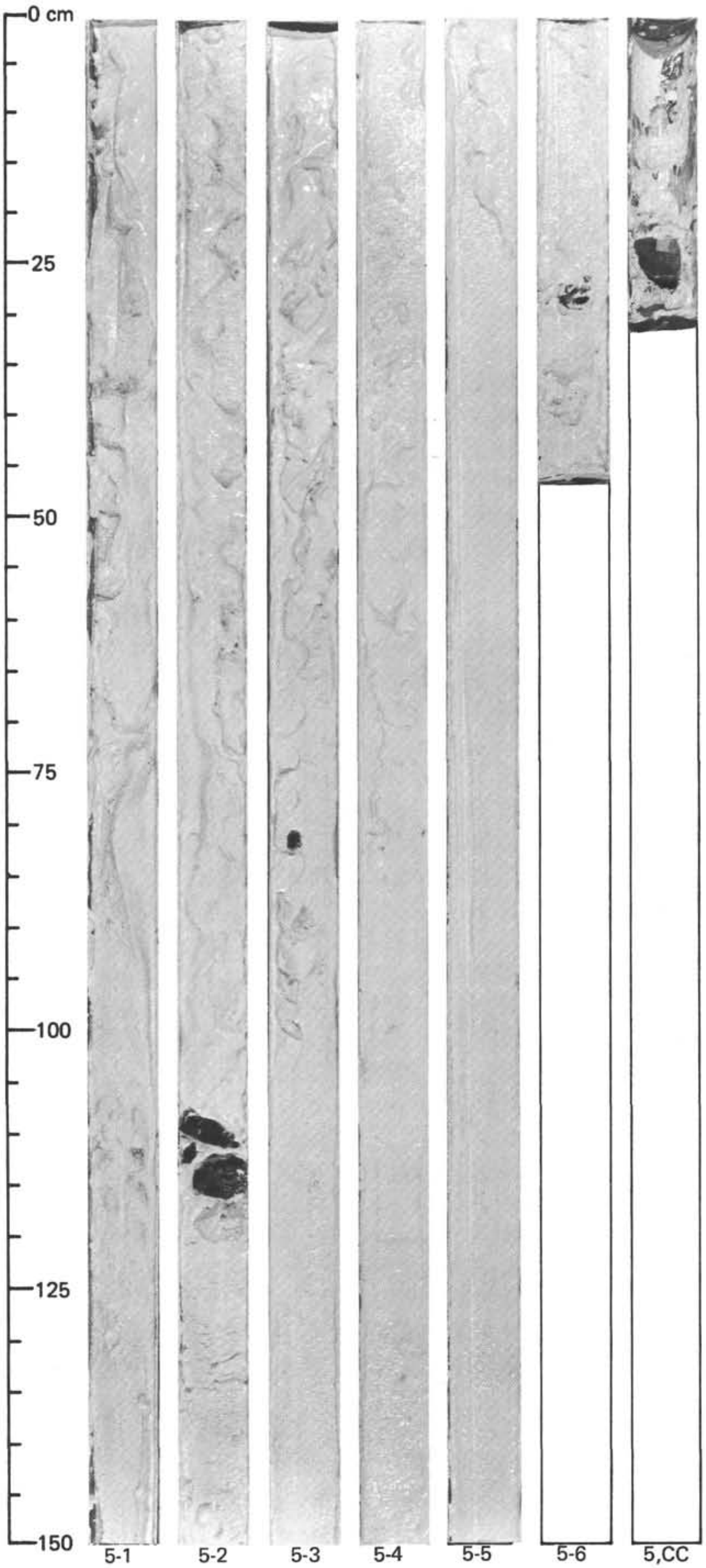
0 cm
25
50
75
100
125
150
5-1
5-2
5-3
5-4
5-5
5-6
5,CC

465-6

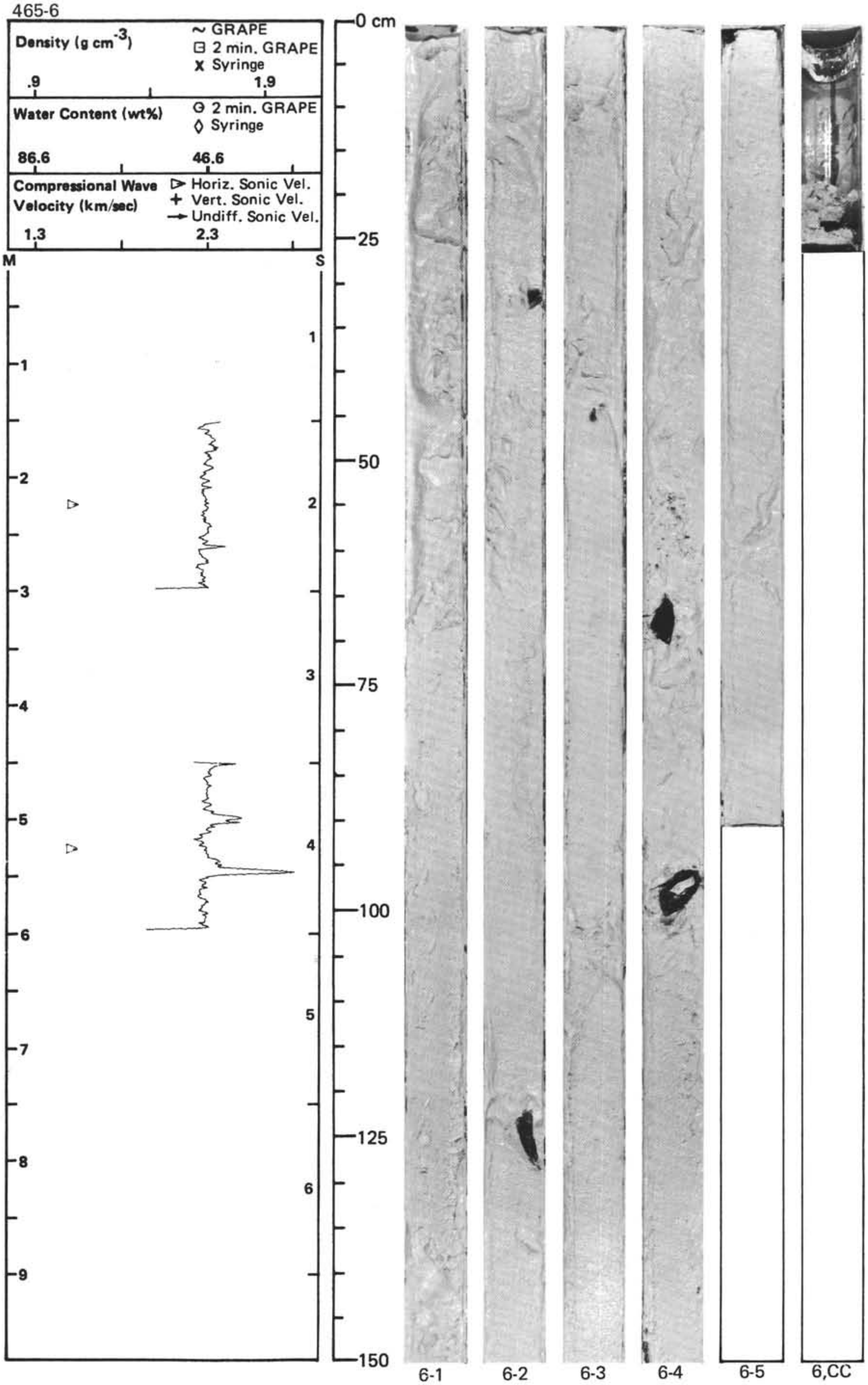
Density (g cm^{-3})
~ GRAPE
⊟ 2 min. GRAPE
X Syringe
.9
1.9
Water Content (wt%)
ʘ 2 min. GRAPE
◊ Syringe
86.6
46.6
Compressional Wave Velocity (km/sec)
▷ Horiz. Sonic Vel.
+ Vert. Sonic Vel.
→ Undiff. Sonic Vel.
1.3
2.3
M
S
1
2
3
4
5
6
7
8
9
0 cm
25
50
75
100
125
150
6-1
6-2
6-3
6-4
6-5
6,CC

465-7, 8, 9 NO DATA

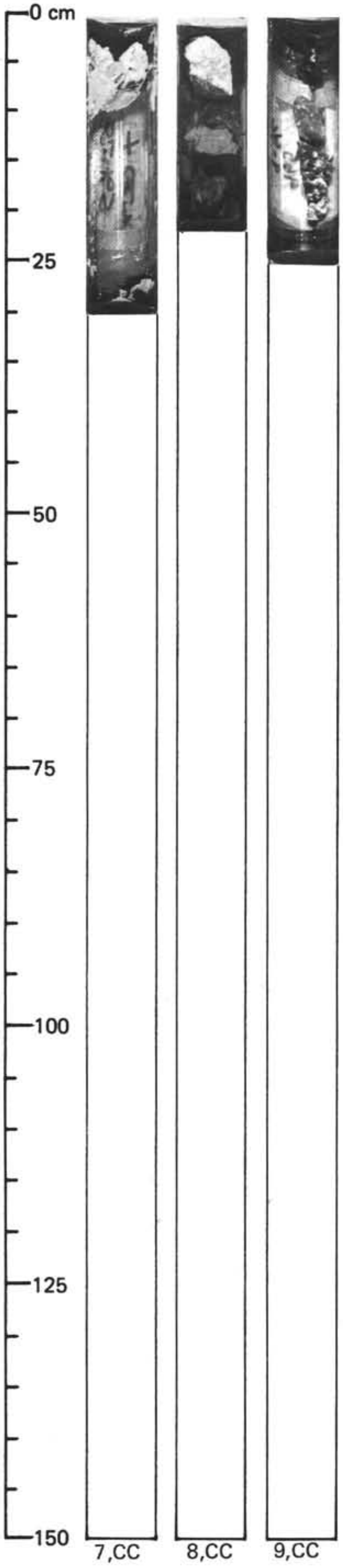

465-10 (465-11 NO DATA)

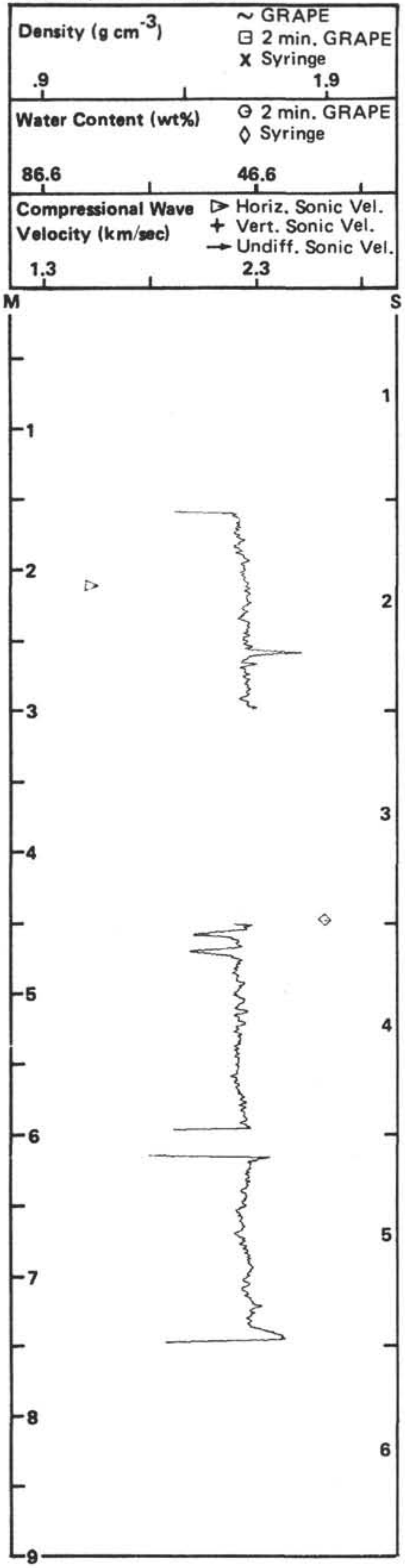

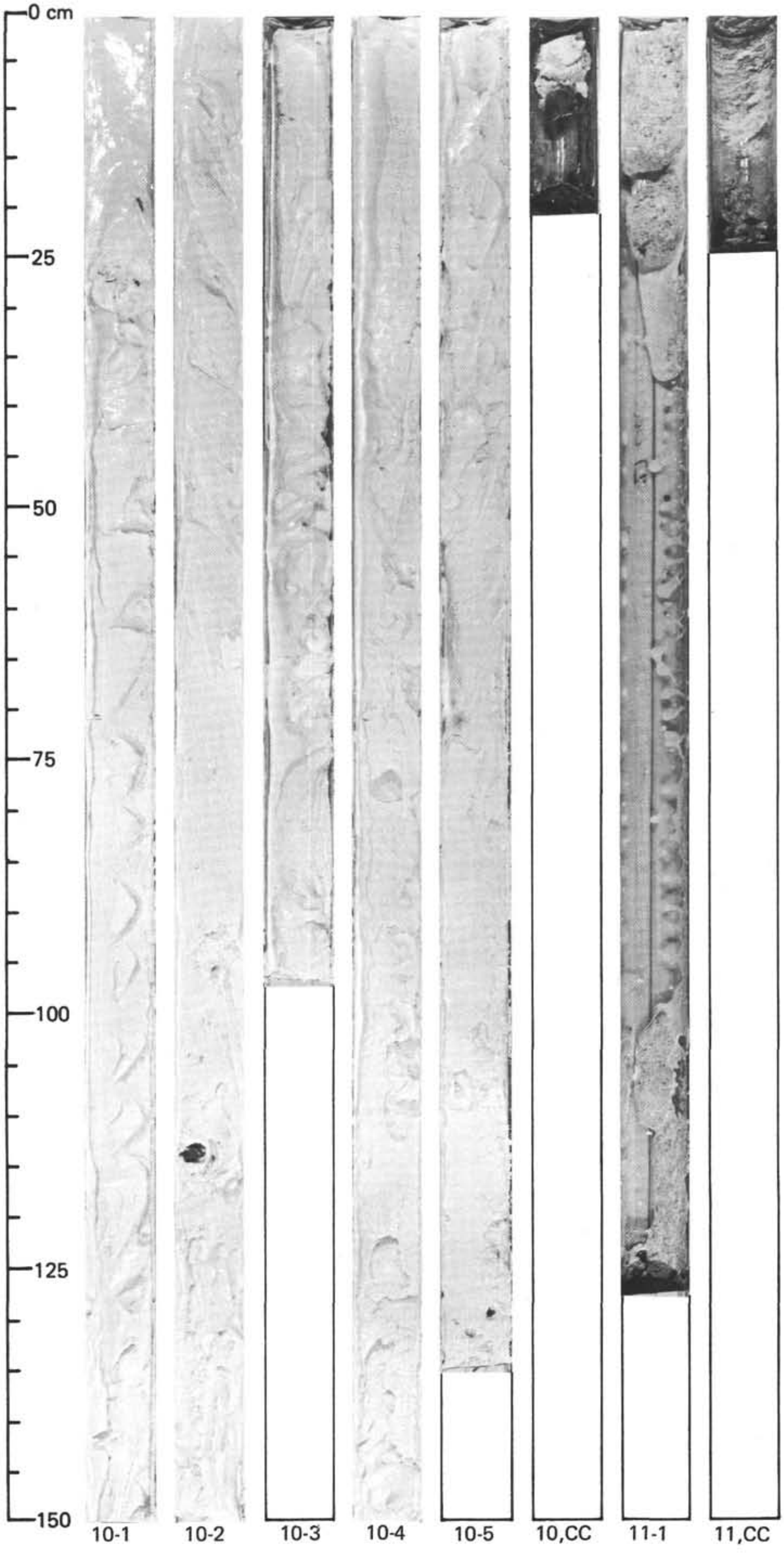

465A-3 (465A-1, 2 NO DATA)

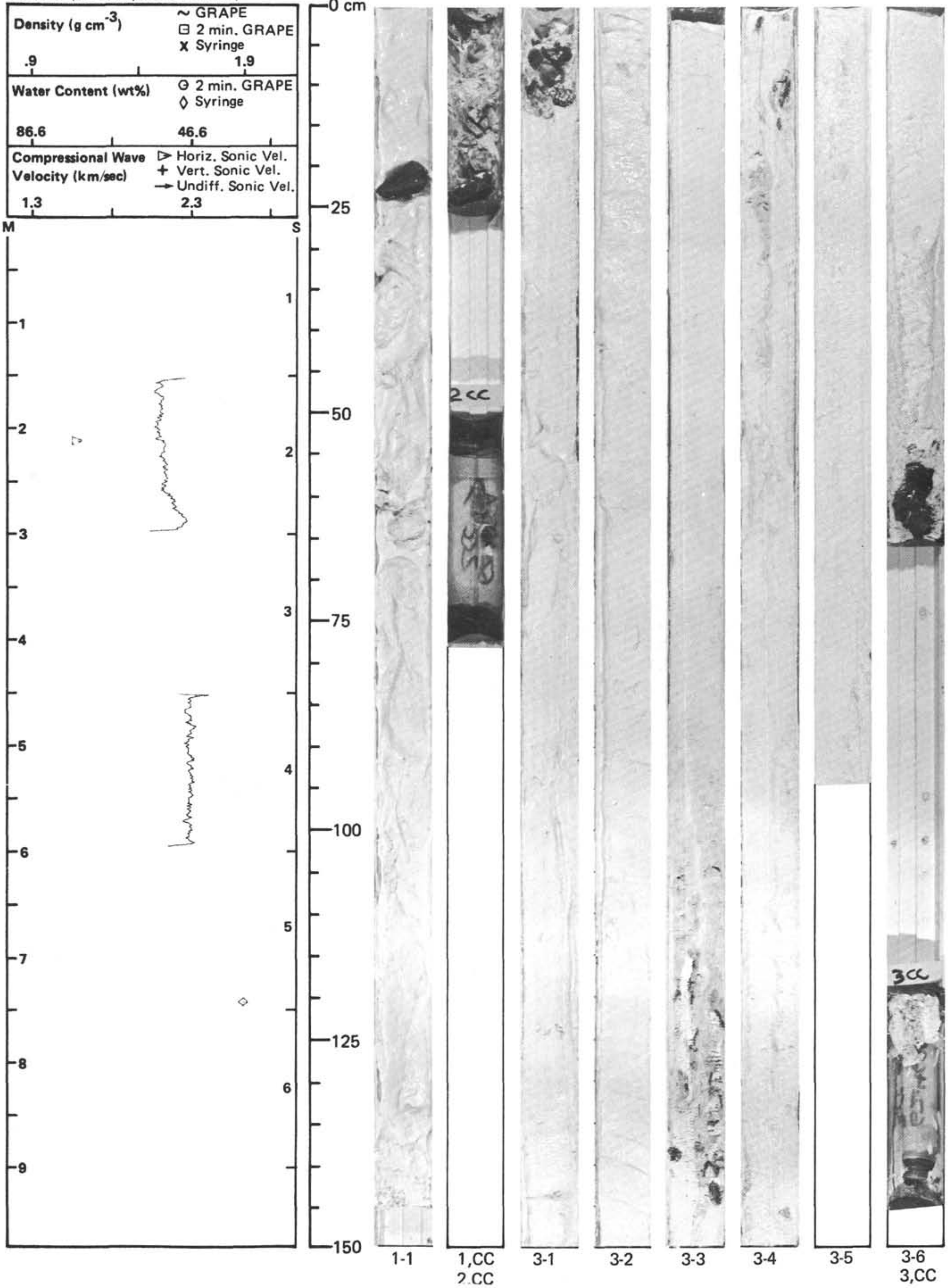

465A-4, 5, 6, 7, 8 NO DATA

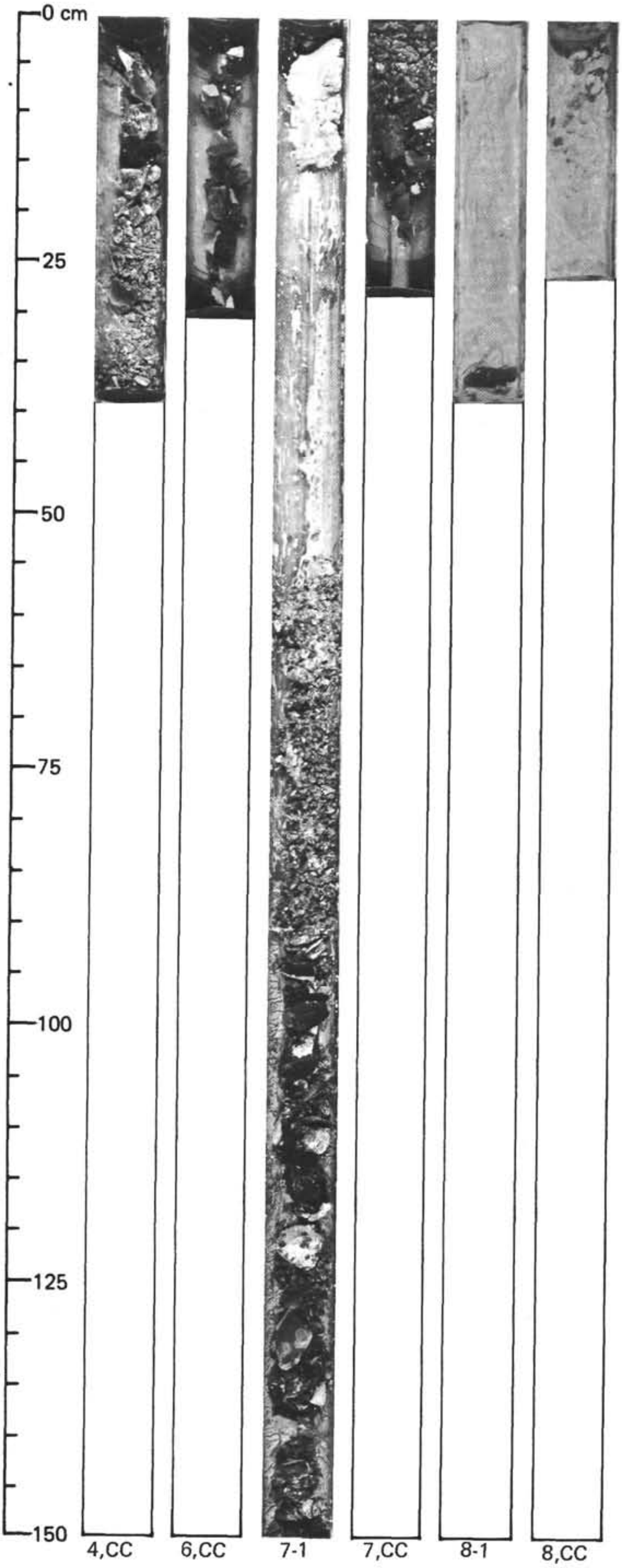

465A-9

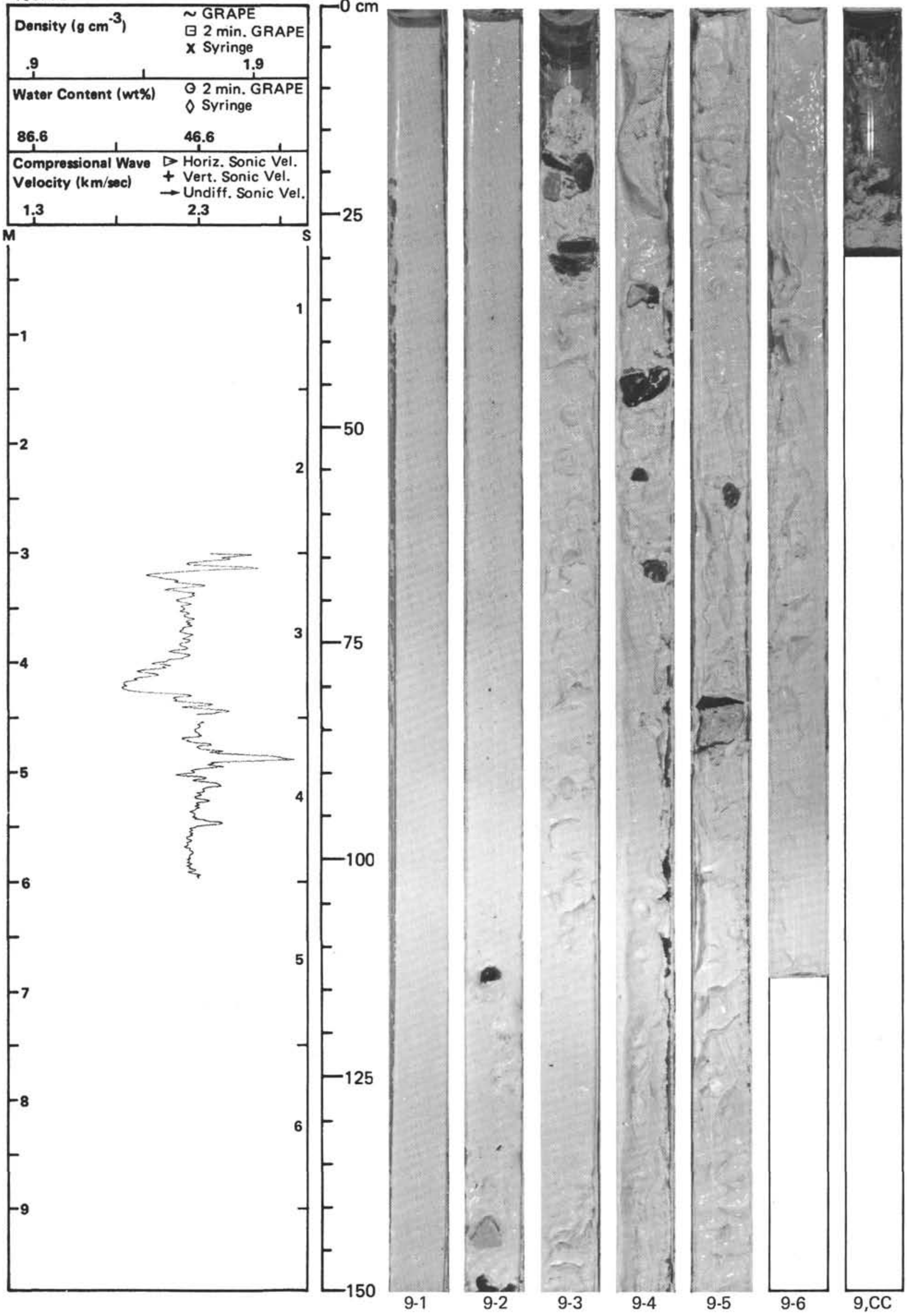
Density (g cm^{-3})
~ GRAPE
⊟ 2 min. GRAPE
X Syringe
.9
1.9
Water Content (wt%)
⊖ 2 min. GRAPE
◊ Syringe
86.6
46.6
Compressional Wave Velocity (km/sec)
▷ Horiz. Sonic Vel.
+ Vert. Sonic Vel.
→ Undiff. Sonic Vel.
1.3
2.3
M
S
1
2
3
4
5
6
7
8
9
0 cm
25
50
75
100
125
150
9-1
9-2
9-3
9-4
9-5
9-6
9,CC

465A-10

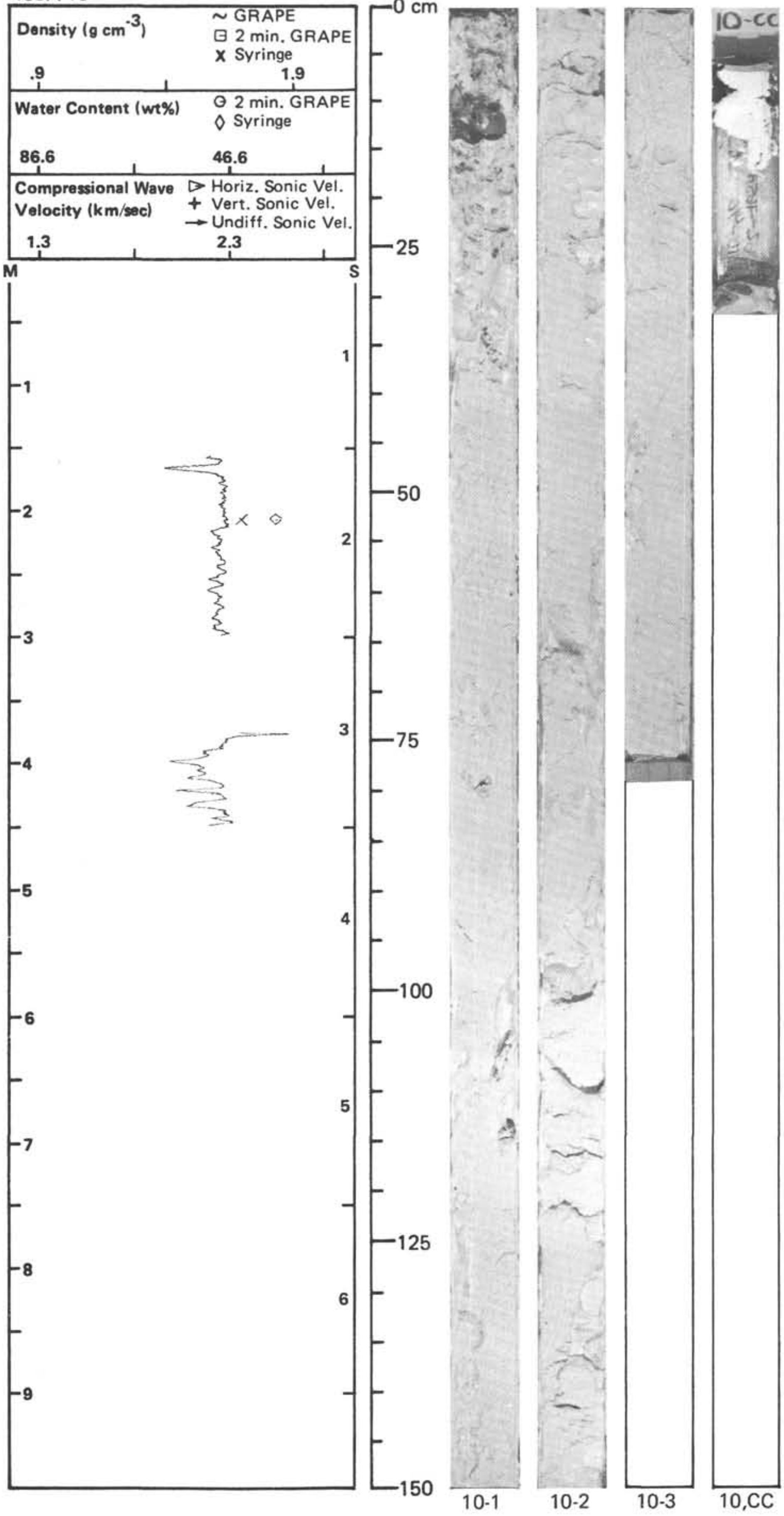
Density (g cm^{-3})
~ GRAPE
⊟ 2 min. GRAPE
X Syringe
.9
1.9
Water Content (wt%)
⊖ 2 min. GRAPE
◊ Syringe
86.6
46.6
Compressional Wave Velocity (km/sec)
▷ Horiz. Sonic Vel.
+ Vert. Sonic Vel.
→ Undiff. Sonic Vel.
1.3
2.3
M
S
1
2
3
4
5
6
7
8
9
0 cm
25
50
75
100
125
150
10-CC
10-1
10-2
10-3
10,CC

465A-11

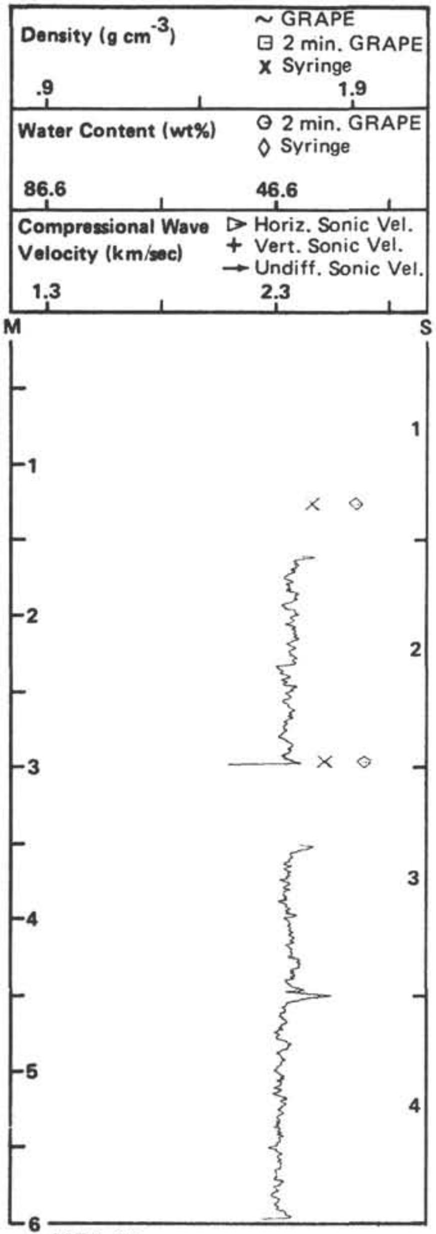

465A-12

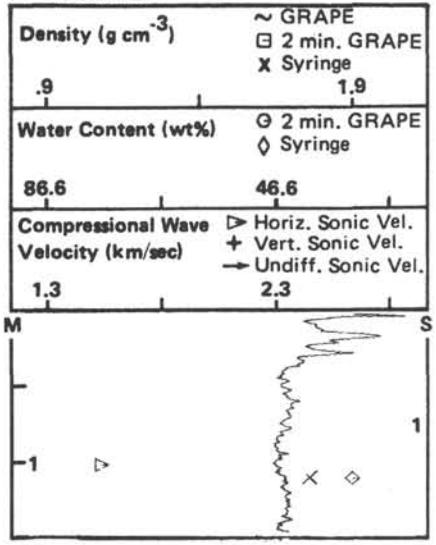

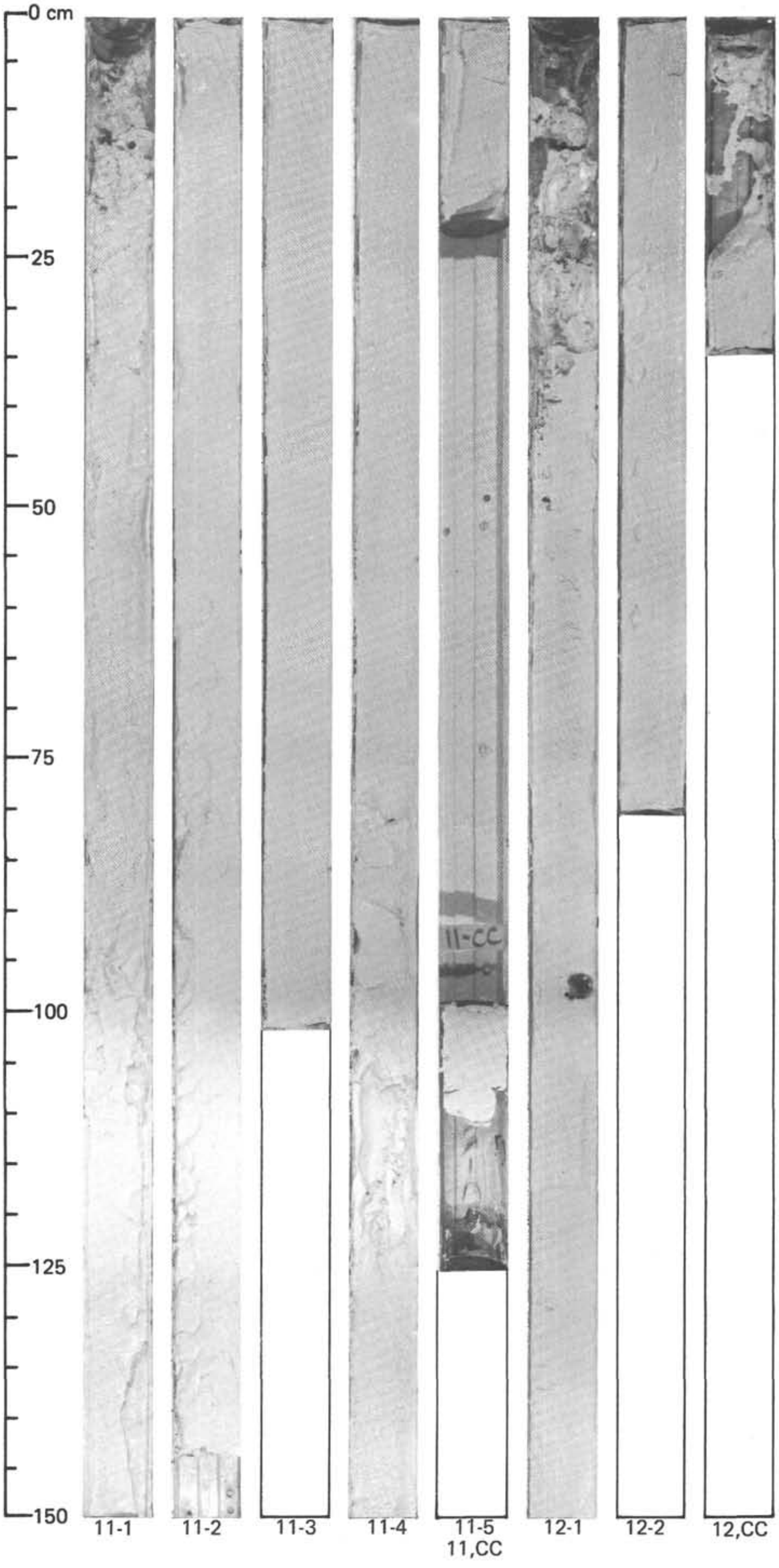

465A-15 (465A-13, 14 NO DATA)

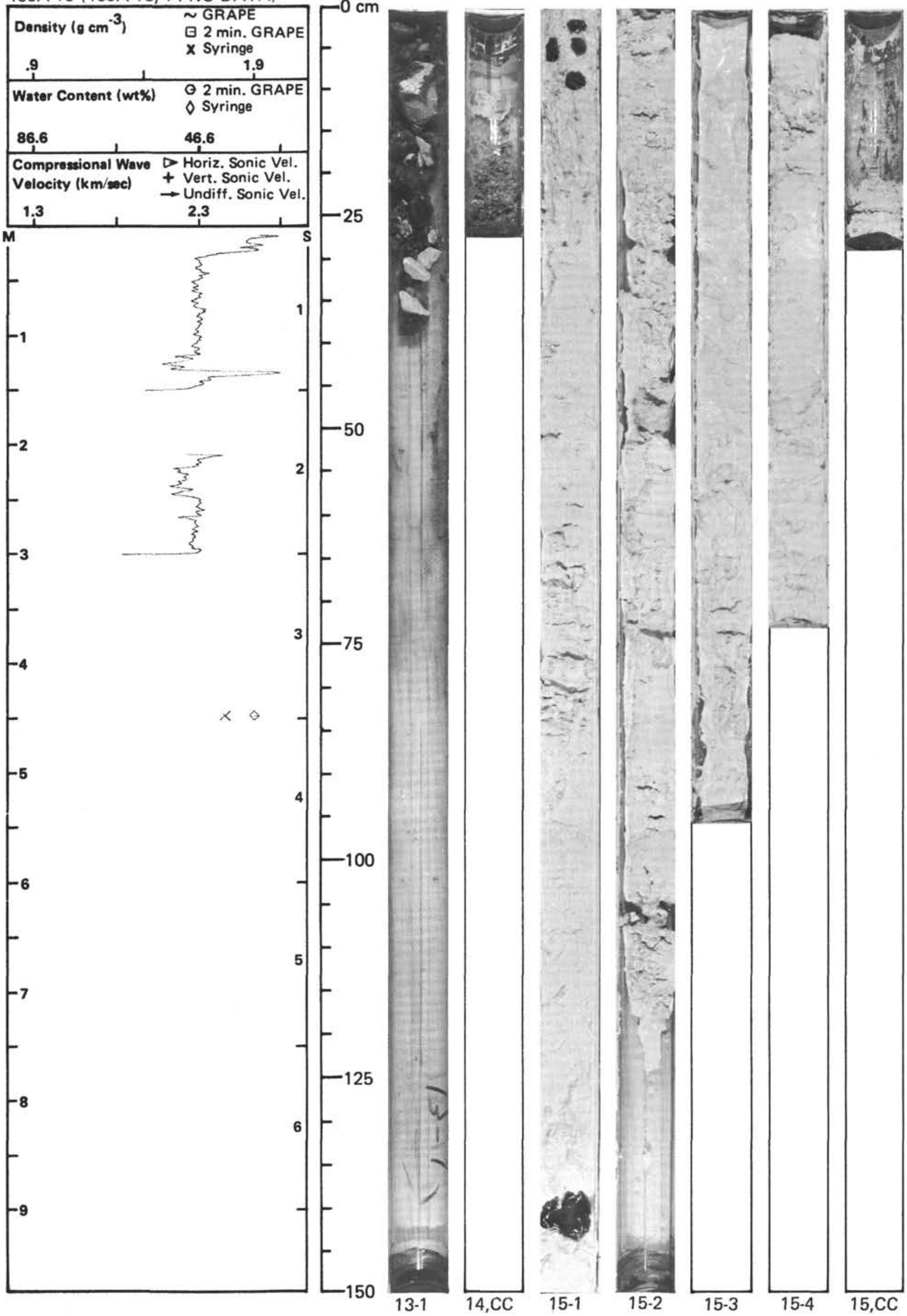

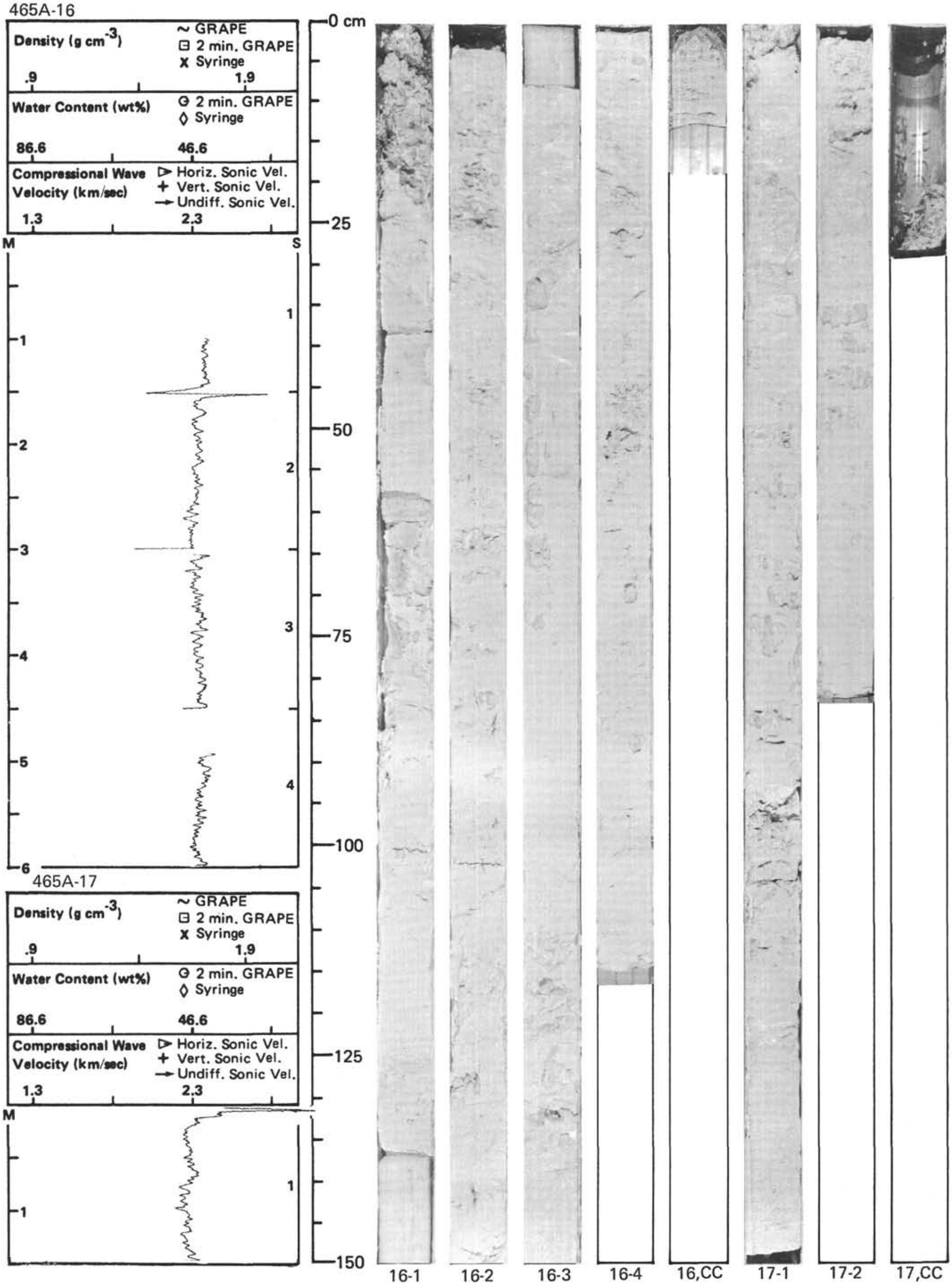
465A-16
Density (g cm^{-3})
~ GRAPE
⊟ 2 min. GRAPE
X Syringe
.9
1.9
Water Content (wt%)
ʘ 2 min. GRAPE
◊ Syringe
86.6
46.6
Compressional Wave Velocity (km/sec)
▷ Horiz. Sonic Vel.
+ Vert. Sonic Vel.
→ Undiff. Sonic Vel.
1.3
2.3
M
S
1
2
3
4
5
6
465A-17
Density (g cm^{-3})
~ GRAPE
⊟ 2 min. GRAPE
X Syringe
.9
1.9
Water Content (wt%)
ʘ 2 min. GRAPE
◊ Syringe
86.6
46.6
Compressional Wave Velocity (km/sec)
▷ Horiz. Sonic Vel.
+ Vert. Sonic Vel.
→ Undiff. Sonic Vel.
1.3
2.3
M
1
0 cm
25
50
75
100
125
150
16-1
16-2
16-3
16-4
16,CC
17-1
17-2
17,CC

465A-18

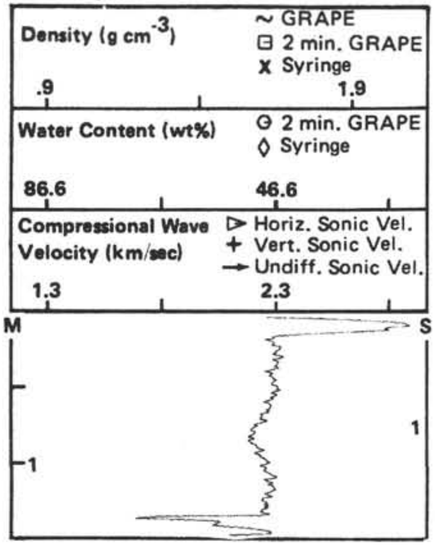

465A-19

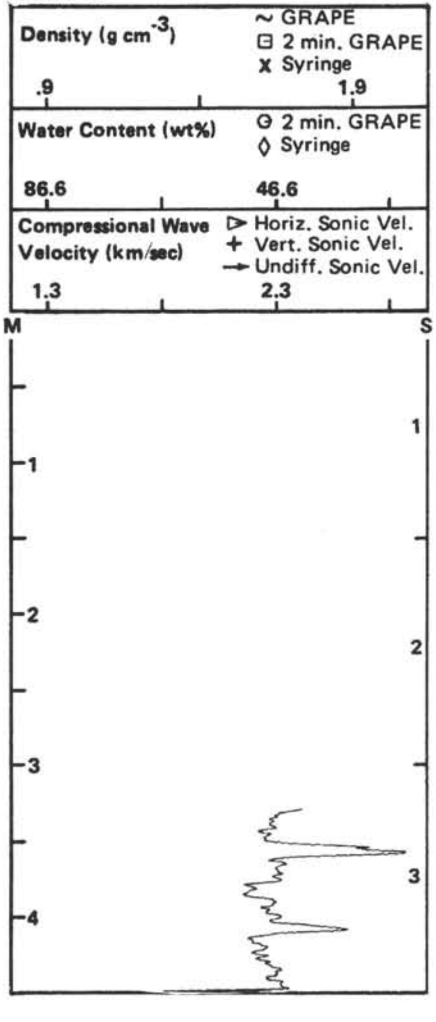

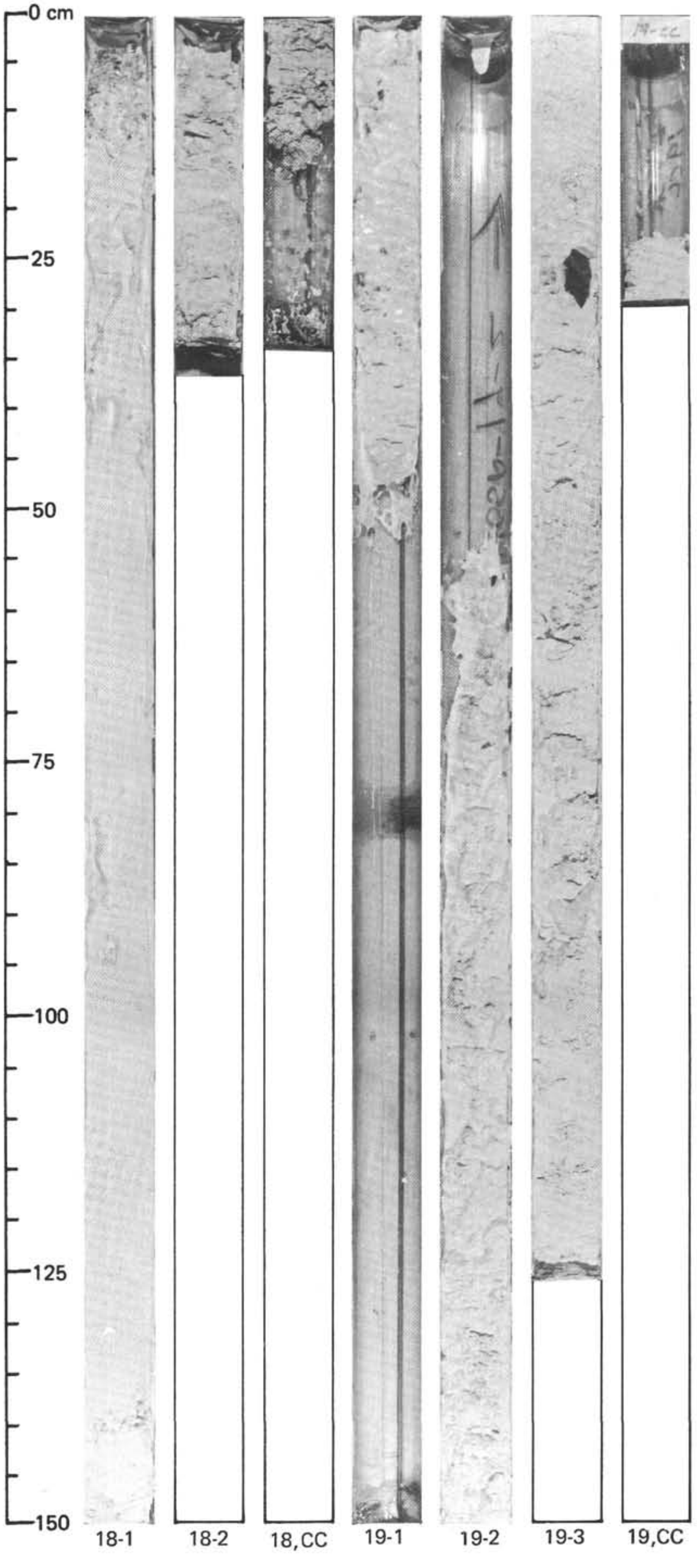

465A-20

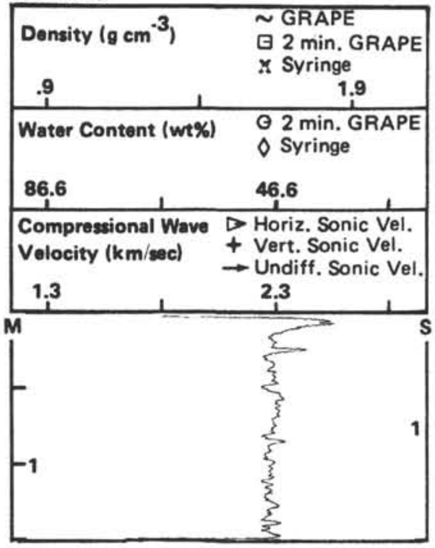

465A-21

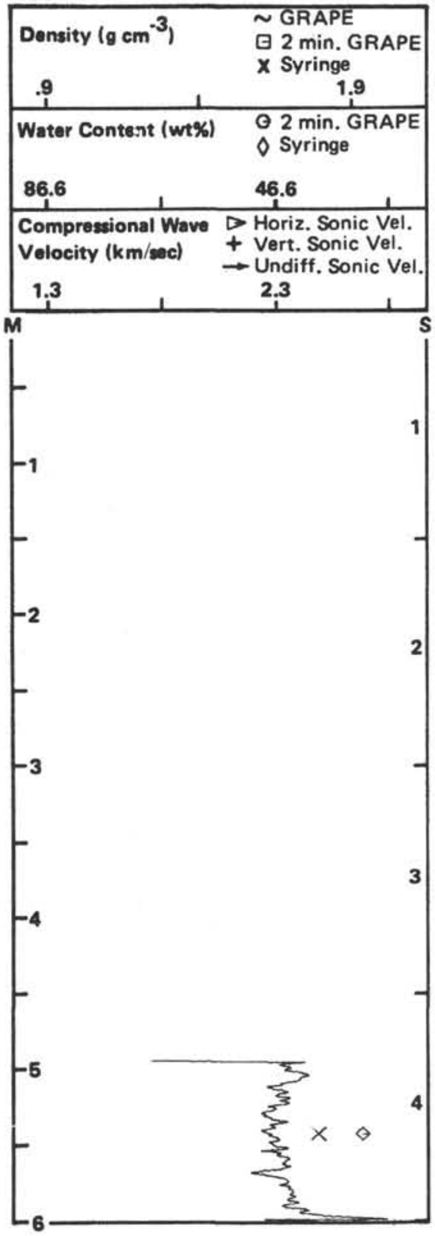

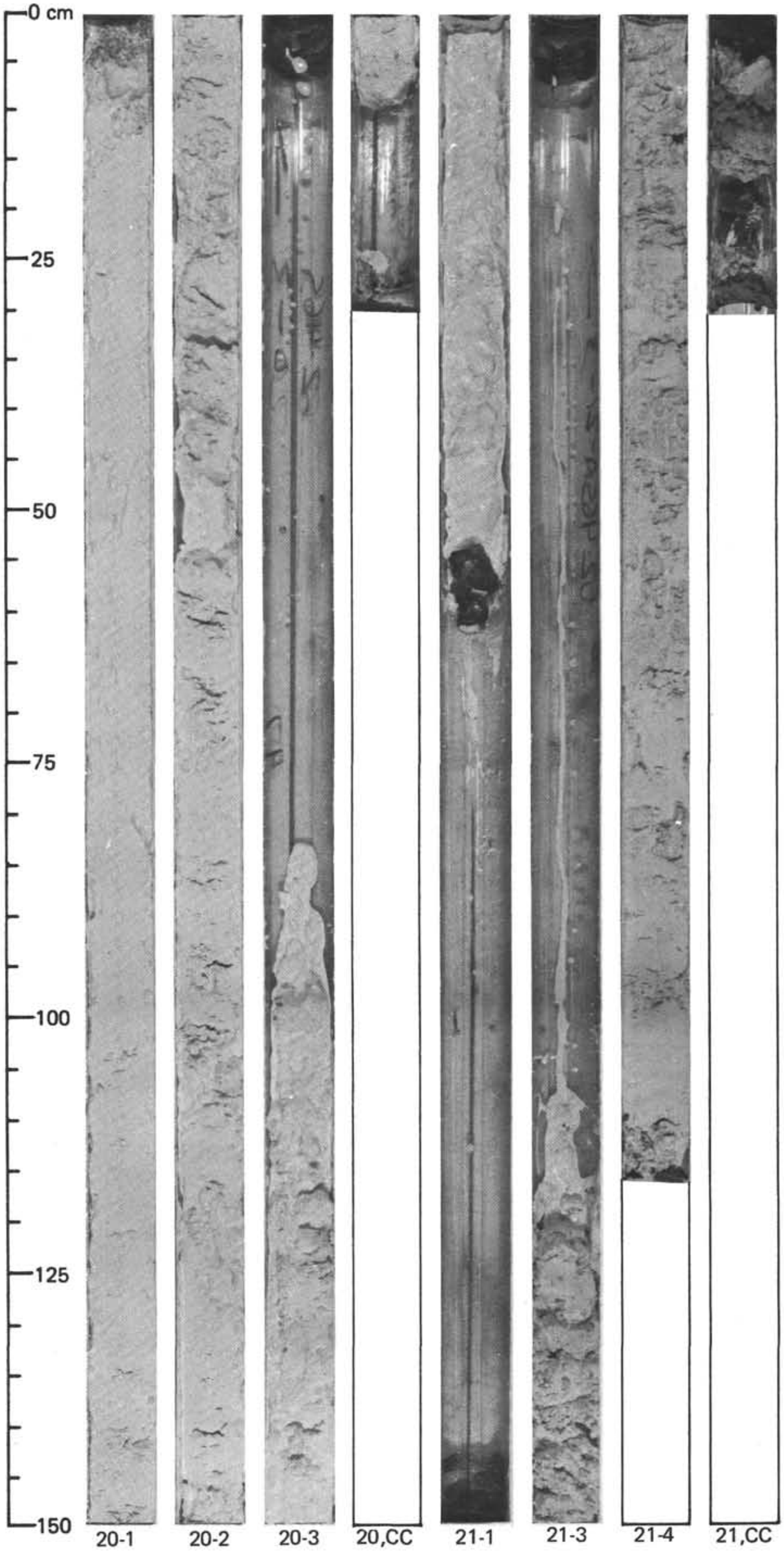

465A-22, 23, 24, 25 NO DATA

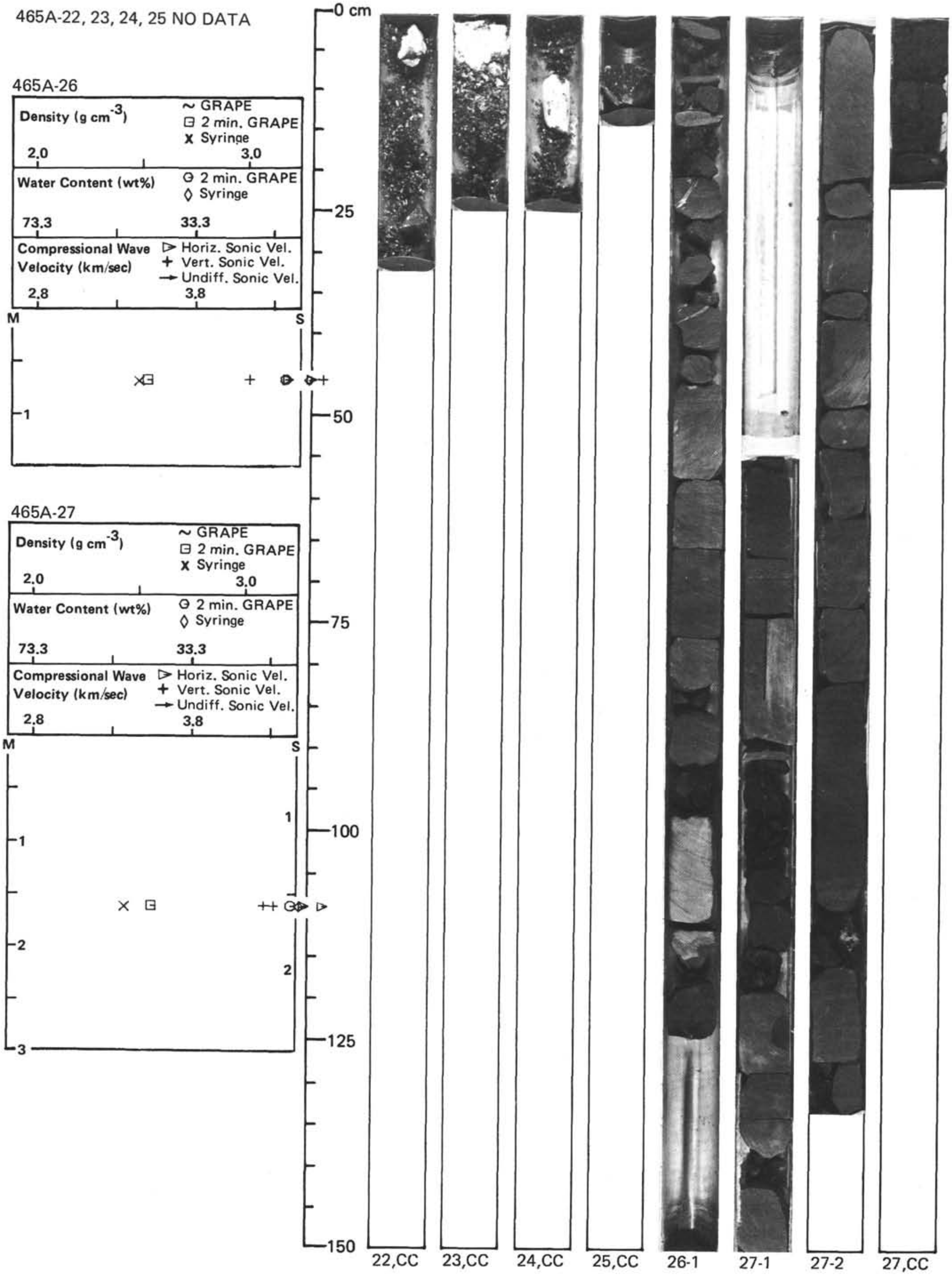

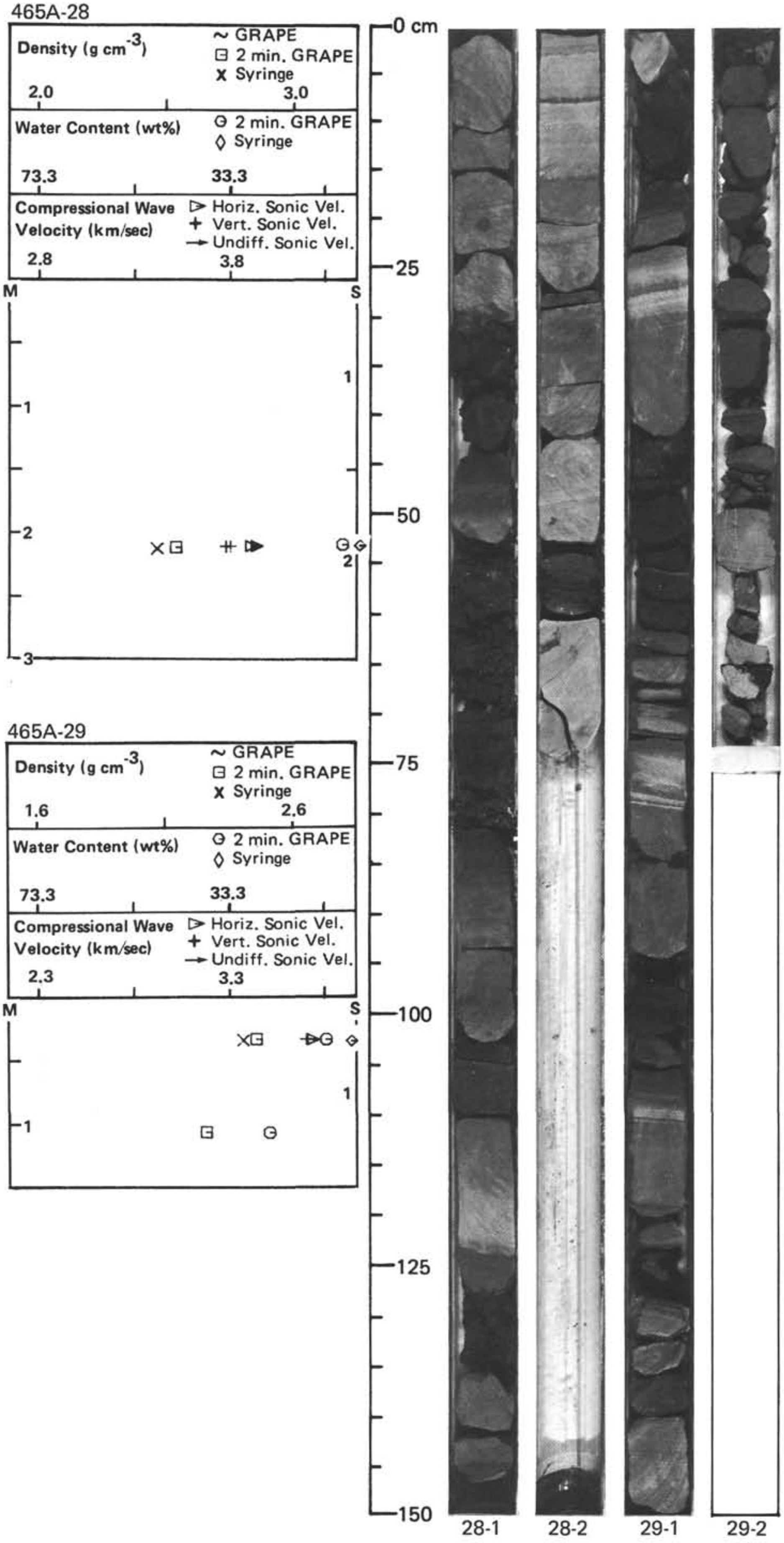
465A-28
Density (g cm^{-3})
~ GRAPE
⊟ 2 min. GRAPE
X Syringe
2.0
3.0
Water Content (wt%)
Θ 2 min. GRAPE
◊ Syringe
73.3
33.3
Compressional Wave Velocity (km/sec)
▷ Horiz. Sonic Vel.
+ Vert. Sonic Vel.
→ Undiff. Sonic Vel.
2.8
3.8
M
S
1
2
3
465A-29
Density (g cm^{-3})
~ GRAPE
⊟ 2 min. GRAPE
X Syringe
1.6
2.6
Water Content (wt%)
Θ 2 min. GRAPE
◊ Syringe
73.3
33.3
Compressional Wave Velocity (km/sec)
▷ Horiz. Sonic Vel.
+ Vert. Sonic Vel.
→ Undiff. Sonic Vel.
2.3
3.3
M
S
1
0 cm
25
50
75
100
125
150
28-1
28-2
29-1
29-2

465A-30

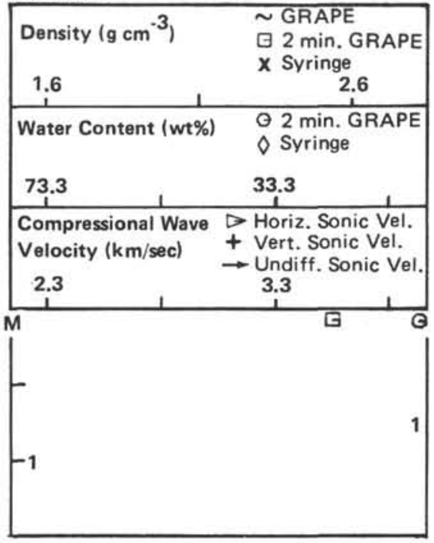

465A-31

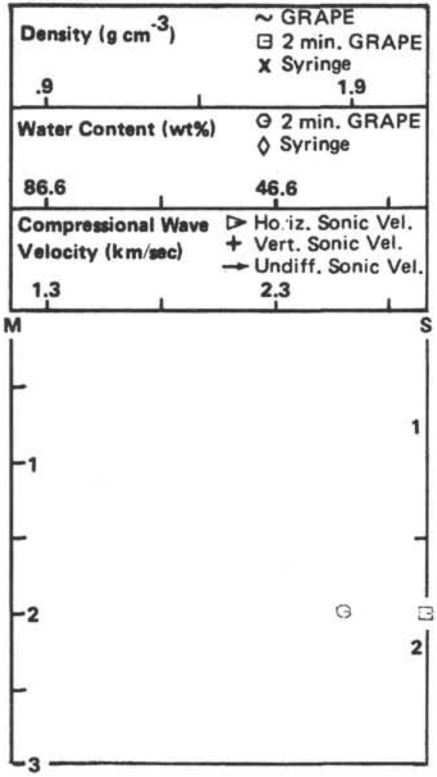

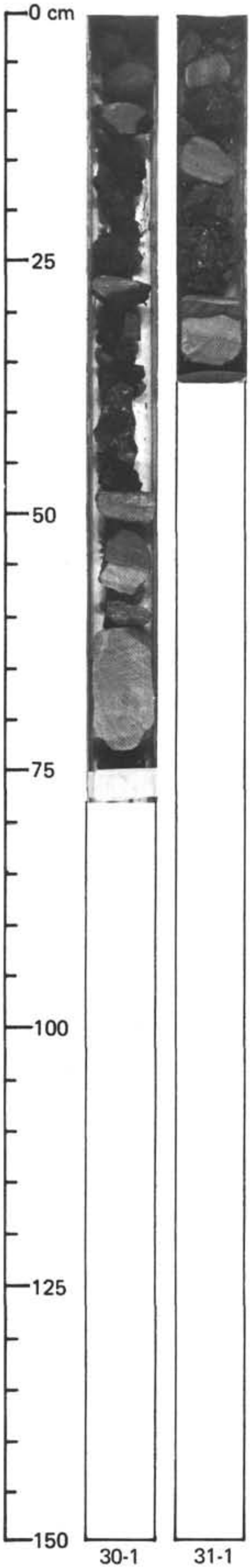

465A-32

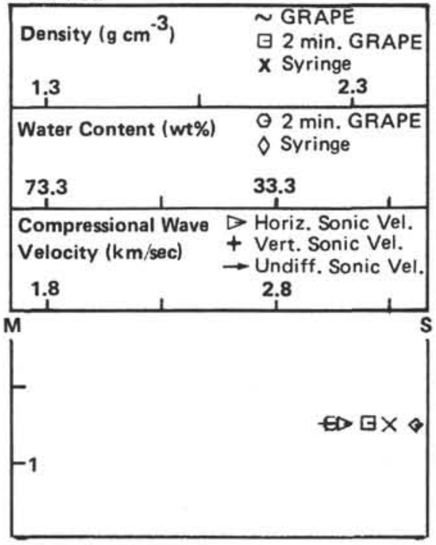

465A-33

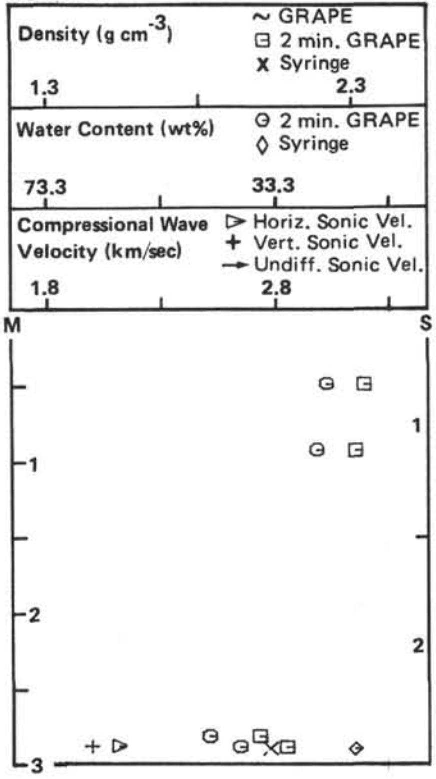

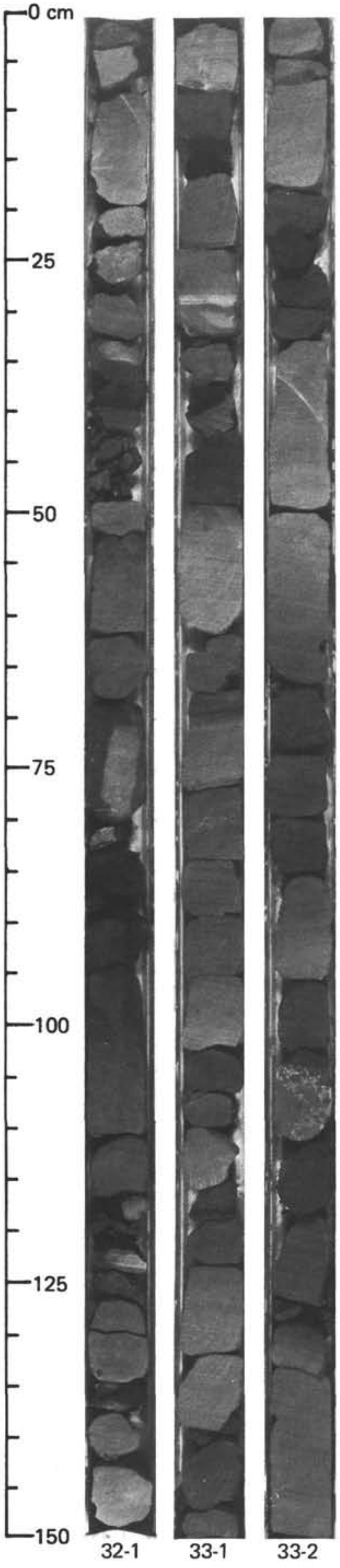

465A-34

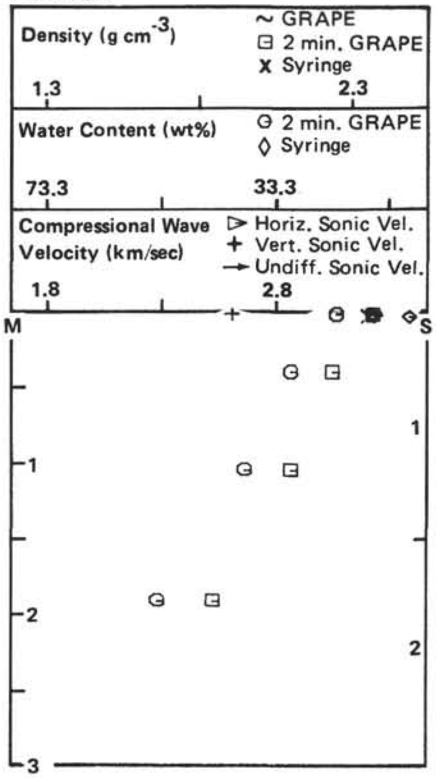

465A-35

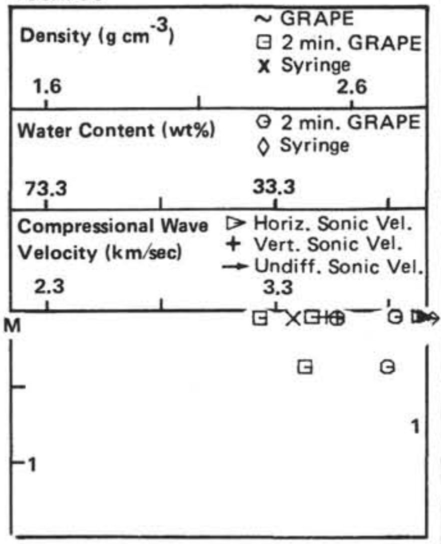

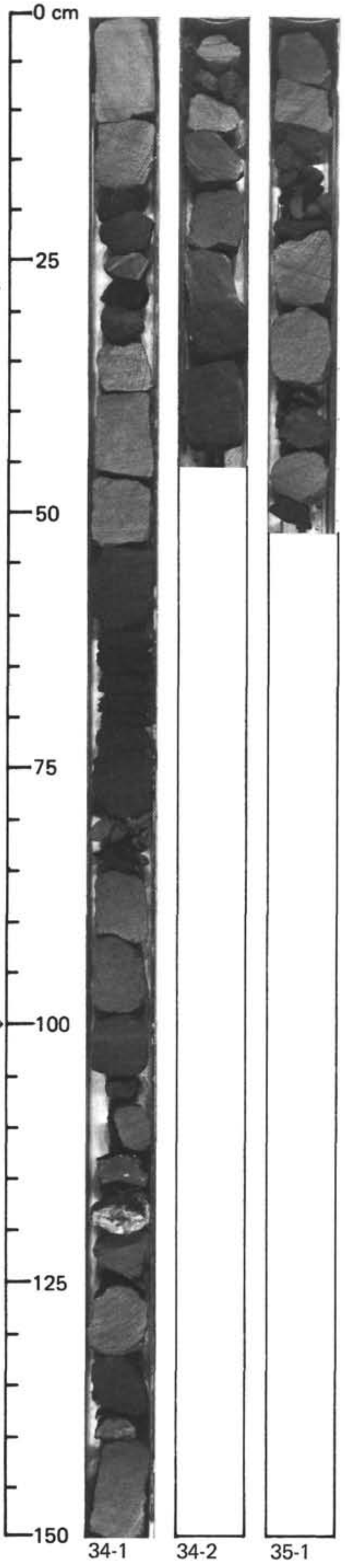

465A-36

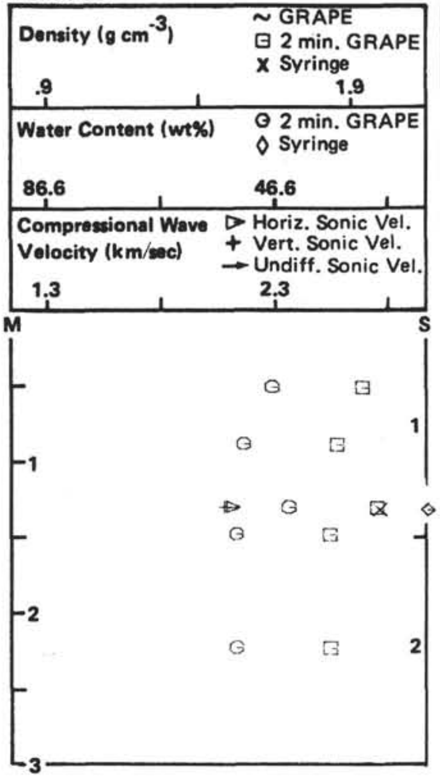

465A-37

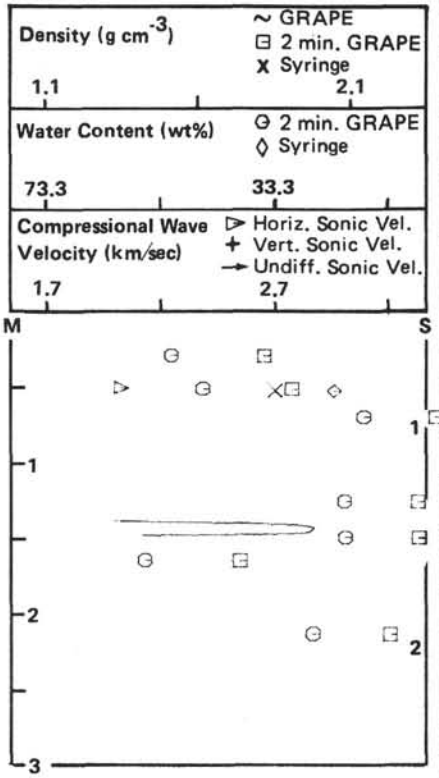

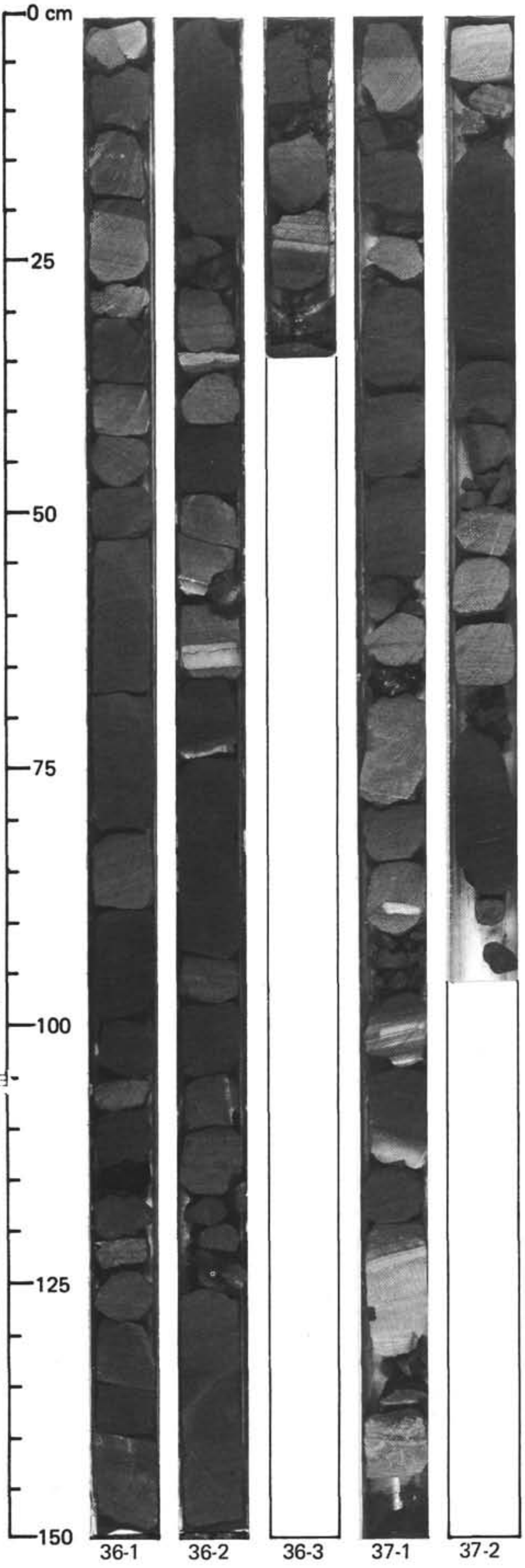

465A-38

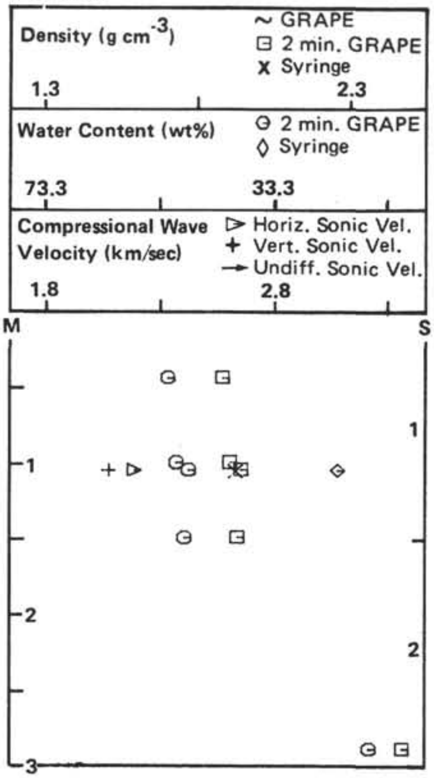

465A-39

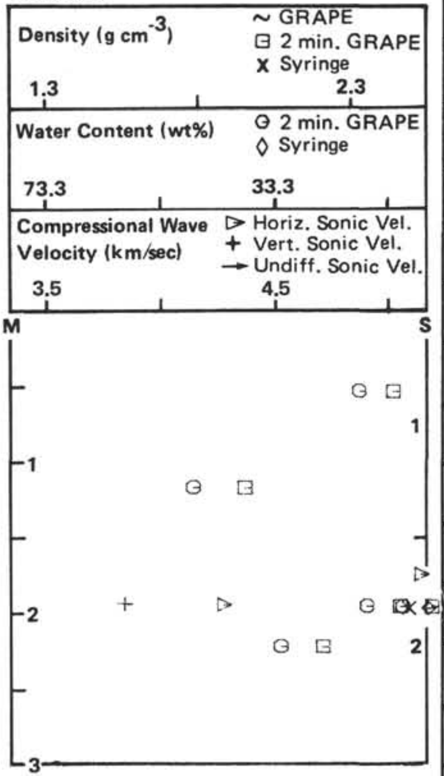

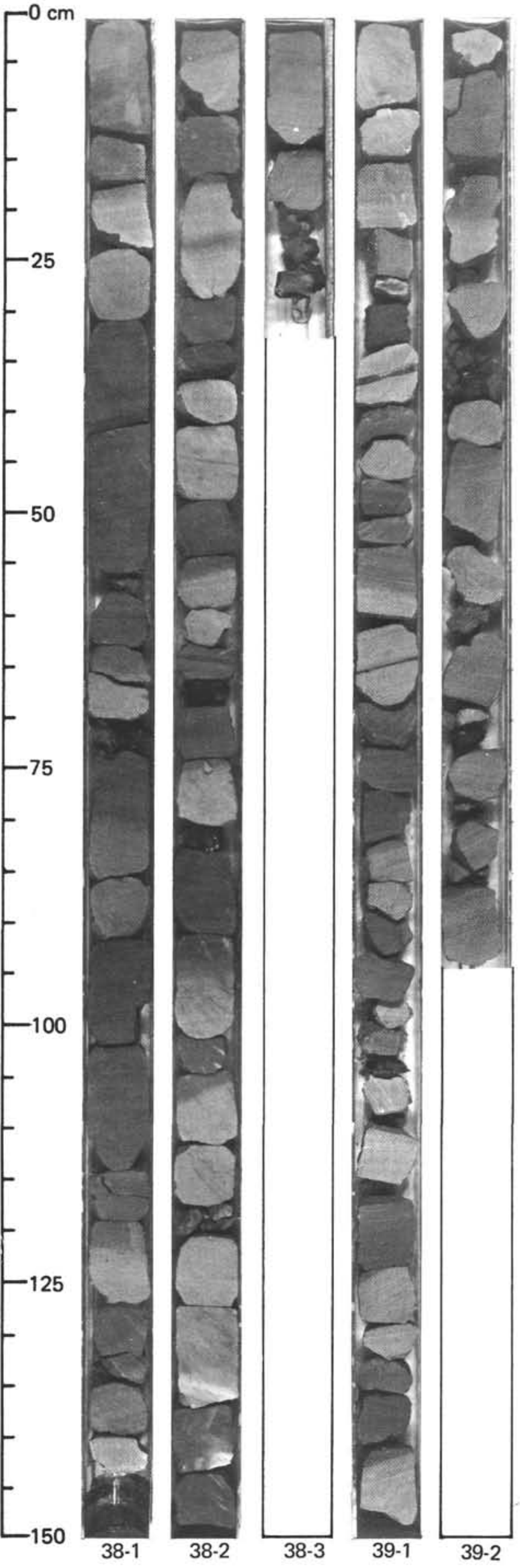

465A-40

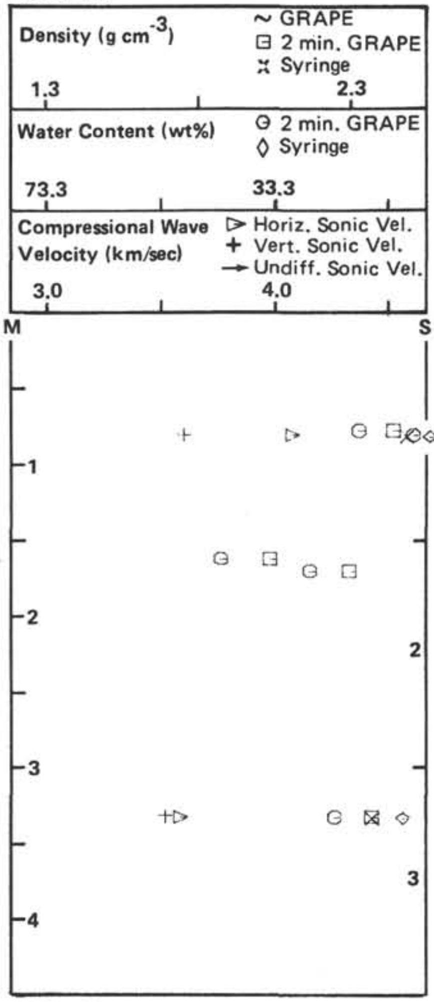

465A-41

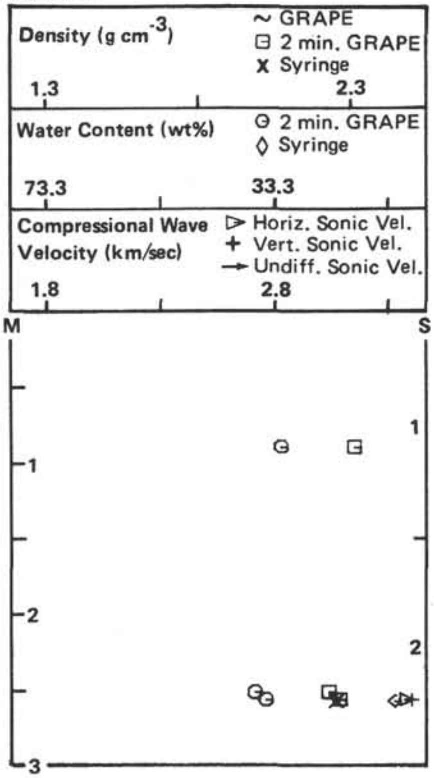

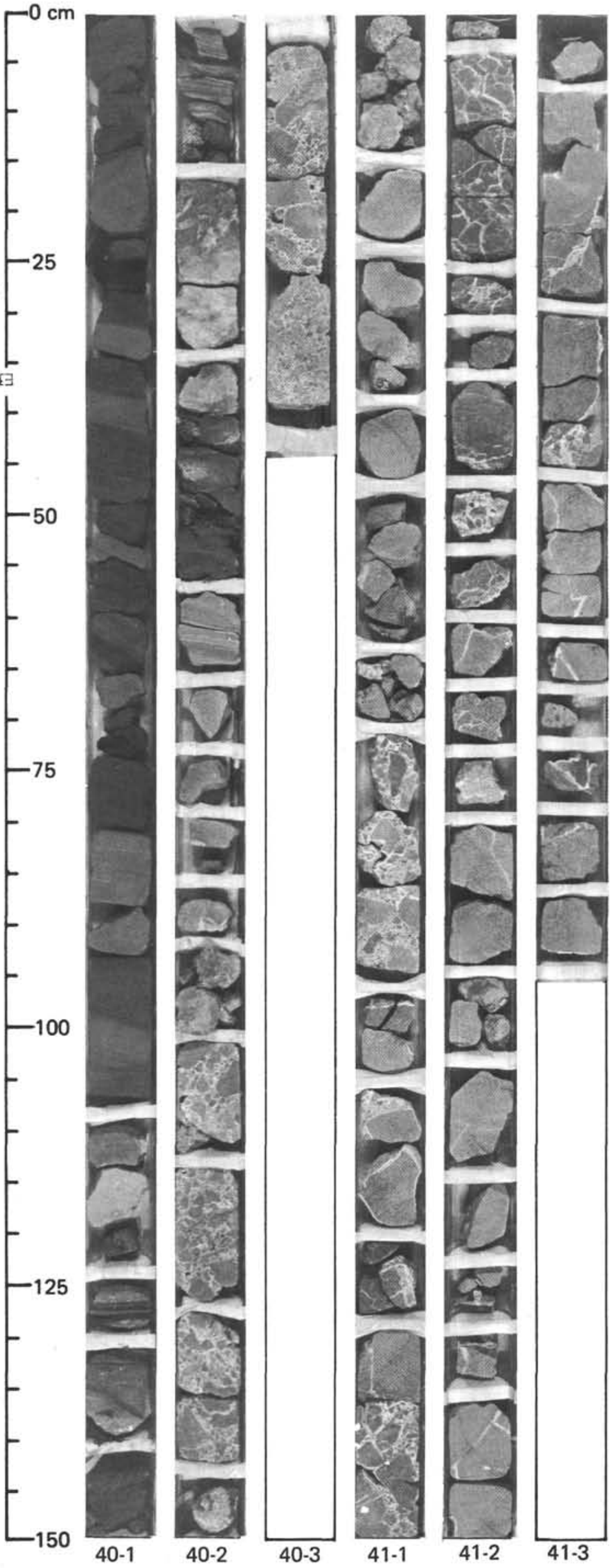

465A-42

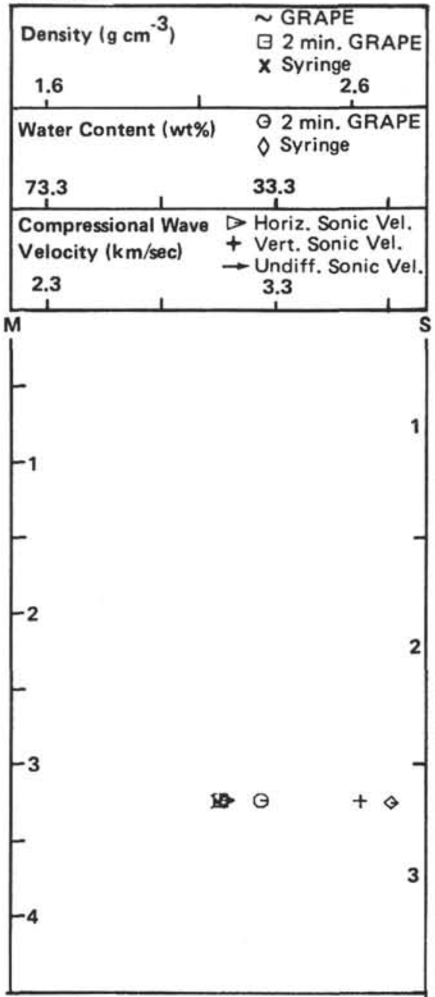

465A-43

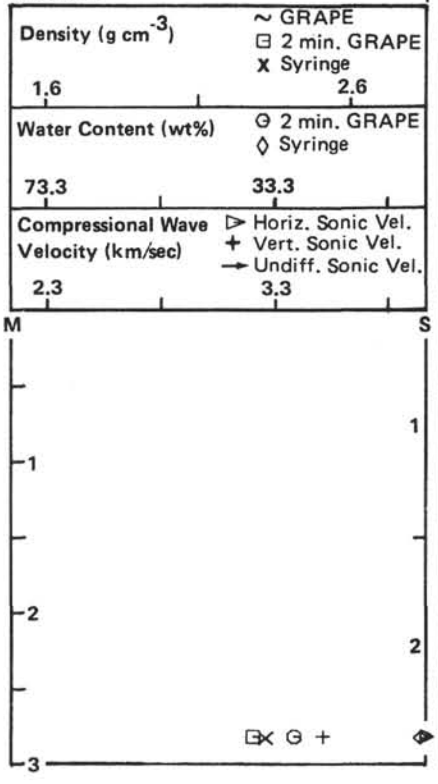

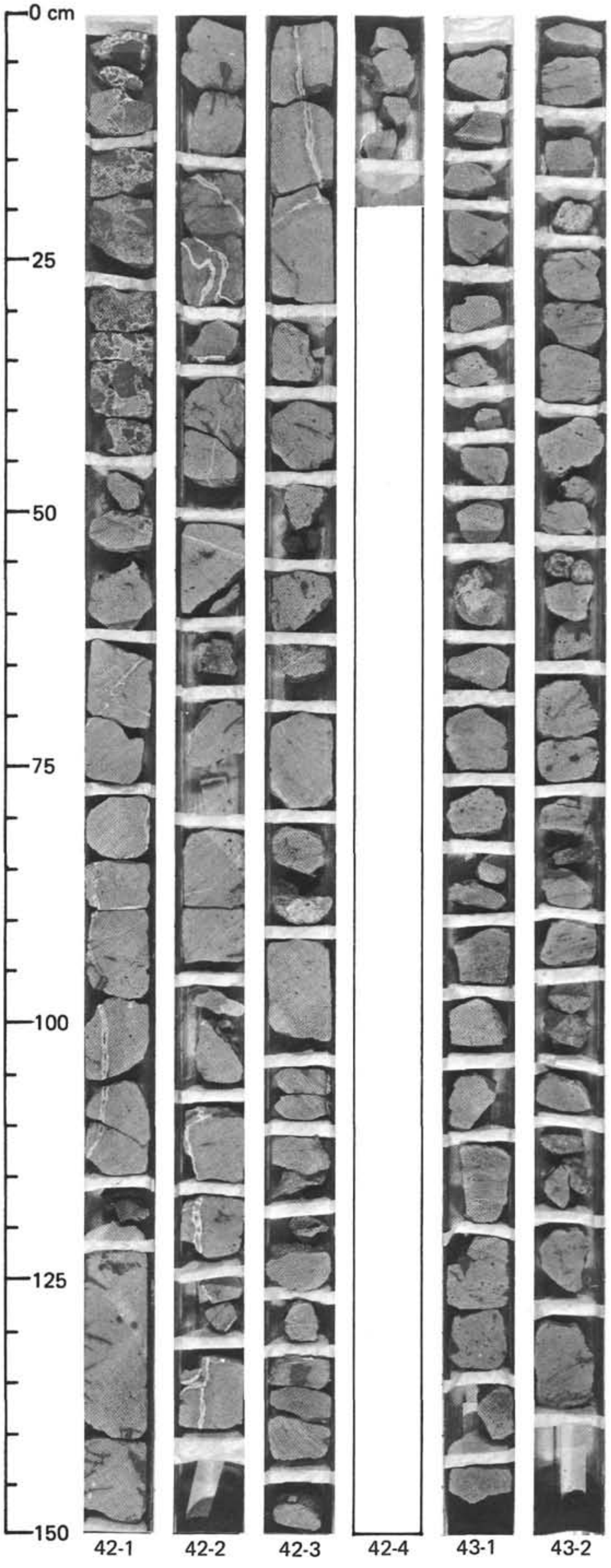

465A-44

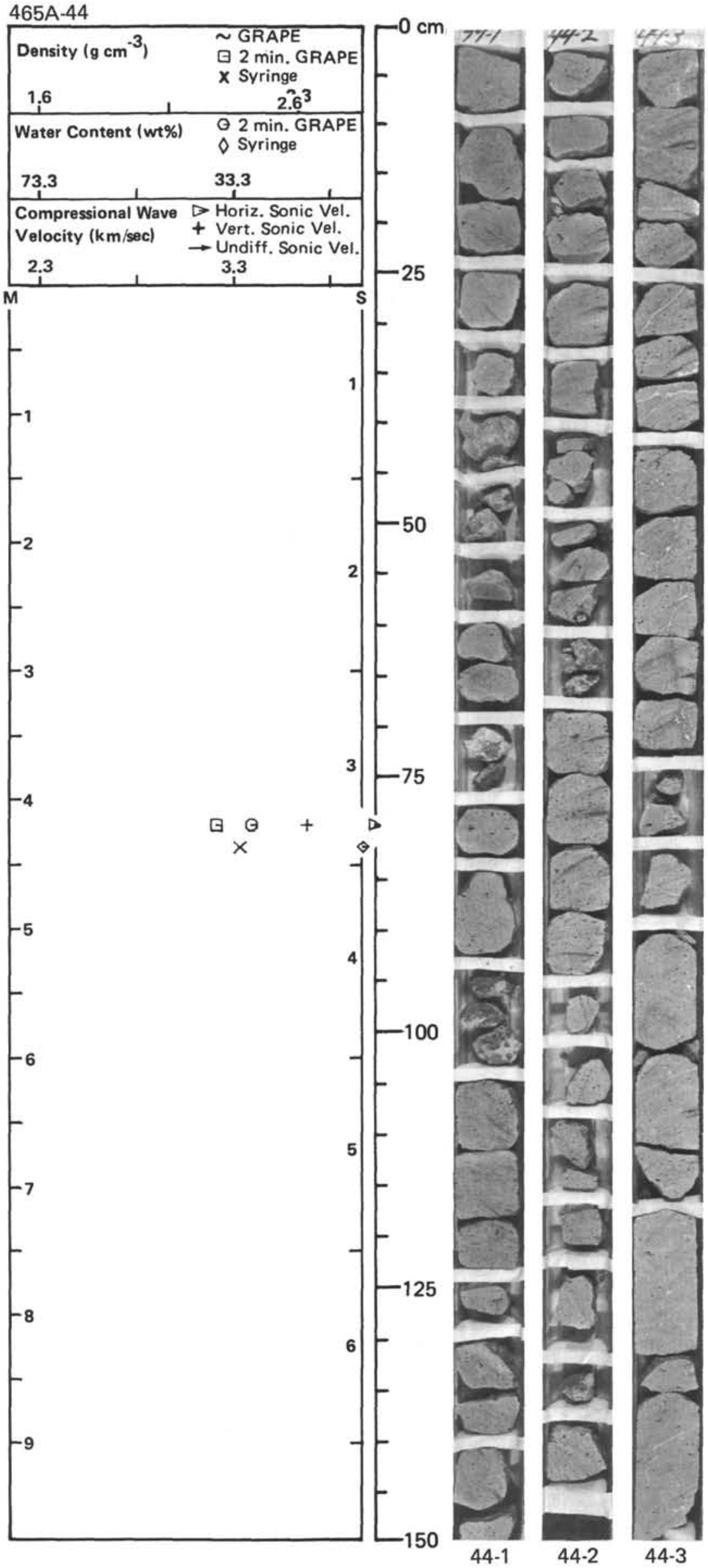
Density (g cm^{-3})
~ GRAPE
⊡ 2 min. GRAPE
X Syringe
1.6
2.6
3
Water Content (wt%)
ϴ 2 min. GRAPE
◊ Syringe
73.3
33.3
Compressional Wave Velocity (km/sec)
▷ Horiz. Sonic Vel.
+ Vert. Sonic Vel.
→ Undiff. Sonic Vel.
2.3
3.3
M
S
1
2
3
4
5
6
7
8
9
0 cm
25
50
75
100
125
150
44-1
44-2
44-3

465A-45

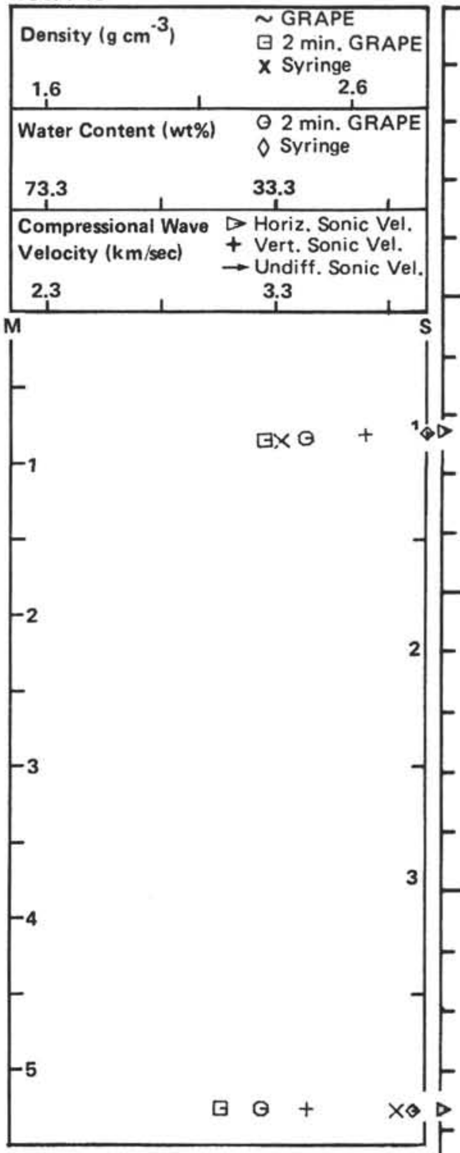

465A-46